Title
Residential HVAC and Distribution Research Implementation

Authors
Sherman, Max
Walker, Iain

Publication Date
2002-05-01

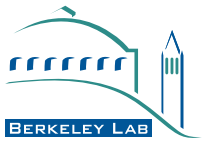

ENVIRONMENTAL ENERGY TECHNOLOGIES DIVISION
INDOOR ENVIRONMENT PROGRAM

May, 2002

Residential HVAC and Distribution Research Implementation

CIEE/PG&E Final Report

Attachments:

"Development of a New Duct Leakage Test: DeltaQ" – LBNL 47308

"Sizing and Comfort Improvements for Residential Forced-Air Heating and Cooling Systems" -LBNL 47309

"Evaluation of flow hood measurements for residential register flows" - LBNL 47382

"Simulation of Residential HVAC System Performance" – LBNL 47622

"Fouling of HVAC Fin and Tube Heat Exchangers" – LBNL 47668

"Deposition of Biological Aerosols on HVAC Heat Exchangers" – LBNL 47669

"Laboratory Study of Pressure Losses in Residential Air Distribution Systems" – LBNL 49293

Lawrence Berkeley National Laboratory
Max Sherman and Iain Walker
One Cyclotron Road, Mailstop 90-3074
Berkeley, CA 94720
Phone: 510-486-4692
E-mail: iswalker@lbl.gov

This study was sponsored by the California Institute for Energy Efficiency (CIEE) through the U.S. Department of Energy. The research reported here was funded by the California Institute for Energy Efficiency (CIEE), a research unit of the University of California. Publication of research results does not imply CIEE endorsement of or agreement with these findings, nor that of any CIEE sponsor.

This page intentionally left blank

Table of Contents

Acknowledgements

This work was supported by the Assistant Secretary for Energy Efficiency and Reneewable Energy. Office of Building Technology, State and Community Programs, Office of Building research and Standards, of the U.S. Department of Energy under Contract No. DE-AC03-76SF00098.

This work was supported by the California Institute for Energy Efficiency under Contract No. S9902A through the U.S. Department of Energy. The research reported here was funded by the California Institute for Energy Efficiency (CIEE), a research unit of the University of California. Publication of research results does not Imply CIEE endorsement of, or agreement with these findings, nor that of any CIEE sponsor.

The Energy performance of Buildings Group of Lawrence Berkeley National Laboratory developed this project for the Pacific Gas and Electric Company (PG&E) under Contract S9902A, to support PG&E's energy-efficiency programs in new and existing residential buildings. The Project manager for PG&E is Lance Elberling, with the assistance of Marshall Hunt. Bruce Wilcox (Berkeley Solar Group) also provided input and guidance.

EPB staff who contributed to this project are: Craig Wray, Jeffrey Siegel, Darryl Dickerhoff, Duo Wang, and Jennifer McWilliams. The following undergraduate summer students also made significant contributions: Gwladys Degenetais, Fabienne Boulieu and Sylvain Masson (students from the National Institute of Applied Sciences, Lyon), Jacob Wempen (from Southern Utah University on a DOE Energy Research Undergraduate Laboratory Fellowship) and Brian Carrol (from University of Texas, Austin on a DOE Energy Research Undergraduate Laboratory Fellowship). Lastly, Chris Niles was a high school student who joined EPB as a summer intern as part of an LBNL Center for Science and Engineering Education program.

This project was managed by Ed Vine of the California Institute for Energy Efficiency.

Other contractors on this project were:

Richard Heath Associates/California State University Chico:
Jim O'Bannon
Carol Holmes
John Brown

Produced by the Energy Performance of Buildings Group
Lawrence Berkeley National Laboratory
MS 90-3074, One Cyclotron Road, Berkeley,CA 94720

E-mail: iswalker@lbl.gov mhsherman@lbl.gov

Web: http://epb1.lbl.gov/EPB http://ducts.lbl.gov

Executive Summary

The most important results of this study were:

- There are significant energy savings (25%-30%), peak demand reduction (25%-30%) and comfort improvements to be realized from combining good duct systems with correctly sized HVAC systems.
- Cloth duct tapes are the only sealants to fail longevity testing under both cycling and steady temperatures.
- Technical support was provided to the California Energy Commission (CEC) to limit the use of cloth duct tapes in California through changes to Title 24 under the AB970 legislative process.
- Additional technical support was provided to the CEC AB970 energy code changes in the requirements for duct leakage & refrigerant change checking, and requirements for TXV controls for air conditioners.
- Testing of splitter boxes has shown that splitter box leakage can be a significant source of duct leakage (up to 3 cfm per box).
- The round-to-round connections have not shown the extremely rapid failure we found with previously tested collars. However, the same tape samples that failed in previous testing have shown considerable visual degradation and their measured leakage is slowly increasing.
- Field tests showed that failure of plastic flex duct is usually limited to the exterior layer. Although this does not lead to duct leakage, there is significant insulation degradation, due to insulation falling off the duct systems.
- Pioneering laboratory experiments on coil fouling have shown that typical coils are effective at removing airborne particles from the air stream. Significant advances were made in the modeling of particle deposition on coils.
- Experiments with solid dust particles have shown that pressure drops can be significantly increased by fouled coils – adding up to 30 Pa to the pressure drop across the coil in our experiments.
- A coil fouling webpage has been developed based on the experimental and modeling and work: http://epb.lbl.gov/coilfouling/
- Evaluation of a new flow-plate air-handler flow measurement technique has shown that this device underpredicts air handler flows by about 10% compared to our standard pressure matching method. For systems with central air handler filter slots, this method can be quick and easy to perform, however, in typical new California systems with filters at the return grille, significant air flow adjustments are required to account for return duct leakage that introduce additional flow errors and additional measurements that increase the time required for the test.
- Laboratory and field tests of flow hoods has shown that commercially available devices are poor at measuring residential register flows. Typical errors are in the range of 20% to 30%, mostly due to non-uniformity of flow entering the flow hoods and backpressure issues.
- Powered flow hoods were found to be much more accurate, with uncertainties of about 2% to 3%.

- Preliminary work on a simple and inexpensive non-powered flowhood has shown encouraging results compared to commercially available flow hoods, with accuracy almost as good as powered flow hoods, but with less expense for equipment and time required for testing. We plan to pursue the development of these flow hoods in the future with possible funding from DOE.
- New application standards for flow hoods need to be developed in collaboration with ASTM and ASHRAE.
- Over one hundred houses (mostly between 5 and 15 years old) were tested by CSUC staff for duct leakage. The average duct leakage for these houses was typical of other surveys at 10% supply and 12% return leakage.
- The DeltaQ test was performed in all these houses and small changes to the measurement procedure resulted from these field experiences. In particular a method of eliminating the measurement of plenum pressures (thus making the test simpler and faster) has been developed. The DeltaQ test is now being used by many field practitioners (including researchers, building science experts and Building America partners) and is being evaluated by ASHRAE and DOE sponsored research programs.
- The DeltaQ test was found to take about 30 minutes on average – this time should be reduced by removing the requirement to measure plenum pressures.
- Considerable differences (typically half of the measured flows) were found between DeltaQ and fan pressurization results. This result is expected because the DeltaQ test measures leakage flows at operating conditions and the pressurization tests measures the size of the holes in the duct system. However, if we look at screening, compliance or quality control tests where a low leakage limit is imposed, then better agreement was found between the two test methods, with the pressurization test tending to overpredict leakage (i.e., it is a conservative test of leakage).
- Potential users of the DeltaQ test like its straightforward procedure (no registers to be covered), the fact that it uses existing blower door equipment, the short time requirements and the fact that the test includes envelope leakage.
- Repeatability testing of the DeltaQ test has indicated that the repeatability is excellent for this test method over a range of duct leakage and supply/return leakage imbalance. The results show the repeatability uncertainty is less than 1% of fan flow.
- Laboratory tests have produced new duct fitting loss coefficients for use in duct design calculations. The new coefficients are for fittings not currently found in design guides.
- Laboratory tests have shown how compression of flexible plastic duct significantly increases the pressure losses for duct systems – with typically compressed duct having about five times the flow resistance and pressure drop of fully stretched duct. A simple calculation procedure for compressibility effects has been developed that is suitable for use in standard calculation procedures, e.g., ASHRAE or ACCA.
- A full scale “typical” California duct system test facility has been built at LBNL. This facility has been used in the duct fitting and flow hood development testing. We are planning to use this facility in future residential HVAC research projects for developing diagnostic techniques and evaluation of potential residential HVAC performance and comfort improvements.

Introduction

This report provides information to support energy efficiency and peak demand reduction in residential thermal distribution systems. The study had eight tasks:

Task 1: Whole Building Approaches to New Residential Construction

This task examines the integration of the HVAC system with innovative house construction techniques using field evaluations. For example, bringing duct systems inside the thermal envelope of the house.

Task 2: Sizing and Operation of Cooling Systems

This task is developing new system sizing techniques and looking at how system controls influence performance. A key objective of this task is to provide information that will reduce the current oversizing of residential cooling systems.

Task 3: Duct Leakage Test Method
Improvements in accuracy and reductions in cost for duct leakage testing are being investigated in this task that will result in a new ASTM standard test method. A new test method (called DeltaQ) is being developed under this task.

Task 4: Duct Sealant Longevity

Using good duct seals is very important. This task includes laboratory evaluation of sealants and developing an ASTM standard test method.

Task 5. Coil Fouling

Dirty coils can have significant effects on indoor air quality. In addition, reduced air flow reduces the efficiency of HVAC equipment and increases air handler fan power requirements. This is a pioneering study of HVAC system air coil fouling.

Task 6. Duct Fittings Survey and Performance Testing

Many duct system fittings in common use in California duct systems are not found in standard fitting loss tables. This task aims to evaluate these fittings using a full scale laboratory duct system, that will also be used to evaluate duct system air flow measurement devices.

Task 7. Improved Energy Efficiency Modeling

Technical assistance is being provided to the California Energy Commission regarding efficiency calculations in California building codes and standards.

Task 8. Field Research on Duct Systems in Older Homes

In collaboration with Richard Heath & Associates and California State University Chico, this task is evaluating the thermal distribution systems in over one hundred California homes more than 5 years old.

Review of findings from individual tasks

Task 1: Whole Building Approaches to New Residential Construction

Production delays for the structural panels mean that construction and field testing will occur in November 2001. Some preliminary diagnostic test results are given in Appendix C, however, due to time constraints, no additional testing or analysis will be possible for this project.

In conjunction with the LBNL residential commissioning project, we gave presentations at PAC meetings and for CEC commissioner Rosenfeld (and other CEC staff) in Sacramento that showed how this project is developing field test procedures and setting norms for house performance.

We have also attended Natural Resources Defense Council (NRDC) “Future of T24”

meetings to discuss how thermal distribution systems will be treated in future T24 standards.

We have performed analyses on some of the effects of these new construction techniques in Tasks 2 and 7 (e.g., duct improvements and related equipment capacity reduction).

Task 2: Sizing and Operation of Cooling Systems

This task uses the LBNL REGCAP simulation tool to look at four key questions:

- Can heating and cooling systems be downsized (and by how much) in California if distribution systems are improved?
- Does the downsizing result in poor comfort?
- What peak power and energy savings are associated with improved systems?
- What other system parameters can have a significant impact on energy use and peak load?

The REGCAP model is a state-of-the-art simulation program that performs minute-by-minute simulations of house, attic and HVAC system heat and air transport. It includes conduction, radiation (including solar gains) and airflows (duct leakage and natural ventilation of house and attic). The house and attic are treated separately and are linked by conduction and airflow through the ceiling. The equipment model accounts for coil airflow, outdoor weather and refrigerant charge and gives a good match to measured temperatures and energy use.

A total of 368 different simulations were performed in eight California climate zones for cooling and 480 for heating (in all 16 California climate zones). In each climate zone two different days were simulated. One day represented the design conditions, and the second day represented the peak weather conditions (i.e., the coldest and hottest days of the year). The design day is most useful for system sizing, and the peak day is more sensitive to comfort issues, e.g., lack of temperature control. The results of peak-day simulations can also be applied to peak demand calculations where performance in more extreme weather is of great importance.

The simulations investigated a large number of system parameters over a wide range of conditions. The key system parameters were: refrigerant charge, evaporator air flow, duct leakage (including imbalance effects on air infiltration), duct insulation, different thermostat strategies (constant temperature, pulldown and the Title 24 standard of: "on" in the a.m. and "off" during peak, then "on" again in the p.m.) and sizing (4, 3, 2 tons). To evaluate these parameters we determined Tons At the Register (TAR), energy consumption, equipment efficiency, duct efficiency, peak indoor temp, time above setpoint+1°C, pulldown time (peak and daily mean).

The main outcome of this study is that correctly sized systems can provide equal or better comfort than oversized systems. However, comfort improvement and energy savings depend on the climate: more extreme climates have less energy savings and comfort change. Comfort and energy advantages can also result from improving duct characteristics (reduced leakage and increased insulation). The results showed that builders may find it profitable to design and install ducts with minimized area (using shorter duct runs) and improved insulation materials in new houses. In addition to reducing the installation and materials costs, they can then use a smaller and therefore less expensive air-conditioning unit. Further improvements can be obtained by moving ducts into conditioned space. Details of the simulation procedure, including the house and weather data are given in LBNL 47622 and 47309 (see the publications list at the end of this report). Additional validation work has been performed by comparing simulation results to measured data taken by LBNL over the last couple of years. This

validation work is being prepared for an ASHRAE symposium paper (LBNL 50008).

For cooling systems, the results showed that cooling systems can be downsized by about 25% without compromising comfort. A simple comparison can be done between good ducts and typical ducts in California new construction for two systems: one where the systems is built into a cathedralized attic (like those used in the Building America Project in Task 1) so that the duct system is almost all inside the conditioned space; and a second system where the ducts are still in a standard vented attic, but they have little leakage and good insulation. The resized cathedralized system has 20% greater TAR, 60% less energy use, and uses 30% less peak power. The resized, vented attic system has 3% less TAR, 27% less energy use and 22% less peak power. The peak power demand scales with the reduction in capacity: for a typical three ton system, the peak savings are about 1.5 kW.

There are significant energy savings associated (up to 50% for conventional systems) with turning off air conditioning systems during the day and then turning them back on in the late afternoon (between 3:00 and 4:00 p.m.) However, there are significant thermal comfort issues associated with this type of operation. A typical California cooling system takes too long to pull down the interior house temperature to an acceptable level, resulting in indoor temperatures being too high for several hours. In addition, this operation method would have many air conditioners coming on at the same time, which results in excessive peak demand for electric utilities.

The REGCAP simulations for heating show that heating systems can be successfully downsized (by about 25%) without compromising comfort, if systems are well sealed and insulated and/or are brought more inside the conditioned space. A resized system in a cathedralized attic with 25% less capacity than a typical new California system reduces the peak gas and electricity consumption by 25%. In addition to consuming less energy, this system is able to deliver 12% more energy to the conditioned space.

The reductions in energy consumption that can be obtained using well-installed duct systems, or systems inside conditioned space depend strongly on climate. A typical energy reduction is about 35% for a house in Sacramento at design conditions. In addition, thermostat strategies that allow the house to be cooler at night result in energy savings of about 7% for attic duct systems at design conditions.

Another important sizing issue that was studied as part of this simulation work was the systematic oversizing of heating and cooling equipment. The oversizing of cooling equipment has been well documented in other studies. For the heating simulations we performed ACCA Manual J sizing calculations that already have some oversizing built in to the methodology. These calculations showed that in most climate zones (except climate zone 16 that requires 45 kBtu/hr) a 35 kBtu/hr system is the right size for the standard house. For comparison, the Title 24 default value (used in the base case simulations) has a furnace with 60 kBtu/hr capacity - almost a factor of two in oversizing. Additional anecdotal evidence suggests that systems in real houses are even further oversized. A key reason for this is that the same duct system is used for heating and cooling, and the duct size and fan flow requirements are greater for cooling than for heating. The air handler and furnace (that come together as a unit) are therefore oversized for heating systems. This oversizing leads to very short furnace cycles, even for resized systems, as shown in the simulation results of Figure 1. In this figure, the lowest line is the outdoor temperature. The next highest line is the attic temperature that shows the same diurnal cycle as the outdoor temperature. The indoor temperature shows small fluctuations around the 68°F setpoint. The

supply air temperature shows the large temperature swings up to 120°F. The short furnace cycles are easily seen in the rapid supply temperature changes. Note that in order to capture the dynamic performance of the house and duct system our sophisticated model capable of short time step calculations is essential.

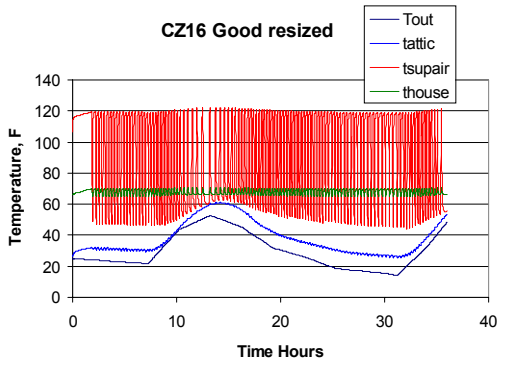

Figure 1. Short Furnace Cycles Indicating Excess Capacity

In August 2000 we presented a paper titled "Delivering Tons to the Register: Energy Efficient Design and Operation of Residential Cooling Systems" at the ACEEE Summer Study 2000, Asilomar, CA. This paper summarized comparisons of REGCAP to measured field data for both conventional and cathedralized attics. REGCAP was then used to simulate several different duct/HVAC systems to determine the potential for system downsizing while maintaining comfort.

We have given a presentation discussing Performance Testing of HVAC system operation at the Affordable Comfort Workshop in December 2000. At the same Affordable Comfort meeting, we gave field demonstrations of new protocols and techniques for Performance Testing of Residences in a new house in Livermore, CA. Presentations on HVAC system sizing issues have been given at: a California Association of Building Energy Consultants meeting (May 2001), HVAC Comfortech Conference in Nashville (September 2001) and a forum at the Energy and Environmental Building Association Conference (October 2001). These activities were performed in conjunction with LBNL's CEC PIER and DOE Research Programs.

Task 3: Duct Leakage Test Method

This task focuses on the development of a new duct leakage test method to determine the supply and return duct leakage at system operating conditions. Many details of the work performed for this task are given the attachment: "Development of a New Duct Leakage Test: DeltaQ" - LBNL 47308.

For this task LBNL and CSUC have performed both field evaluations and repeatability testing. The field evaluations were intended to find if there are conditions for which the test gives poor results and to find which parts of the test are difficult to perform and/or are time consuming. For the field evaluations, LBNL has trained CSUC staff and provided test protocols and automated software for the DeltaQ test. Additional field evaluations have been performed by other researchers and building scientists (e.g., Chitwood Energy Management, ECOTOPE, Inc., and Brookhaven National Laboratory Staff) in over 100 houses. This developing database indicates that the DeltaQ test provides a quick, easy and robust method for estimating duct leakage flows.

We received field data from CSUC for 110 houses in which the DeltaQ test was performed, together with duct pressurization testing and observations of flexible duct longevity. More detail on these field tests, in addition to other tests performed by CSUC, can be found in quarterly reports from CSUC.

The DeltaQ test shows that the average leakage for these houses is typical of those seen in previous surveys (Cummings et al. (1990), Downey and Proctor (1994a), Jump et al. (1996a) and Modera and Wilcox (1995)) with 99 cfm (47 l/s or 10% of air handler flow) for supply and 107 cfm (51 l/s or (12% of air handler flow)) for returns.

The supply leakage ranged from zero to 330 cfm (156 l/s or 35% of air handler flow). The return leakage ranged from zero to 600 cfm (283 l/s or 73% of air handler flow).

There was a large range of envelope leakage from 760 to 7000 cfm50 (357 to 3300 l/s at 50 Pa). The corresponding 4 Pa ELAs are about 40 to 370 in^2 (260 cm^2 to 2400 cm^2). The average envelope leakage was 2500 cfm50 (1180 l/s at 50 Pa), with a standard deviation of 1100 cfm50 (520 l/s at 50 Pa). Testing over this wide range of envelope leakage is important because the DeltaQ test uses the change in flow through the envelope caused by duct leakage imbalances to calculate the duct leakage. Other tests that use the envelope pressure difference work best only when the envelope is not very leaky. Our field experience with the DeltaQ test has shown that for the houses in this study, the automated DeltaQ test produced reasonable results, even with leaky envelopes. This is because many data pairs are used in the analysis over a range of envelope pressures that was greater in magnitude than the weather induced envelope pressure fluctuations. In addition, the automated software used long time averages to reduce weather induced fluctuations and automatically took data until prescribed limits on standard deviation of measured pressures were reached.

By changing the duct pressures and reanalyzing the data it was found that even fairly large changes in duct reference pressure did not change the final result a great deal. Typically, the reference pressure can be changed by a factor of two and only change the supply and return leakage by about 10% to 15%.

When the duct leakage is small the DeltaQ analysis can sometimes yield negative numbers for supply or return leakage. This is a combination of the precision of the test being limited to about 10 to 20 cfm (5 to 10 l/s) and at these low leakage levels, the results become more sensitive to "outliers" in the measured data. The precision is estimated based on the resolution of the envelope pressure measurements (roughly 0.1 Pa, although this can be effectively reduced by taking many data points) and the corresponding envelope flows, combined with the observed magnitude of the small negative numbers generated by the calculation procedure. Generally, when negative numbers result from the test this shows that the duct system is not leaky and the test result should be interpreted to mean that the leakage is less than this precision of the test procedure, i.e., less than 10 to 20 cfm. This implies that the leakage flows are going to be less than about 1% of fan flow and therefore not significant in terms of energy losses or poor distribution. Also, any system with this little leakage is going to pass any of the existing (and probably future) leakage limits found in energy codes (e.g., CEC (1998) gives a 6% of fan flow limit) or voluntary programs (EPA Energy Star ducts have a 10% of fan flow limit).

In terms of ease of use, the field tests showed a problem (and one that we have found while using the test in houses as part of our CEC Commissioning project) with having too tight a limit on the range of allowable blower door pressures. This led to multiple changes of blower door rings that was both time consuming and frustrating for the operators. A new version of the automated software has been developed to reduce this problem.

Two sets of repeatability testing of the DeltaQ test have been performed using a trailer at LBNL. This testing was augmented by support from DOE Energy Research Undergraduate Laboratory Fellowship awards to two engineering students: Jacob Wempen and Brian Carrol.

The first round of testing evaluated the same duct system 20 times over several days. These results showed that the repeatability errors were quite reasonable and within a few cfm of values obtained in other studies for direct duct pressurization (Walker et al. 1998). Table 1 summarizes these

repeatability testing results for DeltaQ. Both the standard deviation and 95% confidence interval (C.I.) are given.

Table 1. Repeatability Results for DeltaQ Testing

Average Supply Leakage (Q_s), cfm	19
Average Return Leakage (Q_r), cfm	66
Standard deviation of supply leakage, σ_s	11
Standard deviation of return leakage, σ_r	16
Supply Leak 95% C.I., cfm	5
Return Leak 95% C.I., cfm	7

Rather than analyze the repeatability results in absolute terms (cfm), it is better to look at them in terms of the fraction of fan flow. This is because the leakage test results to be used in either energy calculations or verification of low leakage compliance will express the leakage as a fraction of fan flow. This is done because the energy losses are proportional to the fraction of fan flow, and compliance testing needs to scale with the size of the equipment and therefore, the fan flow. Flow hood and tracer gas measurements showed that the air handler flow was approximately 1000 cfm, so the 95% C.I. for the repeatability uncertainty was very small compared to the air handler flow: <1%. In addition, the trailer where the tests were performed was fairly leaky for a small building (1000 cfm50, ELA 80 in^2). The small duct leakage and leaky envelope is the situation that we expect to be most difficult for the DeltaQ test due to the resulting small envelope pressure changes. Therefore, the results so far are extremely encouraging. Figure 2 shows the variability in the test results as a function of measured pressure variability. In Figure 2, the supply and return leakage (Qs and Qr) are expressed as fractions of the air handler fan flow. In addition, the effective leakage area (ELA) of the trailer taken from the Air Handler fan off measurements is shown. This ELA data is another indicator of the repeatability of the test. In this figure, the less scatter from test to test, the less the repeatability uncertainty. Although this is a limited data set the test variability does not increase very much with the measured envelope pressure variability. This is a good result, because we would like the test to be relatively insensitive to these pressure fluctuations, so that it will provide accurate results under a wide range of weather conditions.

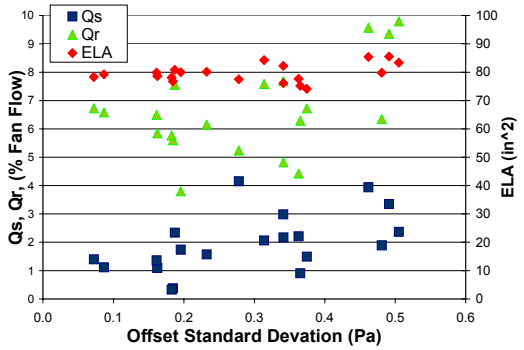

Figure 2. DeltaQ Repeatability Test Results

For the second round of repeatability testing, leaks were added to the duct system. The added leaks were carefully installed so that the leakage flow could be accurately monitored. The air flow from registers was ducted directly to outside through flow meters so that the true leakage flow to outside could be measured. The system was sealed and measured before the leaks were added and this background leakage (less than 2% of fan flow) was added to the directly measured leakage flows. Four combinations of added leakage were examined:

1. **Large supply and return leakage**: 22% supply leakage, 14% return.
2. **High supply and no added return leakage**: 15% supply leakage, 2% return.
3. **Moderate supply and no added return leakage**: 9% supply leakage and 2% return.
4. **Small supply and no added return leakage**: 4.5% supply leakage and 1.5% return (the changes in "no added return" leakage are due to

changing system operating pressures that vary as the supply leakage increases).

Each leakage combination was tested several times to see if repeatability changed significantly with leakage magnitude and distribution between supply and return. The test results showed that the repeatability was excellent, with a 95% CI of about 0.2% of fan flow (2 cfm). In addition, there were no significant changes in repeatability as the leakage changed. Figure 3 illustrates supply leakage repeatability results for the four different leakage levels.

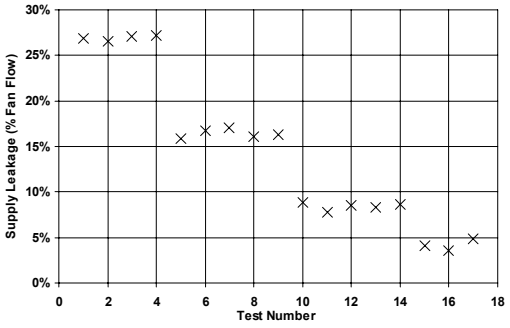

Figure 3. Supply leakage repeatability results for four leakage configurations

In terms of accuracy, the RMS difference between the DeltaQ results and the combined measured and background leakage for all the leakage configurations was about 2.5% of fan flow (25 cfm (12 l/s)) for returns and 1.3% of fan flow (13 cfm (6 l/s)) for supplies. Most of this uncertainty is due to the overprediction of leakage flows with the large supply and return leakage. This overprediction may be due to the nature of the added leaks. The added leaks were flow meters that have significantly different flow coefficients and exponents depending on flow direction. During the DeltaQ tests, the flow direction changes through the leaks. Because the DeltaQ method assumes the flow coefficients and exponents do not change, it results in experimental errors. In real houses, it is unlikely that the leaks will be single large leaks with coefficients and exponents that change with flow direction, so this error is less likely to occur in real systems. Unfortunately, it is difficult to measure the true leakage of duct systems in order to estimate test method accuracy without using some flow meter device whose flow characteristics dominate the leakage of the system. We will continue to investigate these accuracy issues in the future.

Pressure Selection

During the development of the DeltaQ test we came up with the idea that the pressures used in the calculation data could be fitted to the measured data at the same time as the supply and return leakage flow rates. This is possible because the DeltaQ test takes several data pairs over a wide range of pressure and flow conditions. The main advantages of fitting the pressures are:

- The time and effort required to perform the test are reduced because the plenum pressures do not have to be measured. This can be a considerable saving for many residential systems whose air handlers are difficult to access. Also, no holes need to be drilled into the plenums (and sealed after the testing is completed).
- It makes use of the measured data from the actual system rather than relying on modeling assumptions about duct pressures scaling with plenum pressures. This has the potential to increase the accuracy of the test method.

The potential drawbacks of this pressure fitting technique primarily result from the data analysis. For example, reducing the number of degrees of freedom when fitting to the measured data may reduce the accuracy of the fit to the data. Also, noisy measurements may result in the fitting routine being less robust and causing larger errors for noisy data.

We have applied the pressure fitting technique to the over 100 houses measured by CSUC for this study. In addition, we

have also used this technique on 7 houses (tested in more then 60 leakage configurations) measured by ECOTOPE as part of an ASHRAE Research project. Lastly, we used the second set of repeatability tests to examine this pressure fitting technique in addition to a couple of other options for selecting the characteristic system pressures: using half the plenum pressures and fixing the pressures at 25 and 100 Pa for the supply and return respectively.

From the controlled repeatability tests with carefully measured duct leakage we found that the fitted pressures gave the best results, followed by the plenum pressures. Table 2 summarizes the error estimates for each characteristic pressure technique. Figure 4 illustrates the differences between the DeltaQ predictions with these four characteristic pressure methods for supply leaks.

Table 2. RMS errors (cfm) for four different characteristic DeltaQ pressure estimates

	Actual Plenum Pressure	Fixed Pressure	Half Plenum Pressure	"Best Fit" Pressure
Supply	17	57	33	25
Return	29	14	34	13

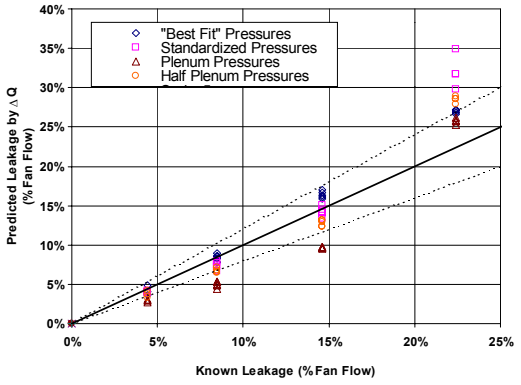

Figure 4. Variation in DeltaQ predicted supply leakage flows depending on characteristic pressures for four leakage configurations (solid line is for DeltaQ leakage equal to known leakage and the dashed lines represent ±20% variation form the equality line

The details of the first round of testing were given in an attachment to the interim report: "Repeatability of the DeltaQ Duct Leakage Test Method". More details of the second round of repeatability testing are in Appendix A of this report.

We tested an additional four houses using DeltaQ as part of the CEC commissioning project. These houses showed a large range in duct leakage from unmeasurably small (less than 20 cfm) for a new house in Sacramento (built to SMUD Advantage Homes specification – guaranteed to use half the energy of a Title 24 house) to substantial (30% supply and 60% return) for an older home in Concord.

A more detailed report on the development of the DeltaQ test is given in Attachment C - "Development of a New Duct Leakage Test: DeltaQ".

There has been continued development of the revisions to ASTM E1554 (Standard Test Methods for Determining External Air Leakage of Air Distribution Systems by Fan Pressurization). The field data taken for this task has been used in supporting documentation for this standard. The standard will be reballoted in January 2002.

Task 4: Duct Sealant Longevity

In this task, we are testing a wide range of duct sealants using an existing test facility whose construction was funded by previous DOE activities. This facility can simultaneously perform different tests: heating only, cooling only and temperature cycling. The comparison of these different test methods is being used in the development of an ASTM standard for duct sealant longevity testing.

The test results continue to show that only cloth-backed rubber adhesive tapes fail. However, the range of time to failure for these types of tape is large - with some failing in a few days and others failing very slowly. So far, over fifty samples have been tested in the new apparatus. Some samples

have been removed after 100 days of testing in order to make space on the test apparatus for new samples. The removed samples were those that had shown no measurable changes in the 100 days of testing.

The new samples included some innovative duct sealing products, e.g., a new experimental butyl tape that is UL-181 listed and a pre-caulked duct fitting system. The pre-caulked sample in the heating-only test had the caulking melt and run out of the groove. However, the leakage measurement results show that leakage is still not very high. This is because this sample is tightly inserted into a well-cut circular hole that has little leakage, even if it unsealed. After demonstrating these results to the manufacturer, they plan to change the caulk formulation for higher temperature resistance. We are continuing to collaborate with the manufacturer as they improve and change this product. The experimental butyl tape showed no failure.

Other connections have been tested: flex duct to collar connections, a straight circular to circular connection (instead of the inside 90 degree samples we currently use), and a sample duct board splitter box. These connections should answer questions raised by the sealant and building industry regarding the applicability of the test samples we are currently using to the wide range of joints seen in many duct systems.

A very important result is that the testing has shown that failure is fastest for heating only, followed by cycling, with cooling having no failure as yet (although a few samples are close to failure). The same samples fail in cycling mode as in heating-only, they just take longer to fail. This indicates that the quick and easy heating only test is suitable for longevity evaluation. These results were presented to the ASTM sub-committee members at the ASTM meetings in October 2000, and all those present agreed that the simpler testing would be preferable. This simpler test is more acceptable to manufacturers and allows a simpler ASTM test procedure. We have prepared a new draft longevity standard for heating only that will be balloted in February 2002. The work done for this task will be included in supporting documentation for this ballot.

Unfortunately, longevity testing was delayed due to several equipment breakdowns – with failed fan bearings and heater systems. The bearings have been replaced, and their housings redesigned to direct cold air over the bearings. This has significantly reduced the bearing operating temperature and will lead to longer bearing life.

We presented a paper titled "Stopping Duct Quacks: Longevity of Residential Duct Sealants" at the ACEEE Summer Study 2000, Asilomar, CA.

Task 5. Coil Fouling

The objective of this task is to find out more about coil fouling. Fouling of heat exchangers used in heating, ventilating, and air conditioning (HVAC) systems is important both because of their widespread use in commercial, residential and industrial buildings and the energy and indoor air quality impacts that can result from fouling. Fouling of indoor fin-and-tube heat exchangers, particularly air conditioner evaporators, is especially important because space cooling in buildings is an key contributor to overall energy use and peak electric demand. Furthermore, the location of heat exchangers in HVAC systems means that if bioaerosols containing bacteria, fungi, and viruses deposit on heat exchangers and remain viable, they can quickly spread through an indoor space if they are re-entrained in the airflow. Fouled coils restrict airflow and reduce heat transfer coefficients, which leads to system inefficiencies and poor distribution. In addition, they can be a significant health hazard due to the nature of the matter that is deposited on coils and the likelihood that coils are moist due to condensation. Examples of a clean coil and a fouled coil are given in Figure 5.

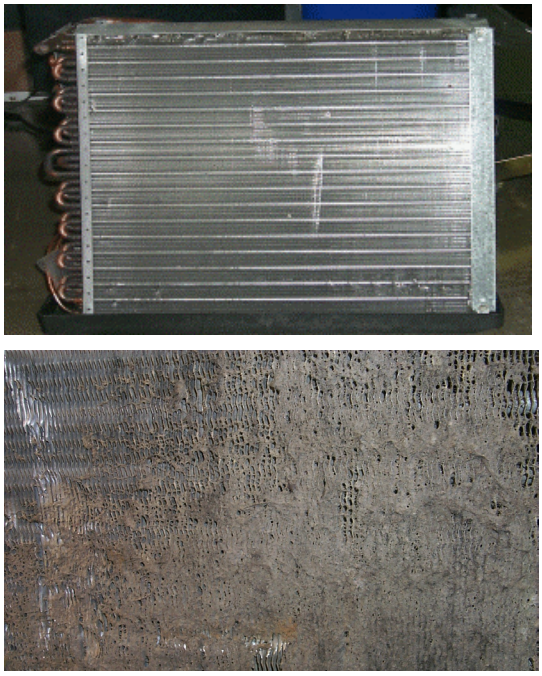

Figure 5. Face of a clean coil and a fouled coil

Because this is a new area of research, the first element of this task was to perform a literature survey. The literature search found a large base of water/liquid coil fouling – but almost nothing on air fouling (the focus of this study). As far as we know, our laboratory study will be the first of its kind. There have been several anecdotal reports of heat exchanger fouling (e.g., Anonymous, 1987; Neal, 1992). In the engineering literature, Krafthefter & Bonne (1986) report that a typical residential heat pump system will foul sufficiently to cause a 20 % reduction in performance over a 4 to 7 year period. They further report substantial reductions in fouling from large dust particles by the installation of electric air cleaners. Muyshondt et al. (1998) used a computational fluid dynamic (CFD) approach to predict aerosol deposition on fin and tube heat exchangers for a matrix of velocities, heat exchanger geometries, and horizontal and vertical fin orientations. Their work suggests, "… the evaporator coil will collect significant amounts of aerosol in the particle size range of 5 – 100 µm." While both of these works contribute significantly to our understanding of coil fouling, there is still a gap in the literature of our understanding of the mechanisms that lead to coil fouling as well as a lack of particle size resolved experimental data of deposition on a typical fin and tube heat exchanger.

The experimental work was designed to validate a model of particle deposition. The purpose of this model is to predict particle deposition depending on particle size, air flow rate, and fin/tube geometry. The model includes both aerodynamic and particle/surface interactions. The model is discussed in detail in the attached report: "Fouling of HVAC Fin and Tube Heat Exchangers" LBNL 47668.

More detailed information can be found in two papers that are attached to this report (LBNL 47668 and 47669). The energy implications of fouling and additional modeling and experimental work is described in a paper for the ACEEE 2002 conference (Siegel et al. LBNL 49757).

Typical heat exchangers in residential HVAC systems consist of horizontal refrigerant tubes with attached thin vertical fins to increase heat transfer. The heat exchangers have two staggered sets of 0.95 cm (3/8 inch) copper refrigerant tubes that run horizontally through vertical aluminum fins. Commercial and industrial systems can have much larger tubes. Fin spacings range from 2.4 to 7.9 fins/cm (6 - 20 fins/inch or FPI), with typical systems having 4.7 fins/cm (12 FPI). The fins are approximately 100 µm thick and are often corrugated to increase surface area for heat transfer. Heat exchanger depth can vary, but typical residential and small industrial and commercial heat exchangers are about 5 cm (2 inch) thick and are often grouped together for larger capacities. Air velocities range from 1 to 5 m/s (197 – 984 ft/min) in these systems.

Monodisperse particles, tagged with fluorescein, are generated with a vibrating orifice aerosol generator and then charge

neutralized. The particles are mixed with a HEPA filtered air stream designed to eliminate ambient particles, and sent into 24 m (80 ft) of straight 15 cm (6 inch) square duct. A schematic of the apparatus is shown in Figure 6, and a photograph of the apparatus is shown in Figure 7.

The duct air velocity can be varied continuously over the 1 - 5 m/s (197 - 984 ft/min) range of interest. The tested heat exchanger is similar those used in residential and small commercial applications. Several honeycomb flow straighteners are used to promote fully developed turbulent flow with a uniform concentration of test particles. The particle-laden air then passes through an experimental evaporator, which consists of a 4.7 fin/cm (12 FPI) coil that entirely fills the duct.

Particle air concentrations are measured up and down stream of the duct by isokinetically sampling the air onto filter paper, which is later subjected to fluorometric techniques to determine the particle air concentrations. Isokinetic sampling means that the air samples are drawn out with a pump from a sample tube pointing directly into the air flow. The sample flow is controlled so that the velocity of air entering the sample tube is the same as the air velocity in the duct. This ensures that our measured particle concentrations are the same as those seen by the coil and the sampling procedure does not disturb the flow. A confirmation of the deposition results is made by removing the test coil from the duct and extracting the deposited particles with a buffer solution and using fluorometric techniques to determine the mass of deposited particles. In order to better understand the deposition mechanisms that lead to the accumulated material on the coil, a coil extraction technique was developed that allowed separate measurement of the material on the leading edge from material in the core of the coil.

The air flow in the duct needs to be known in detail, so pitot tube velocity measurements are made at many locations across the cross section of the duct at several stations along the duct.

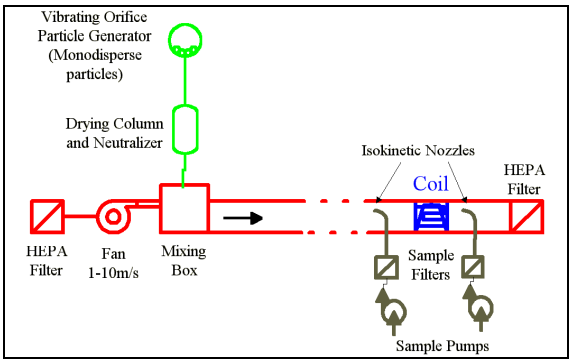

Figure 6. Schematic of Coil Fouling Test Apparatus.

Figure 7. Illustration of Coil Fouling Apparatus showing the Duct and Particle Samplers

The fouling results for a single velocity appear in Figure 8. The horizontal error bars represent one standard deviation in particle diameter for a given experiment and vertical error bars indicate experiment uncertainty calculated from an analysis

based on standard error estimates and confirmed with experimental repetitions. Deposition plots for additional velocities are given in LBNL 47668 and 47669.

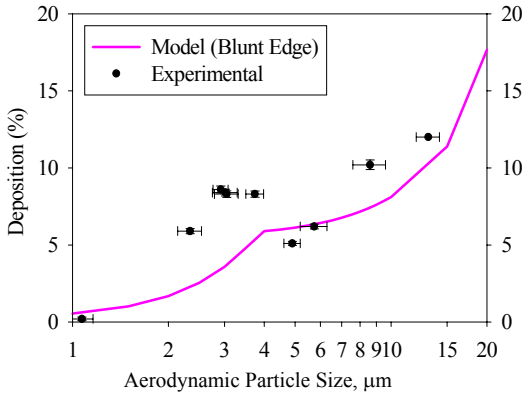

Figure 8: Experimental and Modeled Deposition for 1.5 m/s (295 ft/min)

The results depicted in Figure 8, suggest that increasing particle size leads to increased fouling. The results also indicate that for particle sizes up to about 20 µm particles, increasing velocity leads to increasing deposition. The dip for 4-5 µm particles in Figure 8 is not well understood, but is repeatable, and suggests an anomaly in particle mixing. These results suggest that impaction is an important deposition mechanism for 2-20 µm particles. The experimental results agree reasonably well with the model of the system.

In addition to measuring how many particles deposit in the system, we also investigated the effect they have on pressure drop of the coil. An experiment was performed using the same apparatus described in Figures 5 and 6, but the particles used were a standard test dust (SAE coarse) rather than the fluorescent liquid particles. Details of these experiments are given in Appendix D. An example of the experimental results for solid dust particles is given in Figure 9. This figure shows how the coil pressure drop increases relative to the pressure drop for a clean coil. A relative pressure drop of 2 means that the dirty coil has twice the pressure drop of the clean coil. The results suggest that rate of coil fouling increases with the amount deposited on the coil. As the coil becomes more fouled it is better at filtering out particles from the air stream, resulting in an increase in deposition rate. The majority of the fouling that caused pressure drop was due to build-up on the leading edge of the coil, which suggests that regular mechanical cleaning of the exposed face of the coil may be a useful strategy to minimize the effects of coil fouling on pressure drop.

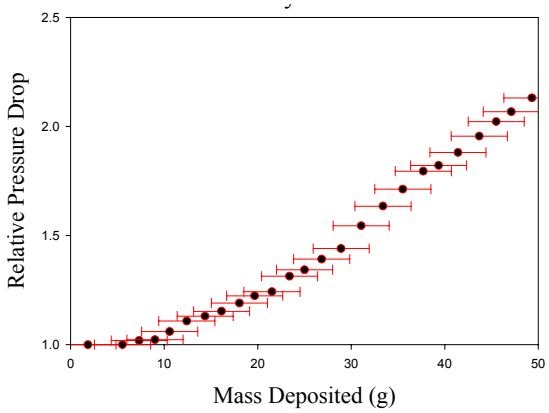

Figure 9: Experimental deposition for 2 m/s (393 ft/min). Horizontal error bars indicate uncertainty in the mass deposited on the coil

These experimental results can be combined with information about indoor dust and particle concentrations and filtration are known, to determine the fouling rate and the resulting pressure drop. We obtained some dirty coils and have begun to perform visual and chemical analysis. The analysis of the matter from these coils will be used to verify that the laboratory experiments are using the appropriate size of particle because this is a critical parameter for coil fouling. Our original focus was on particles in the 1-10 µm range. Smaller particles in the range of 0.1 to 1µm are typical of those found in Environmental Tobacco Smoke (ETS), whereas larger particles (10 to 100 µm) are more typical of household dust.

Cooled Coil Effects

Air conditioning coils often serve to condense water and thus dehumidify the air stream. Additional experiments are currently being done to quantify the effect of

cooling on particle deposition, preliminary results of this work appear in Figure 10. Cooling is expected to enhance deposition through three phenomena: thermophoresis, the motion of particles down temperature gradients, diffusiophoresis, the motion of particles towards a condensing surface, and impaction on condensed moisture that has not yet drained off the coil. Figure 10 shows the results of a cold (air-to-surface temperature difference of 6 °C (11 °F)), but not condensing coil for 8 and 12 µm particles. The results suggest that thermophoresis enhances deposition slightly more than the model predicts. The two cooled and condensing experiments a 9.5 µm suggest that condensation dramatically increases deposition. The lower point had condensation on the coil for approximately half of the experiment, the upper point had deposition for the entire experiment. These results suggest that impaction on condensed water is the dominant deposition mechanism for a cooled coil and that a coil that is condensing water makes an extremely good filter. These results should be considered preliminary until deposition on cooled coils for smaller particles is performed.

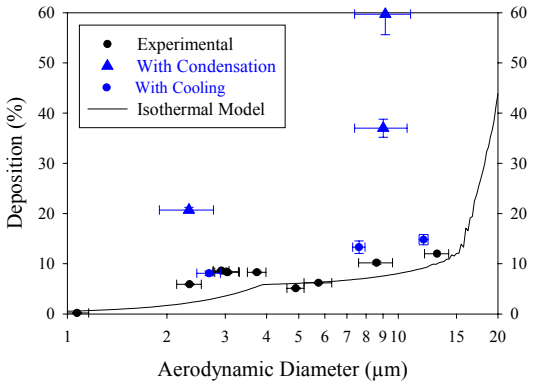

Figure 10. Comparison of isothermal coil deposition to cooled coil deposition

Fouling Agents

Optical and electronic microscopy methods were used to determine the nature of the particles that cause fouling. One caveat with these results is that only the material on the leading edge of coils can be examined. Two example pictures from the same evaporator, shown below in Figures 11 (optical microscope) and 12 (electron microscope), show images of typical fouling agents.

These figures show that many fibers deposit on the leading edge. The fibers are typically quite long (i.e. on the order of mm to cm), and are in some cases very small in diameter (<10 µm). This, as well as their color on the optical microscope (Figure 11), suggests that they are likely to be carpet or clothing fibers. The microscopic scans indicate that in addition to long fibers, smaller particles in the rage of 1-30 µm also deposit. Many smaller, more spherical, particles collect on the fibers and on the coil as well. Chemical analysis (done using x-ray diffraction techniques on an electron microscope) suggests that almost all of the material on most residential coils is household dust (chemically consisting mostly of carbon and silicon).

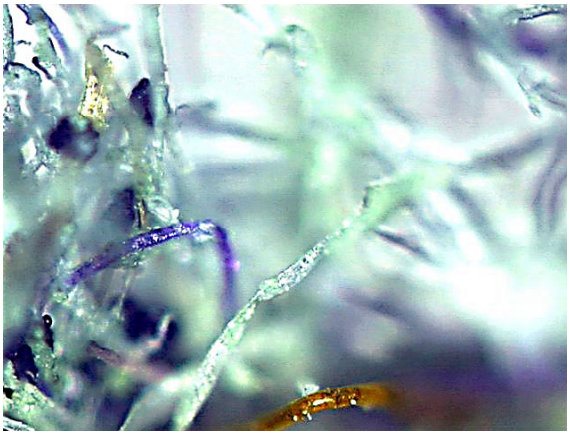

Figure 11. Optical microscope image of material from the coil leading edge

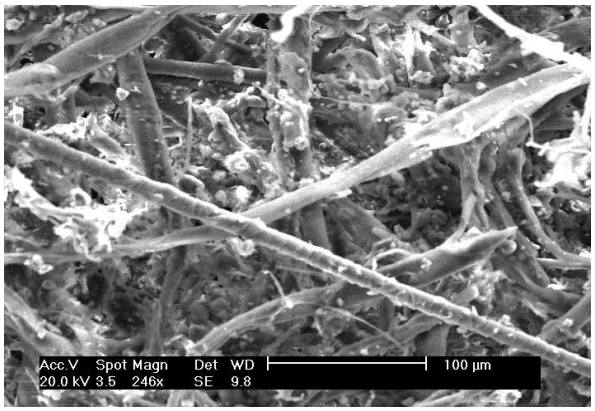

Figure 12. Electron microscope image of material from the coil leading edge

Energy Implications of Fouling

There are two potential energy impactions of fouling. The first is a reduction in heat transfer because the coil is coated with a layer of the fouling agent. Fin heat transfer analysis, as well as the fact that a large amount of fouling material collects on the leading edge and at fin discontinuities in the coil (i.e. locations unimportant for heat transfer), suggest that this is relatively unimportant energy consequence. This was confirmed by Krafthefter and Bonne (1986) who suggest the change in heat transfer due to the insulating effects of the fouling layer are about an order of magnitude less than the change in heat transfer due to the reduction in airflow that results from an increased pressure drop. There has been considerable research on how reduced flow affects air conditioner performance (Proctor and Parker (2000), Palani et al. (1992). This research suggests that fouled coils lead to reduced sensible capacity. The effect on air handler performance is less clear because it depends on the efficiency and pressure-flow relationships of the air handler. The range of fouling can be great, and work is still ongoing to determine typical fouling rates, but a scaling analysis suggests that 5-20% capacity degradations for an evaporator that has been in service for 5 years are typical. Efficiency (EER) reductions are much smaller, ranging from 1-10% for most of these systems. This result is consistent with results in Krafthefter and Bonne (1986).

Solutions to Fouling

Frequent washing of coils is often cited as the suggested method for cleaning coils (e.g., Turpin, 2001). There are several problems with this approach. The first is that the cleaning agents are often very acidic or very basic (pHs of 1 or 13 are typical) and have the potential to irritate or injure technicians as well as building occupants. Additionally, the byproducts of cleaning can often remain in the system causing further health and safety problems. A third problem is that residential evaporators are often located in hard to reach and inspect areas – most homes probably have fouled coils without their occupants even knowing. A much better approach to mitigating coil fouling is the proper use of filtration. Much of the particulate matter that responsible for fouling is made up of large dust particles that are filtered easily by even a low efficiency filter (i.e., a MERV 6 filter used to comply with ASHRAE 62.2). The problem comes from filter bypass – air that bypasses the filter because of incorrect filter size, poor filter installation or return duct leakage between the filter and the coil. Although filter bypass has not yet been addressed by the technical community (ASHRAE standard 52.2 for filter efficiency does not address it, for example), it is a common problem, as shown in the following photographs.

Also, a coil fouling webpage has been set-up at: http://epb.lbl.gov/coilfouling.

Figure 13. Filter bypass examples: filter wrapped around fan, bag bypassed filter into fan blades, wrong size filter forced into filter slot (the first photograph is from Paul Francisco of Ecotope)

Task 6. Duct Fittings Survey and Performance Testing

We have completed the laboratory testing of a large range of duct fittings and plastic flexible ducts. A total of about 50 different configurations were tested and for each configuration a large range of flows and pressure drops were measured. The measurements have been analyzed to reduce the multiple pressure and flow measurements to loss coefficients comparable to those used in standard duct design practice. The results are summarized in report LBNL 49293. A key result is that the compression effects on flex duct flow resistance are much more significant than indicated by the estimating techniques published by ASHRAE and ACCA. A simple algebraic algorithm has been developed that duct designers and installers can use to estimate the effects of flex duct compression. A draft paper titled "Compression Effects on Pressure Loss in Flexible HVAC Ducts" by Abushakra, Walker and Sherman has been prepared for submission to ASHRAE as a technical publication. We intend to follow-up this paper with recommendations to the relevant ASHRAE technical committees to make appropriate changes to the ASHRAE Handbook of Fundamentals.

A new full-scale duct system test laboratory was constructed at LBNL to evaluate the pressure drop of residential duct system components that are either not available or poorly described in existing duct design literature (for instance, ASHRAE Fundamentals, and ACCA Manual D). The design is based on the CSUC field survey of 20 California duct systems. The prototype system is illustrated in Figure 14. The tests were designed to examine cases normally found in typical residential and light commercial installations.

The study was divided in two parts: individual component analysis and complete system analysis. The component analysis included three different sizes of flexible ducts under different compression configurations and different bending angles, splitter boxes, supply boots, and a fresh air intake hood. The experimental tests followed the proposed ASHRAE Standard 120P – Methods of Testing to Determine Flow Resistance of HVAC Air Ducts and Fittings. The complete system analysis included the calculation of total pressure drop in the supply section of a typical residential air distribution system, based on the pressure drop results from the component analysis. The calculations were

compared with calculations based on available literature (ASHRAE Fundamentals and ACCA Manual D). These calculated pressure drops were compared to the measured system pressures.

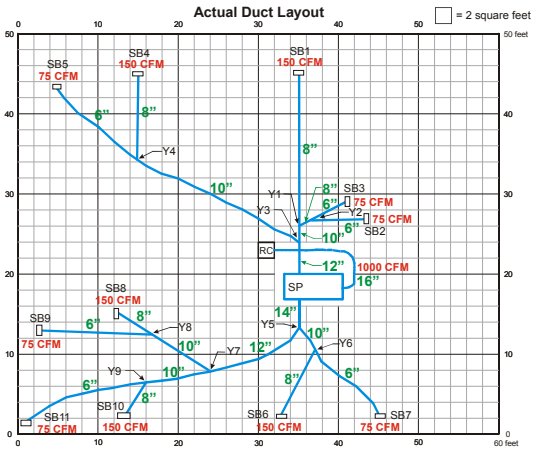

Figure 14. Prototype Duct System for Laboratory testing

Individual Component Analysis

Experiments were performed on fully stretched and compressed ducts of 6 inch (0.15 m) , 8 inch (0.2 m) and 10 inch (0.25 m) diameter, in both straight and bent configurations. A pressure drop correction factor, PDCF, was developed to account or compressibility effects. The PDCF mulitplies the pressure drop for fully stretched uncompressed duct to find the pressure drop for the compressed case. The PDCF is a function of the geometry of the duct and the compression ratio. A simple empirical relationship was developed to allow easy calculation of PDCF, using and simple compression ratio (CR) multiplyer:

$$PDCF = Y \times CR$$

The CR is the amount of duct compression, e.g., for a duct 30% shorter than fully stretched, C.R. = 0.3. Y was determined by fitting to measured data, and has the value of 25, 21 and 16 for 6 inch (0.15 m) , 8 inch (0.2 m) and 10 inch (0.25 m) diameter ducts respectively. Further analysis has shown that the empirical coefficient is a function of the pitch to diameter ratio of the metal wire spiral in the inner flex duct liner. Y can be approximated by multiplying the pitch to diameter ratio by a factor of 100. These simple empirical predictors of PDCF are within 3% of the measured values, which is close to the experimental measurement uncertainty limit, so more complex PDCF calculation methods cannot be justified. These results are illustrated in Figure 15, that shows both measured and predicted PDCF values. Further testing is required to confirm the universality of this empirical correlation including pitch to diameter ratio, but the good results achieved in this study by using these techniques is encouraging.

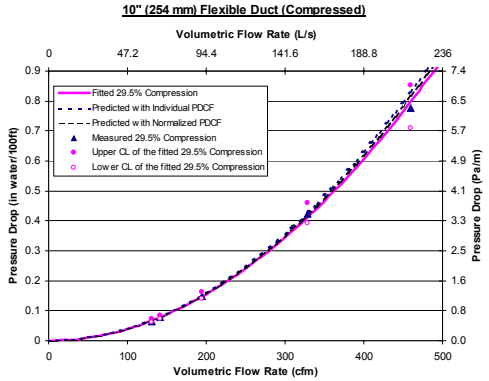

Figure 15. Comparison between measured, power-law-fitted, and predicted pressure drop with PDCF models in a compressed 0.25 m (10") diameter flexible duct

The results also showed that ASHRAE Fundamentals and ACCA Manual D underestimate the pressure drop in compressed flexible ducts. The ASHRAE calculations underestimate the PDCF by about 35% and the ACCA calculations do not account for different compressibilty effects (however, our test results show that the flex duct flow resistance values given by ACCA correspond to partly compressed ducts). The laboratory experimental work showed that the test procedures in proposed ASHRAE Standard 120P should be changed. In the proposed standard the duct specimen is attached by clamping the outer jacket. Our experiments showed that this can lead to an unknown (but significant) amount of inner liner compression. To avoid this potentially confusing problem, we recommend that the tests be performed with

the inner liner clamped to the end collars so that inner liner compression can be correctly accounted for.

Three bending angles were tested for flexible duct: 45°, 90° and 135°. Each of the bending configurations was tested with the duct under moderate and extreme compression (around 5% and 30% C.R., respectively). The local loss coefficients values of these "elbows" varied between 0.8 and 3. These loss coefficients are about four times the published values for equivalent sheet metal elbows.

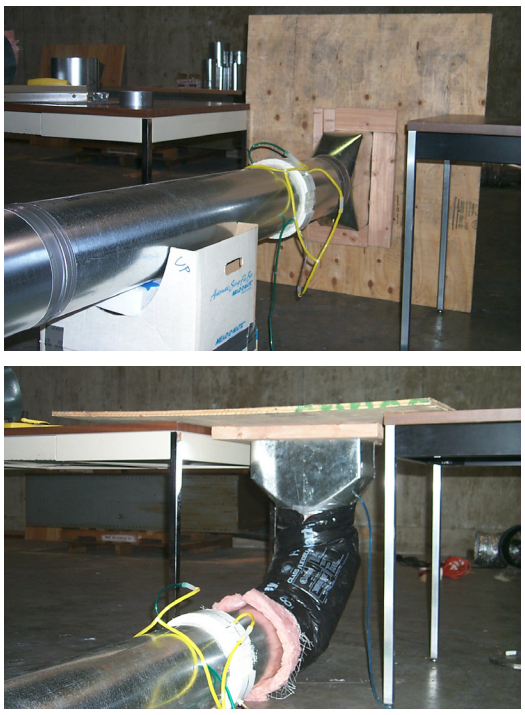

Figure 16. The 0.15 m (8") Straight Supply Boot tested under different configurations: a straight setup, and an angle setup with the flexible duct as an integral part of the boot

Figure 16 illustrates the experimental apparatus used to measure supply boot performance. Supply boot loss coefficients were determined for several configurations including a setup where the flexible duct elbow connection was considered an integral part of the supply boot. The supply boots results showed that diffusers have a major effect on the pressure losses in exit fittings. The diffuser can increase the pressure drop by factors between 0.15 and 2.0, depending on the configuration of the boot connection and the geometry of the diffuser. For a boot with an 8" (0.20 m) intake the loss coefficient is 3.0 without diffuser and 3.8 with diffuser. Additional measurements were made with 90° flex duct elbows connected to the registers boots because this is a common configuration found in new construction. This configuration had pressure drops about 3 and 4 times those of the boot alone. This result indicates that care must be taken to include the details of connections to register boots in pressure drop calculations.

Duct board splitter boxes are commonly used in new California duct systems in place of traditional tees and wyes. These splitter boxes have a triangular plan with a duct connection to the approximate center of each face. Under normal operation one connection is an inlet and the other two are outlets. To evaluate this effect, three sizes of splitter boxes were tested. The splitter box tests used a range of total flows and a range of exiting flow ratios for the two exiting ducts. The results showed that the local loss coefficient through a branch of the splitter box could vary between 0.5 and 6.3 depending on geometry and flow ratios. A typical result is 0.9 and 1.7 for the smaller and the larger branch of a 10"/8"/6" splitter box, respectively, when the flow is balanced. The loss coefficients are within the same range as those given in ASHRAE Fundamentals for rectangular tees and wyes. ACCA Manual D provides pressure drops for splitter boxes in terms of equivalent length (EL), independent of size. We found that the ACCA values tend to slightly overestimate the pressure losses for splitter boxes.

One outside air intake hood was tested. The hood includes a screen and the entering air is parallel to the exterior wall of the building then turns 90^{o} into the fresh air duct. The local loss coefficient of the intake hood was 4.1; a substantial factor in the pressure drop to be considered when designing the ducting system. Much of this pressure drop will be

across the screen as shown in the ASHRAE Fundamentals handbook, where a screen has a loss coefficient between 0.0 and 6.2, depending on the free area ratio of the screen. ASHRAE also gives a loss coefficient value of 0.5 (duct flush with wall) for a "Duct Mounted in Wall".

Complete Duct System

The complete system analysis consisted of calculating the total pressure drop in the supply section of the air distribution system, based on the pressure drop results from the component analysis. The installed system consisted had two main supply branches, and pressure drop estimates were made for both branches. The measured supply plenum static pressure for the two branches was 32.5 Pa (0.130 in. water) and 42 Pa (0.168 in. water). The calculations using the results of our component analysis produced static pressure differences that were reasonably close to these results: 30.5 Pa (0.122 in. water) and 42 Pa (0.168 in. water), respectively. For comparison (using the closest tabulated fittings to those in our system), the ACCA calculations produced static pressures of 30.5 Pa (0.122 in. water) and 48 Pa (0.191 in. water) and the ASHRAE calculations gave results of 21 Pa (0.085 in. water) and 31 Pa (0.123 in. water). One reason for differences between the predicted pressures and the measured pressures is that the full-scale duct system included large diameter flex duct whose flow resistance was estimated by extrapolation. Probably of greater significance is that the individual component measurements have considerable distances upstream and down stream of straight uninterrupted flows, but the complete system has the fittings closely spaced. Therefore, the complete system will have many non-uniform flows through its components, resulting in changed pressure losses.

HVAC system air flow measurements

The full scale duct system facility has also been used to evaluate and improve a wide range of duct system flow measurement techniques. In collaboration with our CEC Commissioning project, we have determined that commercially available flowhoods tend to be extremely sensitive to non-uniformity of register flows, with uncertainties greater than 20% (and substantially larger for some flow hoods). The majority of these measurement errors are due to flow non-uniformity entering the flow capture device and to flow hood back pressure effects. The extra flow resistance of the flow hood significantly reduces the flow through the branch of the system that is being measured. The only flow hood to provide consistently good results (with an accuracy of about ±2%) is a powered flow hood. Automated software has been developed that makes the powered flow hood technique more repeatable, improves quality control, and reduces the time required to perform the measurements. The powered flow hood tests were repeated using several balancing pressure measurement locations, and these tests showed RMS changes in the individual register flows of only 2 to 3 cfm and less than 2% average difference depending balance pressure location. We are continuing our collaboration with at least one manufacturer of flow hoods to examine methods to improve passive flow hood performance. It is clear from our test results that some sort of standard for measuring residential register flows is required so that different flow hoods can be evaluated. Either ASTM or ASHRAE would be suitable venues for developing this test/evaluation procedure.

In conjunction with our CEC Commissioning Project, a prototype simple and inexpensive flow meter for measuring register flows has been developed. Prototype flow meters have been built for both supply and return air flows. Laboratory tests have shown that a single point measurement is sufficient for the return air flow meter but multiple point measurements are required for supplies. These multiple points are obtained by changing the flow

resistance of the flow meter and extrapolating to the flow that would occur at the register with no added flow resistance. Results from our testing this new flow meter in the laboratory and five houses (33 registers in total) indicated that the RMS difference between the experimental flowmeter and our reference flow meter is about 6%, with the experimental flowmeter slightly underpredicting by about 2%, on average. Some simple analytical techniques have been developed that eliminate almost all the bias, however, the RMS uncertainties still remain. These remaining uncertainties are due to sensitivity to flow patterns, extrapolation errors and operational errors, such as having leaks around the base of the flowhood when holding it against the wall or floor containing the register. This is an excellent result compared to RMS errors greater than 20% for commercially available devices. For measuring commercial registers with higher flows, we found that the original design has too much flow resistance resulting in negative biases of about 5%, and RMS uncertainties of 14%. Future work will examine the possibility of creating a lower resistance flow meter for commercial field testing. More details regarding the development of these new register flow meters can be found in Appendix B.

The flowhood tests are summarized in the report "Evaluation of flow hood measurements for residential register flows" (LBNL 47382).

Task 7. Improved Energy Efficiency Modeling

Recent events (high energy prices leading to State of California AB970 legislation on peak demand reduction) changed the emphasis of this task: to provide technical support to the California Energy Commission on changes to Building Efficiency Standards (T24) and Appliance Standards (T20). This effort has included reviewing and analyzing potential changes to T24, making suggestions for potential changes and attending CEC meetings in Sacramento in order to keep track of T24 activities. As part of the same work, we have also contributed to improved energy efficiency requirements for appliances in T20.

We have coordinated our activities on this task with another project sponsored by CEC to determine the time value of energy for use in future T24 calculations. After several meetings and consultation with Bruce Wilcox (Berkeley Solar Group) and Mark Modera (Modera Consulting Engineers), it has become clear that the original proposal to use minute-by-minute simulations is too complex and provides results that are too intractable for this application.

We performed a literature review of over 100 papers on the thermal performance of garages, crawlspaces and basements to determine how best to treat them in a combined ventilation and heat transfer model. Unfortunately, there is not much existing research specific to this issue, however, we will be able to construct general prototypes for the simulation modeling. We completed the necessary modeling to simulate cathedralized attics and verification of model performance is almost complete. We completed the verification of model performance for cathedralized attics (see Task 1 results).

We attended Natural Resources Defense Council (NRDC) "Future of T24" meetings to discuss how thermal distribution systems will be treated in future T24 standards.

Our development work on REGCAP continued by performing more comparisons with field measurements as part of our validation and evaluation program. These validation exercises have shown a couple of areas of improvement for input data. One area is the radiation heat transfer characteristics of roofing surfaces. The attic air temperatures are sensitive to the values chosen for emissivity and absorbtivity of the roof surfaces. We are working on developing a list of roofing materials and

their radiation parameters for use in REGCAP. Linked to this radiation problem is the poor representation of cloud cover in weather data files. This has been found to be important because cloud cover determines the long-wave radiation from the roof, and this is particularly important at night when calculating the effect of radiation to the night sky. We are looking at ways of making better estimates of cloud cover. Lastly, the thermal mass of the house has a strong impact on the time response of the indoor air temperatures and, therefore, on heating and cooling system operation. In the future, we will investigate methods of improving the modeling of thermal mass within REGCAP.

Task 8. Field Research on Duct Systems in Older Homes

LBNL trained CSUC staff to perform duct leakage and fan flow measurements that were used in a survey of existing homes. For more details of measurement protocols and preliminary results, see the CSUC quarterly reports (CSUC 2000).

We evaluated a new fan flow measurement technique that is close to being commercially available. This new technique uses a multi-orifice flow plate in place of the air handler filter (corrected for system pressure changes) to determine flow through the system. Preliminary results indicate that for many systems this will be an accurate and quick way to measure flow. The only major drawbacks of this new technique revolve around applications rather than technical issues. For example, many new systems in California do not include a filter slot, and it can be difficult to find a suitable location in the duct system to insert the flow plate. While in Minneapolis for the ASHRAE summer meetings, we attended an open house hosted by the manufacturer of this new device where it was demonstrated on the air handler system in their office/factory. We are also collaborating with this manufacturer on the automation of the DeltaQ testing, measurement of register flows and other methods of making field testing quicker, simpler and more accurate for practitioners.

In conjunction with the LBNL residential commissioning project, we gave presentations at PAC meetings and for CEC commissioner Rosenfeld (and other CEC staff) in Sacramento that showed how this work is using field tests and setting norms for house performance.

References

Anonymous. 1987. Real-Life Residential Air Conditioning, *Refrigeration Service Contractor*, October 1987, pp. 24-26.

ASHRAE Guideline 2-1986 (RA 90), 1990, *Engineering Analysis of Experimental Data*, ASHRAE, Atlanta, GA, p. 4.

CSUC 2000. HVAC Residential Project, Quarterly report #1 and #2. California State University Chico. Chico, CA.

Krafthefter, B., and Bonne U., 1986, Energy Use Implications of Methods to Maintain Heat Exchanger Coil Cleanliness, *ASHRAE Transactions 1986*, American Society for Heating Refrigeration and Air-Conditioning Engineers, Atlanta, GA, Vol. 92(1b), pp. 420-431.

Muyshondt, A., Nutter, D. and Gordon M., 1998, Investigation of a Fin-and-Tube Surface as a Contaminant Sink, *ASHRAE IAQ '98*, American Society for Heating Refrigeration and Air-Conditioning Engineers, Atlanta, GA, pp 207-211.

Neal, L., 1992, Air Conditioner Efficiency in the Real World, *Home Energy*, May/June 1992, pp. 32-39.

Turpin, J., 2001. Clean those evaporators before they get foul, *The Air Conditioning News*, forthcoming article in November 19, 2001 issue.

Walker 1998. Walker, I., Sherman, M., Modera, M. and Siegel, J. Leakage Diagnostics, Sealant Longevity, Sizing and Technology Transfer in Residential Thermal Distribution Systems. LBNL 41118.

Walton, G.N. 1997. "CONTAM96 User Manual". NISTIR 6056. U.S. Department of Commerce, National Institute of Standards and Technology, Building and Fire Research Laboratory. Gaithersburg, Maryland. ftp://ftp.nist.gov/pub/contam/. September.

Technology Transfer

Papers/Reports

Abushakra, B., Walker, I. and Sherman, M. 2002. "A Study of Pressure Losses in Residential air Distribution Systems". ACEEE Summer Study 2002 (in Press). LBNL 49700.

Sherman, M.H., Walker, I.S. and Dickerhoff, D.J. 2000. "Stopping Duct Quacks: Longevity of Residential Duct Sealants". Proc. ACEEE 2000 Summer Study. Vol. 1, pp. 273-284. American Council for an Energy Efficient Economy, Washington, D.C. LBNL 45423.

Siegel, J., Walker, I. and Sherman, M. 2000. "Delivering Tons to the Register: Energy Efficient Design and Operation of Residential Cooling Systems". Proc. ACEEE Summer Study 2000. Vol. 1, pp. 295-306. American Council for an Energy Efficient Economy, Washington, D.C. LBNL 45315.

Walker , I.S., and Sherman, M.H. 2000. "Assessing the Longevity of residential Duct Sealants", Proc. RILEM 3rd International Symposium: Durability of Building and Construction Sealants, February 2000. pp. 71-86. RILEM Publications, Paris, France. LBNL 43381.

Walker, I.S., Siegel, J.A., Degenetais, G. 2001. "Simulation of Residential HVAC System Performance". Proc. ESIM2001 Conference, pp. 43-50. CANMET Energy Technology Centre/Natural Resources Canada, Ottawa, Ontario, Canada. LBNL 47622.

Siegel, J.A., Walker, I.S. 2001. "Deposition of Biological Aerosols on HVAC Heat Exchangers" Proceedings of ASHRAE IAQ 2001, ASHRAE, Atlanta, GA. LBNL 47669.

Siegel, J.A., Walker, I.S. and Sherman, M.H. 2002. Dirty Air Conditioners: Energy Implications of Coil Fouling. ACEEE

Summer Study 2002 (in press). LBNL 49757.

Siegel, J.A., and Carey, V.P. 2001. "Fouling of HVAC Fin and Tube Heat Exchangers". Proceedings of the United Engineering Foundation Conference on Heat Exchanger Fouling 2001. LBNL 47668.

Walker, I.S., Sherman, M.H., Wempen, J., Wang, D. McWilliams, J.A. and Dickerhoff, J.D. (2001). "Development of a new Duct Leakage Test: DeltaQ". LBNL 47308.

Walker, I.S. and Wray, C.P. 2001. "Evaluation of flow hood measurements for residential register flows". LBNL 47382.

Walker, I.S., Degenetais, G., and Siegel, J.A., "Sizing and Comfort Improvements for Residential Forced-Air Heating and Cooling Systems". LBNL 47309.

Walker, I.S., Dickerhoff, D.J. and Sherman, M.H., 2002. The DeltaQ Method of Testing the Air Leakage of Ducts. ACEEE Summer Study 2002 (in press). LBNL 49749.

Wray, C.P., Walker, I.S. and Sherman, M.H., 2002. Accuracy of Flow Hoods in Residential Applications. ACEEE Summer Study 2002 (in press). LBNL 49697.

Draft publications:

Abushakra, B., Walker, I.S. and Sherman, M.H., 2002. "An Experimental Study of Compression Effects on Pressure Loss in Flexible HVAC Ducts". Submitted to ASHRAE. LBNL 49012.

Siegel, J.A., McWilliams, J.A., and Walker, I.S. 2002. "Field evaluation of proposed ASHRAE Standard 152P for Cooling Systems in Standard and Unvented Attics". Submitted to ASHRAE. LBNL 50008.

Walker, I.S., Wray, C.P., Dickerhoff, D.J., and Sherman , M.H., "Advances in Residential Flow Hoods to Measure Residential Register Flows" To be submitted to ASHRAE.

Walker, I.S. and Sherman, M.H. 2002. "Sealant Longevity for Residential Ducts". Submitted to ASTM/RILEM Building Sealant Conference. LBNL 50189.

Revision to ASTM E1554 - "Standard Test Methods for Determining External Air Leakage of Air Distribution Systems by Fan Pressurization".

New ASTM standard: "Standard Test Method for Longevity Testing of Duct Sealant Methods ".

Presentations

"HVAC Performance Testing: New Protocols and Techniques" at the Affordable Comfort Workshop in San Ramon, December 2000.

"Field demonstrations of New Protocols and Techniques for Performance Testing of Residences" for Affordable Comfort in a new house in Livermore, CA. December 2000.

"Fouling of HVAC Fin and Tube Heat Exchangers" United Engineering Foundation Conference on Heat Exchanger Fouling, July 2001.

Max Sherman and Iain Walker gave written and spoken testimony at a California Energy Commission Hearing about restricting the use of duct tape as a duct sealant, June 2001.

"Ducts in New Construction" for CABEC, May 2001.

Other Activities

A coil fouling webpage is available that summarizes our work: http://epb.lbl.gov/coilfouling

We attended Natural Resources Research Council (NRDC) "Future of T24" meetings to discuss how thermal distribution systems will be treated in future T24 standards.

Technical support to the California Energy Commission on changes to Building Energy

Efficiency Standards (T24) and Appliance Standards (T20).

In conjunction with the LBNL PIER residential commissioning project, we gave presentations at PAC meetings and for CEC commissioner Rosenfeld (and other CEC staff) in Sacramento, that showed how this work is using field tests and setting norms for house performance.

LBNL trained CSUC staff and Rick Chitwood (Chitwood Energy Management) to perform duct leakage and fan flow measurements that were used in a survey of existing homes.

Max Sherman was interviewed by CNN regarding our work on duct sealants, May 2001.

Iain Walker was interviewed by the Canadian Newspaper the “National Post” for an article on duct sealants, May 2001.

Appendix A. Repeatability evaluation of the DeltaQ test with changing duct leakage configurations

Introduction

This study evaluates two aspects of the DeltaQ duct leakage test: the repeatability and the accuracy. It continues the repeatability testing that has already been carried out by LBNL (Walker et al. 2001). The repeatability testing was expanded in this study to include several added leakage configurations in addition to the baseline leakage of the system. The accuracy of the DeltaQ test was examined by adding monitored leaks to the system such that the flow through the leaks can be measured precisely. The DeltaQ estimated leakage can then be compared to these carefully monitored added leaks. A refined analytical analysis was also examined that will reduce the time required to perform the test and make the test simpler by eliminating the task of measuring plenum pressures.

Test Setup

The study was performed in a laboratory facility at LBNL in Berkeley, CA. The laboratory building is a single-story structure of about 1200 ft^2 (111 m^2) with two forced air heating and cooling heat pump systems. All the tests in this study were performed on one of the forced air systems, with the other inoperative. The particular HVAC system under study had a total fan flow of 1000 CFM with four supply registers and a single return. The system as-is was relatively well sealed with about 1.5% supply leakage and 1.9% supply leakage (expressed as fractions of fan flow). Because the tests for DeltaQ accuracy add known leaks to the system it is important to have small background leakage in order to reduce the uncertainty in the sum of the background and added leaks when comparing to the DeltaQ results.

The leaks were added by deliberately ducting register flow to outside through the envelope of the building. Figure A1 is a schematic illustrating how the air is ducted to outside for this experiment.

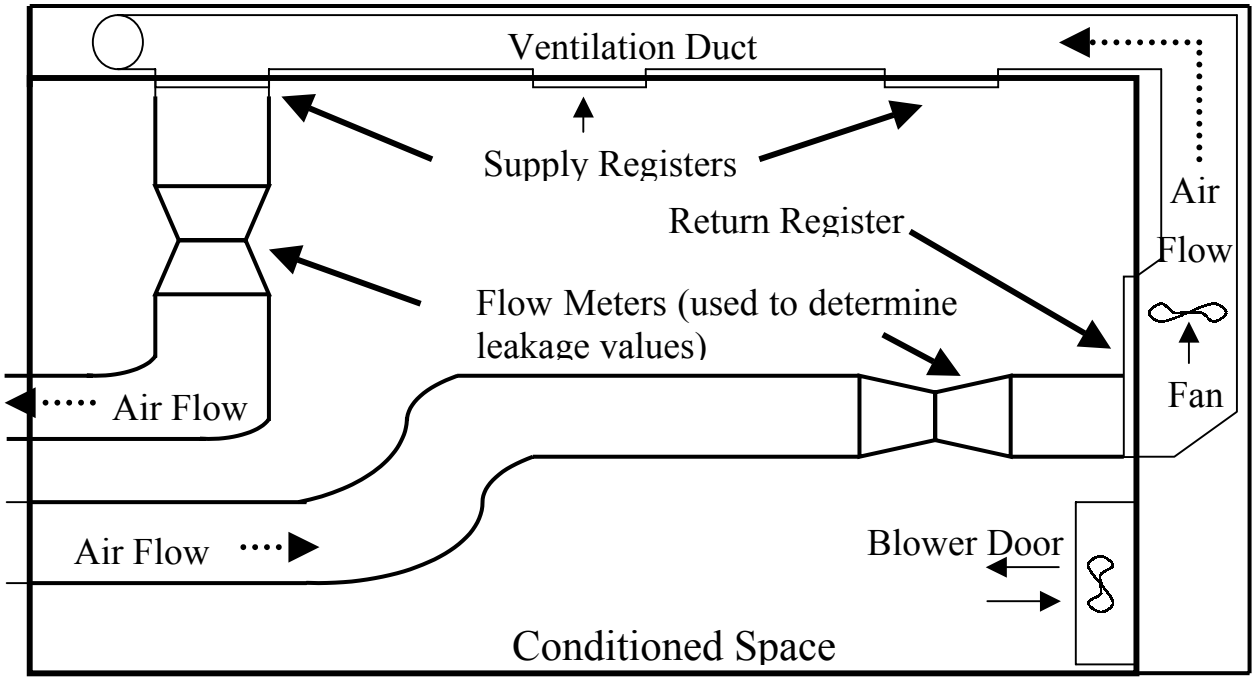

Figure A1. Schematic of added leakage through ducting to outside experiment

Figure A2 shows how spiral flex duct was attached to one of the ceiling registers. The flex duct was attached to a collar that was mechanically fastened to the register grille with sheet metal screws and sealed using pressure sensitive tape.

Figure A2. Flex duct connection to ceiling supply register

Panels were inserted into window openings in order to allow ducting to outside. A fan flowmeter was placed in-line with the flexible duct in order to measure the air flow through the duct. Figure A3 illustrates how the ducting passes to outside through a panel and the location of the inline fan

flowmeter. The fan flowmeter was calibrated in an LBNL calibration facility to have an accuracy better than ±3% of measured flow. The ducting was very carefully sealed to eliminate any air flow that might bypass the flowmeter. With the system on, the pressure drop across the flow meter was recorded and the corresponding flow was calculated using calibrations developed by LBNL. The flowmeter uses different sized orifice plates for different flow ranges, with smaller openings being used at lower flow rates. The use of different plates resulted in a range of flows (leakage) though the ducting. Four different leakage configurations were tested: a balanced supply and return leak and three unbalanced supply leaks ranging from large (25% fan flow) to small leakage flows (3% fan flow).

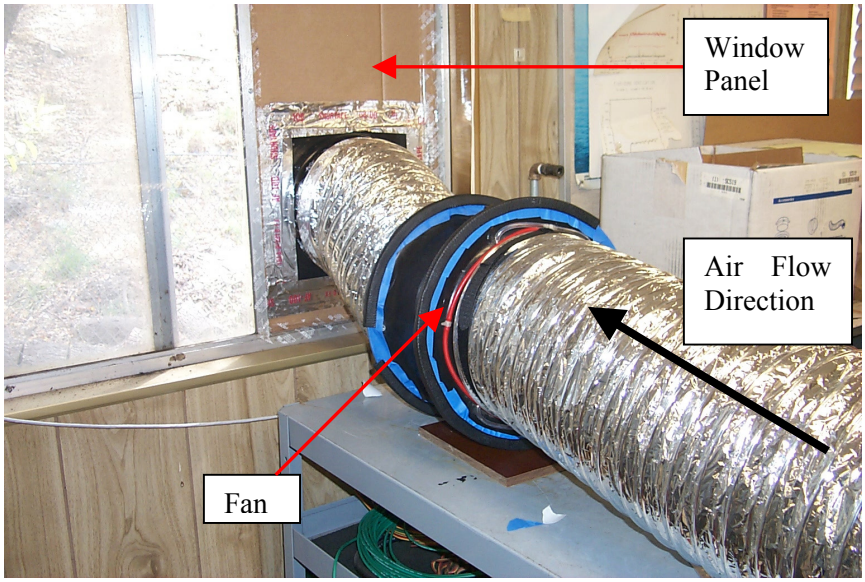

Figure A3. Flex duct connection to window panel and in-line fan/flow meter

Background Duct Leakage

The background duct leakage was measured using the DeltaQ test procedure. The DeltaQ calculation procedure requires characteristic pressures and a pressure exponent. For these background tests half the measured plenum pressures and a pressure exponent of 0.6 were used in the calculation procedure. The operating supply and return plenum pressures were measured at 59.1 and 34.1 Pa, respectively. Thirteen tests were performed on the existing system to establish sufficient background leakage information and to examine the repeatability of the test procedure. Figure A4 shows the variability scatter of the DeltaQ results for the background leakage measurements. The results are also summarized in Table A1 including the standard deviation and 95% confidence interval. Although the variability in the results is a significant fraction of the measured leakage, because this leakage is low, the variability is a very small fraction of the fan flow – from 0.3% to 1.2% (3 to 12 cfm (1.4 to 6 l/s))) depending on the parameter selected. This is an excellent result, however, the sheltered location of the test building and the low on site wind speeds contribute to these stable results and it is expected that the variability would increase for exposed buildings at higher wind speeds. Another issue at these low leakage levels is that the DeltaQ calculation procedure can produce small negative results. This an indicator of the precision of the test because the test procedure cannot resolve with sufficient accuracy leakage flows on the order of 5 to 10 cfm (2.5 to 5 l/s).

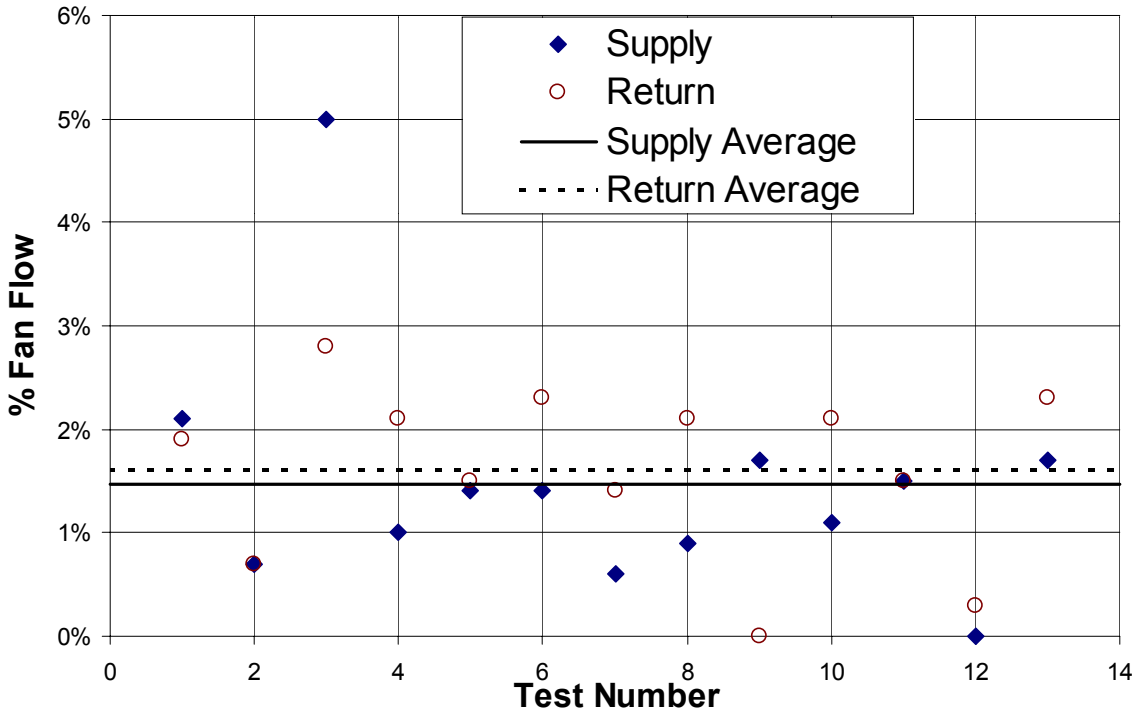

Figure A4. Background leakage and low leakage repeatability individual test results

Table A1. Background Leakage Repeatability: Summary of 13 tests		
	Supply Leakage (cfm)	Return Leakage (cfm)
Average	16	19
Standard Deviation	±11.6	±5.4
95% Confidence Limits	±6.8	±3.2

Testing of Added Leaks

Once the background leakage was established, leaks were installed by routing the airflow to outside from the supply and return grills with flex duct, through a fan/flow meter. This measured leakage flow was added to the initial background leakage to provide an expected new rate of leakage. Each added leakage case was repeated several times to examine the repeatability at different leakage levels. Due to time constraints the number or repetitions was limited to four for case 1, five for cases 2 and 3 and three for case 4.

When these leaks were added, the system operating pressures were changed. The background leakage was adjusted for these changes in operating pressures by assuming that the duct leakage scaled with the measured duct system pressures, using Equation A1:

$$Q_{BG} = Q_o(P/P_o)^{0.6} \quad \textbf{(A1)}$$

The subscript "BG" denotes the corrected background leakage value and "o" the initial operating conditions. The measured additional leakage was added to the corrected background leakage to determine the total system leakage in each configuration.

Four combinations of added leakage were examined:

1. **Large supply and return leakage**: With the system on, flow rates of 208 cfm (98 l/s) and 120 cfm (57 l/s) were measured through the supply and return leaks, respectively. The system plenum pressures were also measured at Ps = 65 and Pr = -29 Pa, indicating a slight change in operating pressures with the leaks installed. In this case, the total leakage flow rate for the supply was Q_s = 208 cfm + 16 cfm $(65/59.1)^{.6}$ = 224 cfm (106 l/s). Likewise for the return, Q_r = 124 cfm + 19 cfm $(29/34.1)^{.6}$ = 141 cfm (67 l/s).
2. **High supply and no added return leakage**: Added leakage was 130 cfm (61 l/s) supply and zero return. The new system operating pressures were 59 and 31 Pa for supply and return, respectively. The expected flows are therefore: Qs = 130 cfm + 16 cfm $(59 / 59.1)^{.6}$ = 146 cfm (69 l/s) for the supply and Qr = 19 $(31 / 34.1)^{.6}$ = 18 cfm (9 l/s) for the return.
3. **Moderate supply and no added return leakage**: Added leakage was 69 cfm (33 l/s) supply and zero return. The new plenum pressures were measured to be 59 and 30.5 Pa for the supply and return, respectively. Using Equation 1 and adding the result to the new installed leakage value, the expected leakage rates were 85 cfm (40 l/s) for the supply and 18 cfm (9 l/s) for the return.
4. **Small supply and no added return leakage**: Added leakage was 29 cfm (15 l/s) supply and zero return. The new operating pressures were 59.8 Pa for the supply and 30.3 Pa for the return. This produced an expected leakage flow of 44 (21 l/s) and 14 cfm (7 l/s) for the supply and return, respectively.

Selection of Characteristic Pressures

The DeltaQ calculation procedure uses a characteristic pressure for both the supply and return leaks. The current DeltaQ procedure uses the measured plenum static pressures. In order to investigate the sensitivity to the selection of this pressure and to examine the possibility of eliminating this measurement and fitting to the DeltaQ test data to determine these pressures, the data was analyzed using four different characteristic system pressures:

- Measured plenum pressure. This is the standard DeltaQ procedure as given by Walker et al. 2001.
- Half the measured plenum pressure.
- Fixed pressures of 25 and 100 Pa for the supply and return respectively.
- "Best fit" pressures determined by fitting to the measured DeltaQ data.

Although a leakage pressure exponent of 0.6 is generally used in the DeltaQ calculations, a value of 0.5 was used for these calculations because this is characteristic of the flow meter through which the majority of the leakage occurred. The effects of changing the pressure exponent will discussed later. The four different characteristic pressure definitions were applied to the test results from the most leaky case studied. The DeltaQ test measurements were repeated four times and the results presented here are the average of all four tests at high leakage. The comparison of the four different pressure characteristics are provided in Table A2.

Table A2. Variation of DeltaQ results with characteristic pressure for different leakage configurations						
		"Best Fit" Pressure	Fixed Pressure	Actual Plenum Pressure	Half Plenum Pressure	**Measured Leakage Flow Rate**
Large Supply and Return Leakage	Supply Leakage, cfm (l/s)	270 (128)	320 (151)	256 (121)	285 (135)	**224 (106)**
	Return Leakage, cfm (l/s)	164 (77)	128 (60)	85 (87)	206 (97)	**141 (67)**
High added supply and zero added return	Supply Leakage, cfm (l/s)	164 (77)	97 (46)	143 (68)	128 (60)	**146 (69)**
	Return Leakage, cfm (l/s)	13 (6)	0 (0)	9 (4)	6 (3)	**18 (9)**
Moderate supply and no added return leakage	Supply Leakage, cfm (l/s)	84 (40)	50 (24)	74 (35)	67 (32)	**85 (40)**
	Return Leakage, cfm (l/s)	12 (6)	3 (1)	7 (3)	8 (4)	**18 (9)**
Small supply and no added return leakage	Supply Leakage, cfm (l/s)	42 (20)	29 (14)	41 (19)	37 (17)	**44 (21)**
	Return Leakage, cfm (l/s)	9 (4)	6 (3)	6 (3)	8 (4)	**17 (8)**

The results in Table A2 show that unlike some other duct leakage tests (e.g., pressurization) an increase in the characteristic pressure does not necessarily increase the resulting calculated leakage. Overall, the "Best Fit" pressures produce the results closest to the measured leakage flow rate, with an RMS difference of 25 cfm (12 l/s) for returns and 13 cfm (6 l/s) for supplies. Most of this uncertainty is due to the overprediction of leakage flows with the large supply and return leakage. For the sum of return and supply leakage the RMS difference between measured and the DeltaQ using best fit pressures is 36 cfm (17 l/s) and the for the imbalance leakage (supply – return difference) the RMS difference is 17 cfm (8 l/s). The standard DeltaQ procedure that uses the actual plenum pressure was the next best performer of the four characteristic pressure estimates.

Added Leak DeltaQ Repeatability

The repeatability was evaluated by repeating the DeltaQ test several times in each leakage configuration (and with each of the characteristic pressures – discussed above). Figures A5 and

A6 show all the individual test results for supply leakage and return leakage respectively. Tables A3a through A3d summarize the repeatability estimates in terms of standard deviation and 95% confidence interval for each leakage configuration and characteristic pressure. The results show good repeatability for all the tests. For the best fit pressures the typical repeatability uncertainty is about ±4 cfm (0.4% of fan flow). Similarly for the plenum pressures, the typical repeatability uncertainty is about ±2 cfm (0.2% of fan flow). Comparing these two results indicates that the extra variability due to fitting pressures to each DeltaQ experiment instead of using the plenum pressures only adds about ±2 cfm (±1 l/s, 0.2% of fan flow) to the repeatability uncertainty.

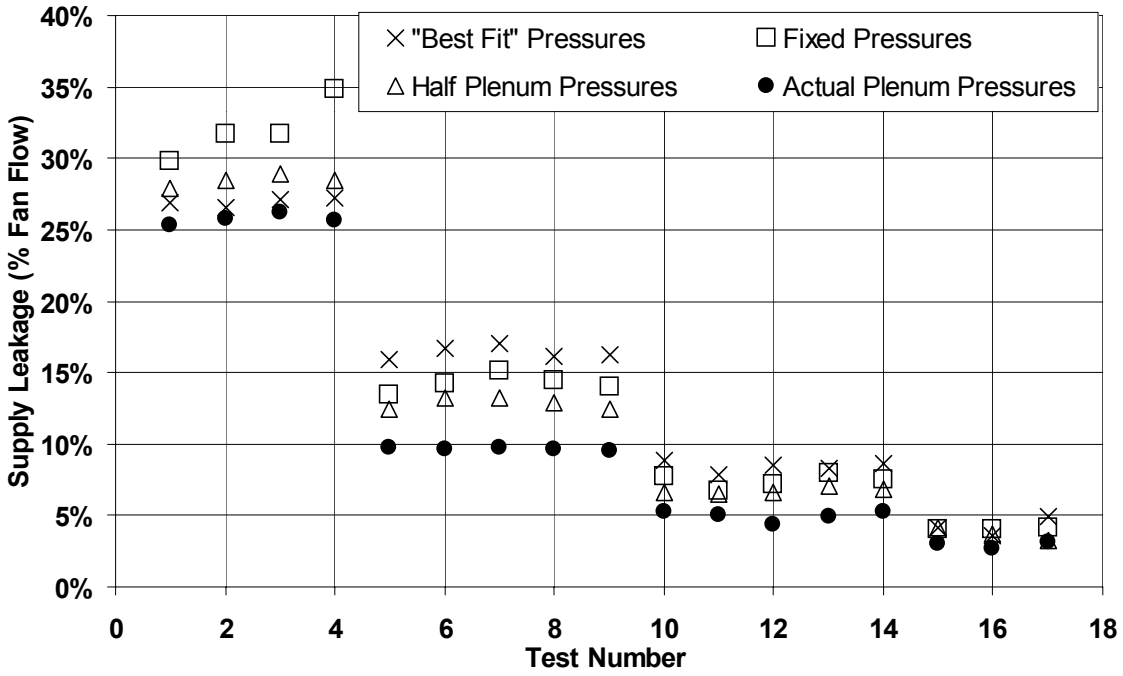

Figure A5. Repeatability of DeltaQ Supply Leakage Measurements

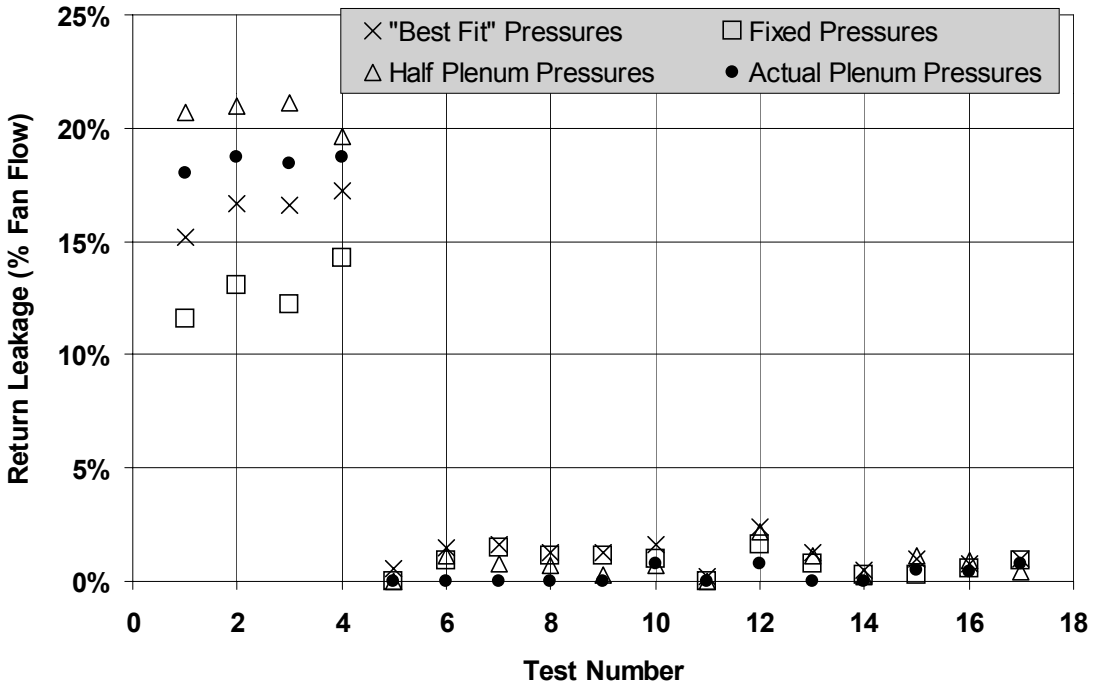

Figure A6. Repeatability of DeltaQ Return Leakage Measurements

Table A3a. Repeatability results for Large Supply and Return Leakage

Characteristic Pressures	Qs Average (CFM)	Qs STD (CFM)	Qs 95% CI (CFM)	Qr Average (CFM)	Qr STD (CFM)	Qr 95% CI (CFM)
"Best Fit"	270	2	2	164	7	7
Fixed	320	18	18	128	10	10
Actual Plenum	258	3	3	185	3	3
Half Plenum	285	4	4	206	6	6

Table A3b. Repeatability results for High added supply and zero added return

Characteristic Pressures	Qs Average (CFM)	Qs STD (CFM)	Qs 95% CI (CFM)	Qr Average (CFM)	Qr STD (CFM)	Qr 95% CI (CFM)
"Best Fit"	164	4	4	13	4	3
Fixed	142	6	5	9	5	4
Actual Plenum	96	1	1	0	0	N/A
Half Plenum	128	4	3	6	4	3

Table A3c. Repeatability results for Moderate supply and no added return leakage						
Characteristic Pressures	Qs Average (CFM)	Qs STD (CFM)	Qs 95% CI (CFM)	Qr Average (CFM)	Qr STD (CFM)	Qr 95% CI (CFM)
"Best Fit"	84	4	3	12	8	7
Fixed	74	4	4	7	6	5
Actual Plenum	50	3	3	3	4	4
Half Plenum	67	2	2	8	8	7

Table A3d. Repeatability results for Small supply and no added return leakage						
Characteristic Pressures	Qs Average (CFM)	Qs STD (CFM)	Qs 95% CI (CFM)	Qr Average (CFM)	Qr STD (CFM)	Qr 95% CI (CFM)
"Best Fit"	42	5	6	9	1	1
Fixed	74	4	4	7	6	5
Actual Plenum	29	2	2	6	2	2
Half Plenum	37	4	4	8	3	3

Accuracy

Using Equation B1 and the results from the initial background leakage, the expected leakage rates were computed for each installed leak. Figures A7 and A8 compare the DeltaQ results using different characteristic pressures to the monitored leakage values.

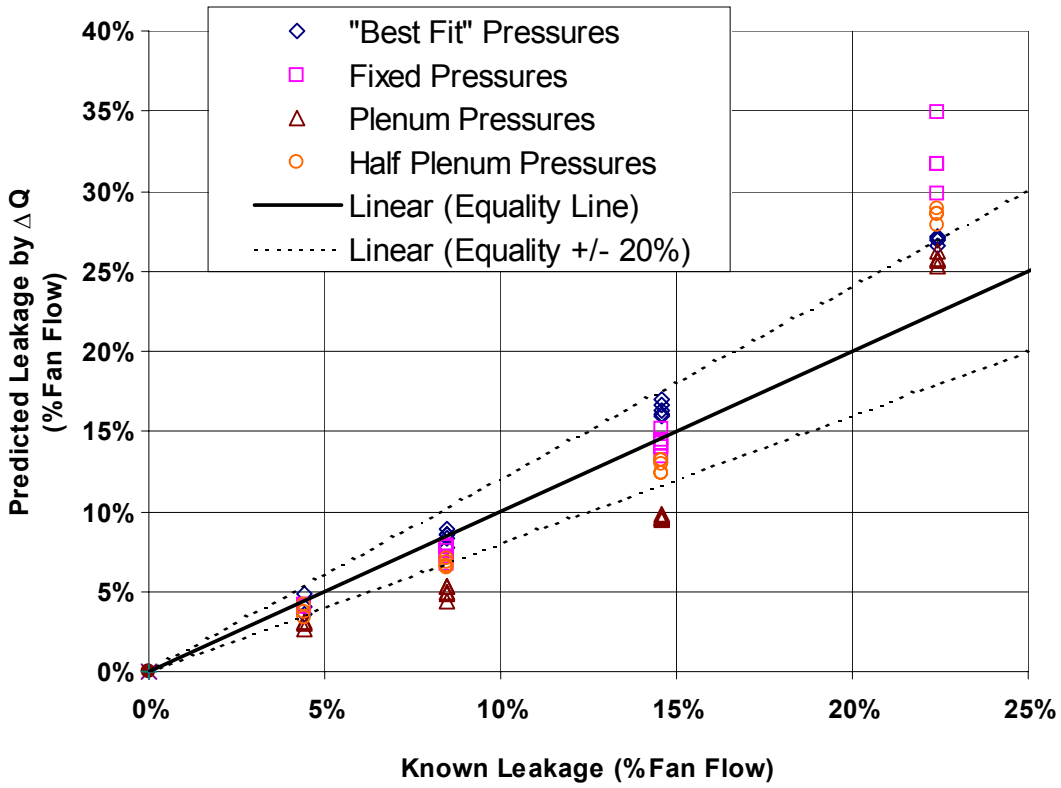

Figure A7. Comparison of DeltaQ results using different characteristic pressures for supply leaks

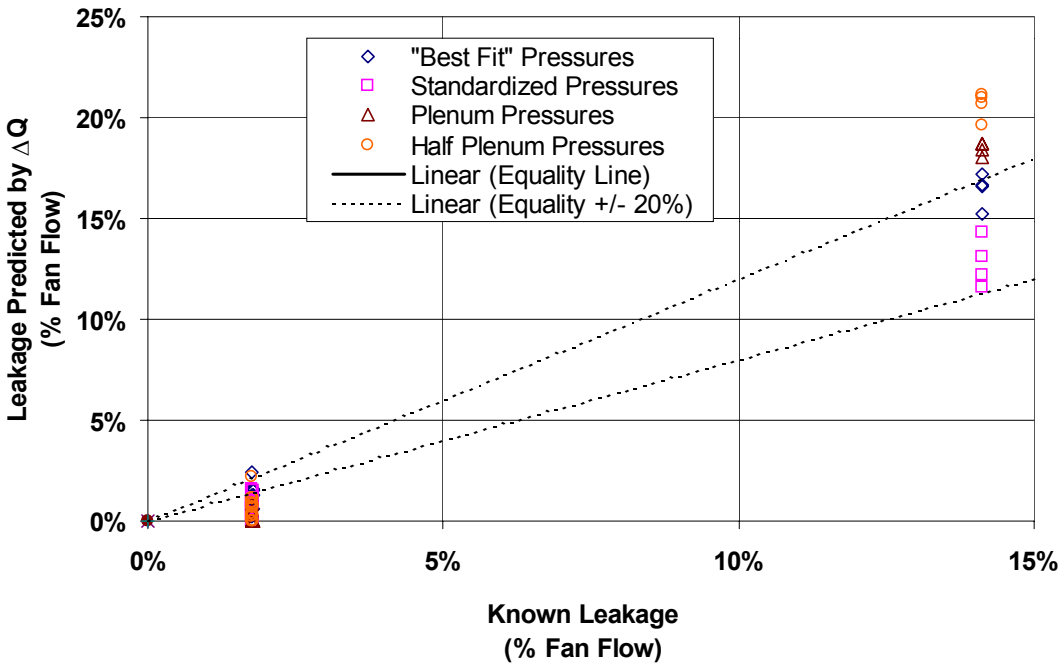

Figure A8. Comparison of DeltaQ results using different characteristic pressures for return leaks

Each technique, with the exception of the actual plenum pressures, produced the expected supply leakage rates with less than 20% error up to 15% fan flow. Past 15% fan flow, each technique overestimated the leakage rates. Half plenum pressure inputs for the return leakages performed poorly for both high and low leakage rates. The "best fit" pressures predicted leakages with an average accuracy of 10%. For the high leakage flows we do not have a good explanation of the DeltaQ overprediction, however, some uncertainty of the supply leakage for low leakage levels can be attributed to flow reversal in the flow meter. The DeltaQ calculations assume the same discharge coefficient and pressure exponent for both flow directions, but the added measured leaks in this experiment had different characteristics depending on flow direction. This change in leak characteristics is only a factor for the highly flow asymmetric leaks used in these experiments. We would not expect this to be a large factor in real duct systems because real systems have many leakage sites, each with different characteristics and driving pressures. The repeatability experiments in this study had leakage completely dominated by the added flow meter leaks. This is convenient from a measurement point of view, but not very realistic. Some leaks in real duct systems may have asymmetric characteristics depending on flow direction: e.g. leaks at flexible duct to collar connections, where the leak is effectively much larger for air escaping from the duct system, and when the pressures change and flow should be into the ducts the flap of flexible duct plastic acts as a valve, severely reducing the effective leakage for reversed flow. However, a lot of other leaks do not exhibit this behavior, e.g, sharp edged leaks through holes in sheet metal.

References

Walker, I.S., Sherman, M.H., Wempen, J., Wang, D., McWilliams, J., Dickerhoff, D.J. 2001. “Development of a new duct leakage test: DeltaQ”. LBNL 47308.

Appendix B: Basket Flow Hood Development

Introduction

Previous work by LBNL (summarized in Walker et al. 2001) has shown that commercially available flow hoods are poor at measuring flows through residential registers. This is primarily because of their sensitivity to flow non-uniformities and the difficulty in accounting for insertion losses on multiple low-pressure branch systems. In addition, these flow hoods are sensitive to the relative position of the register grille – with large variations in indicated flow if not centered over the grille. The LBNL study also showed that powered flow hoods can successfully avoid these problems and produce very accurate (within about 2-3% of measured flow) results. The drawbacks of the powered flow hoods are their weight, complexity and cost. In this study, we aim to develop a simple and cheap device for measuring residential (and commercial) register flows that does not have the drawbacks of existing commercially available devices. This new device is called the "basket hood" due to the use of laundry baskets in the prototype development.

Summary of Existing devices

Existing devices for measuring register air flows can be classified in three categories.

The **standard flow hood** uses a fabric hood that is fixed to a rigid frame that fits over the register. The fabric hood directs the flow over a velocity or pressure-drop sensing element. These devices have built-in electronic signal processing and information displays that include the ability to perform time averaging, temperature compensation and an estimate of insertion loss correction. These flow hoods are fairly expensive – typically costing between $2000 and $3500.

The **propeller flow hood** uses a rigid glass fiber flow capture hood that directs the flow over an axial propeller. As more flow passes through the capture hood the propeller spins faster, and an electronic counter translates the rate of spin into an air flow rate. This flow hood is no longer manufactured, but it is still used by some practitioners.

The **powered flow hood** was originally developed to reduce the effects of backpressure on the flow measurement. It is sometimes referred to as a fan-assisted flow hood. The powered flow hood uses a flow capture device connected to a calibrated fan-flow meter. A length of plastic flex duct and a flow straightener placed between the flow capture device and the fan-flowmeter makes this device insensitive to non-uniform flows at the register grille. A pressure sampling tube array already mounted in the throat of the flow hood is used in the system to measure the pressure inside the hood. The flow resistance of the capture hood, flexible duct and flowmeter is compensated for by adjusting the fan until there is no pressure difference between the room and the hood. This pressure balancing procedure ensures that placing the flow hood over the register does not reduce the flow out of the register. This device is not commercially available as a complete package; however, many practitioners have the fan-flowmeter device used in these tests. Because laboratory results (Walker et al. 2001) showed this flow hood to be very accurate, it was used as the reference flow hood for the field studies.

Basket Hood description

The basket hood uses a calibrated flow resistance to measure the flow through HVAC system registers. The Basket Hood measures the airflow by a pressure drop through a set of calibrated holes in the sides of the basket. The position of the holes has been optimized for the type of

registers (supply or return). The number and size of the holes have been optimized to produce a reasonably accurate pressure signal whilst minimizing the backpressure effects. The basket hood uses a couple of innovations to reduce the flow non-uniformity effects:

The pressure difference between the basket and the room is measured by a "soaker" hose that is fixed on the back of the basket. The "soaker" hose has many small holes that effectively average the pressures over the whole length of the hose, and therefore over a large fraction of the basket. A mesh screen is inserted in the entry of the basket that acts as a diffuser to reduce any flow non-uniformities.

Return registers are often bigger than supply registers because many systems have less returns than supplies resulting in bigger airflows for each return. In addition, because of the different direction of the flow through these registers, two different basket hoods have been developed: a Return Basket Hood and a Supply Basket Hood.

Return basket hood

The design of the return basket hood is less critical than for supplies because the flow into the flow meter is relatively uniform and less affected by boot and grille geometry. The Return Basket Hood (shown in Figures B1 and B2) is designed to fit over most of the return registers in commercial and residential buildings.

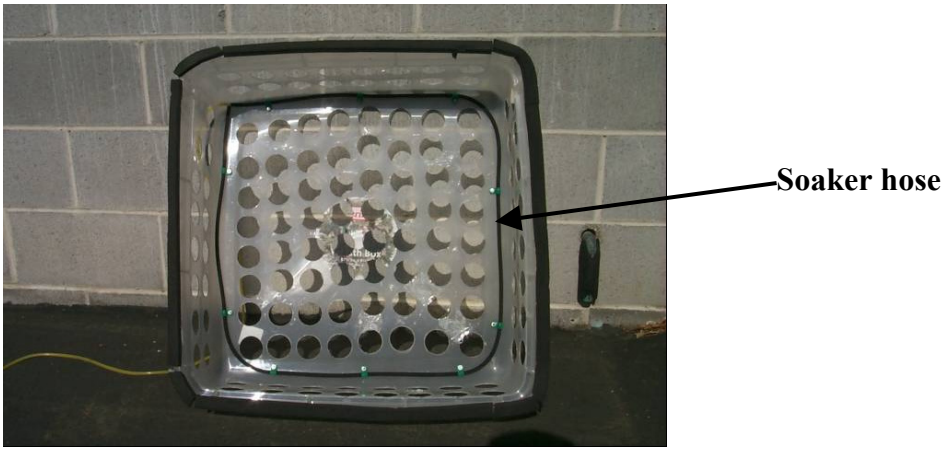

Figure B1. Return Basket Hood, Front view

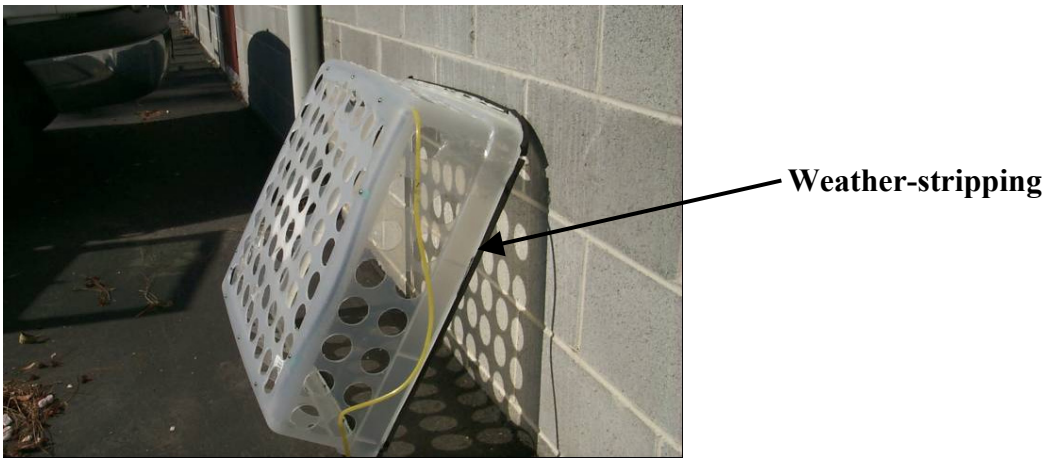

Figure B2. Return Basket Hood, Side view

The Return Basket Hood is constructed from a plastic container to which we added 128 holes of 50 mm (2 inch) diameter. The large number of holes reduces the insertion losses (flow reduction due to the added flow resistance of the flow hood), whilst still providing a large enough pressure signal avoid pressure measurement resolution limits. The pressure resolution is typically 0.1 Pa for good digital manometers. As a reasonable compromise, the return basket hood was designed to have a 5 Pa pressure drop at a flow rate of 1,700 m^3/h (1000 cfm) (see the following section for details of design calculations). The soaker hose is fixed around the inside of the top of the basket (as shown on Figure B1). The pressure difference between the soaker hose and the room the return basket hood is used in is measured using a hand-held digital manometer with a resolution of 0.1 Pa used in a mode that takes five second time averages. The time averaging is an important aspect of the pressure measurement due to the turbulent fluctuating nature of the pressure and flows through the flow meter. In order to assure the airtightness of the device, the edge of the Basket Hood is weather-stripped (as shown on figure 12). Its dimensions are:

Height: 0.673 m (26.5”)

Length: 0.673 m (26.5”)

Width: 0.216 m (8.5”)

Basket Hood design equations

Assuming that the airflow in our system is incompressible (constant density) and steady we use the following equation to design the return Basket Hood. This equation is a standard orifice relationship.

$$Q = \frac{C_0}{\sqrt{(1-\beta^4)}} A \sqrt{\frac{2\Delta P}{\rho}} \qquad \text{(B1)}$$

Where:
Q is the airflow rate through the Basket Hood, in m^3/s (cfm)
A is the total area of the Basket holes, in m^2 (ft^2)
ΔP is the pressure difference across the Basket Hood, in Pa
ρ is the air density, in kg/m^3 (lb/ft^2)
C_0 is the orifice coefficient
β is the ratio of cross-section areas of upstream to that of down stream

Assuming that C_0 is 0.6 and that β is negligible (the down stream cross section area is infinite), we have:

$$Q = A \times 0.6 \times \sqrt{\frac{2\Delta P}{\rho}} \quad \text{(B2)}$$

This can be rearranged:

$$A = \frac{Q}{0.6 \times \sqrt{\frac{2\Delta P}{\rho}}} \quad \text{(B3)}$$

The return basket hood is designed to lead to a 5 Pa pressure drop at a flow rate of 1000 cfm (1,700 m^3/h).

With:
Q = 1000 cfm = 0.4722 m^3/s.
ΔP = 5 Pa
ρ = 1.2 kg/m^3 (Hypothesis: standard conditions)
the required area is 0.2726 m^2 (0.326 ft^2).

The chosen hole diameter is 2" (5.08 cm), so 134 holes are required. Limited by the requirement of retaining some physical rigidity and the physical size of the basket hood led to the use of 128 holes.

Hole Taping Configurations for Basket Flow Hoods

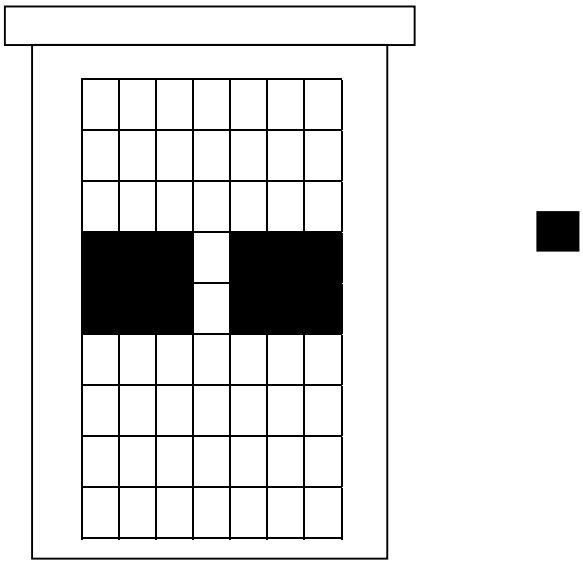

Residential Basket Hood , Configuration : White 1 (24 holes)

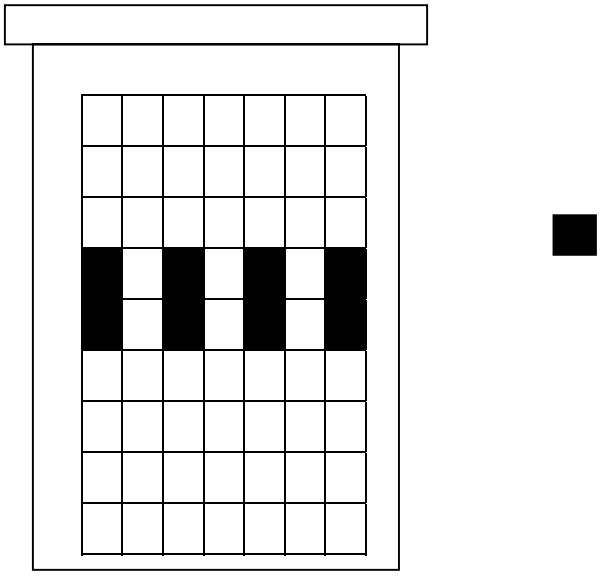

Residential Basket Hood , Configuration : Blue 1 (16 holes)

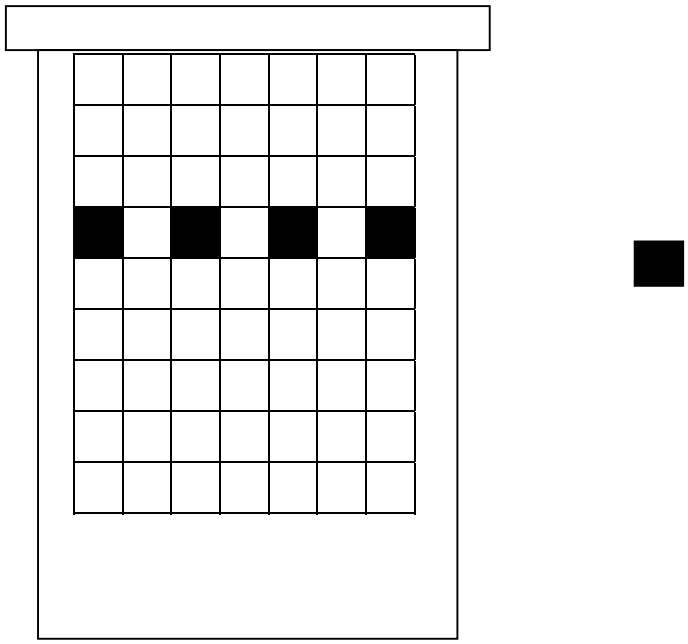

Residential Basket Hood , Configuration : White 2 (8 holes)

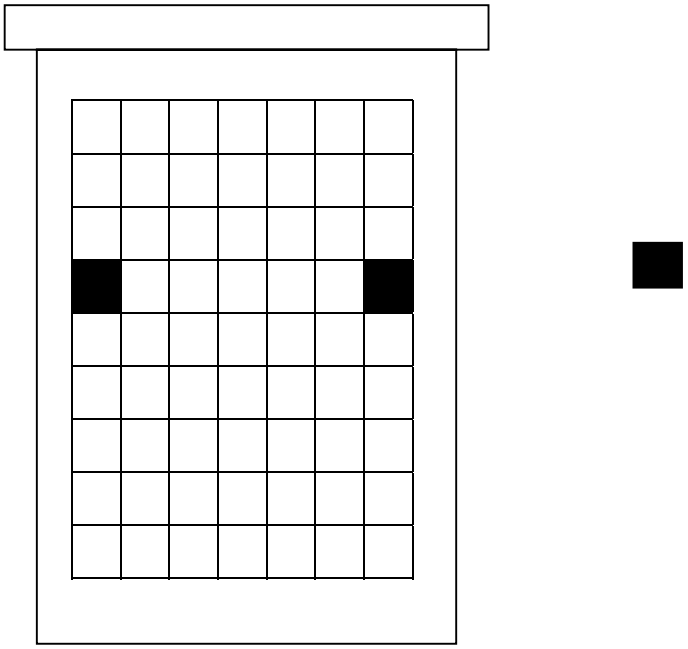

Residential Basket Hood , Configuration : Blue 2 (4 holes)

Return Basket Hood Calibration

In order to calibrate this device, we used a complete duct system that is representative of a typical California house. This duct system is a result of the collaboration between Lawrence Berkeley National Laboratory (LBNL) and California State University at Chico (CSUC). CSUC conducted a site survey at 20 houses selected as representative of present standard practice. Based on the results of the 20 site surveys and the market review, CSUC developed the specifications for a duct system. This duct system has been recreated in a LBNL test facility. The reference airflow is measured by a precise (±0.5% of flow) flow nozzle connected to the duct system within the return plenum. Figure B3 shows the dimensions of the return register used in the calibration procedure.

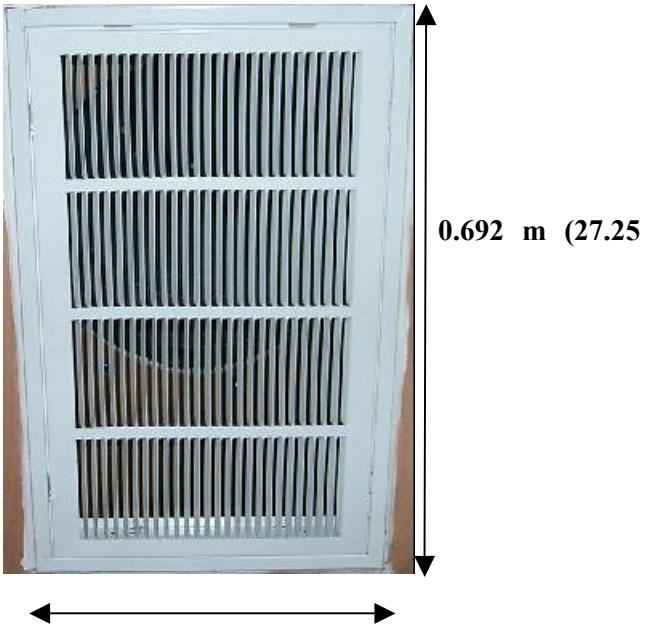

Figure B3. Laboratory calibration system test return register

The return basket hood calibration is based on a power law relationship:

$$Q = C \times \Delta P^n \tag{B4}$$

where C and n are constants. To determine these two constants, the pressure difference was measured over a range of air flows. Because the air handler fan used in the calibration apparatus was not designed to provide different airflows, the airflow was modified by blocking the return register with tape using a grid pattern. Figure B4 illustrates the calibration data for the return basket hood. C and n were determined by least squares fitting to these data and C = 484 and n = 0.469. The 95% confidence interval (C.I.) for C was 460/509 and for n it was 0.434/0.505.

These laboratory tests also included measurements of air flow through the system with and without the flow meter in place. These tests showed that he added flow resistance of the return basket hood decreases the system flow by only 0.5 %. Because this small change was the same as the accuracy of the reference flow meter it was neglected in the calibration procedure and does not need to be accounted for in field measurements of single returns. For multiple branch return systems, this effect would be further reduced because only part of the return duct system would be affected.

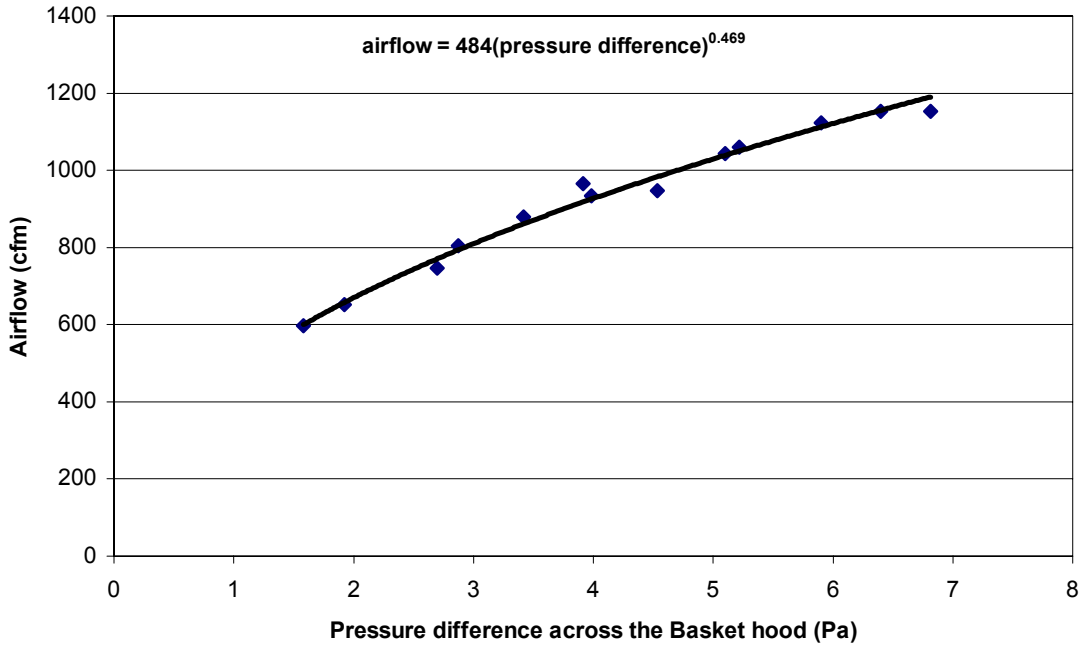

Figure B4. Return Basket Hood calibration equation

The basket hood was also tested for its sensitivity to centering over the register because previous LBNL studies (Walker et al 2001) showed that commercially available flow hoods were sensitive to being centered over registers. A second set of measurements were taken with the basket hood deliberately off-centered as shown in Figure B5. The results showed the fact that the return basket hood is not very sensitive to centering over the register, with less than 1% difference in the calibration results compared to the centered results.

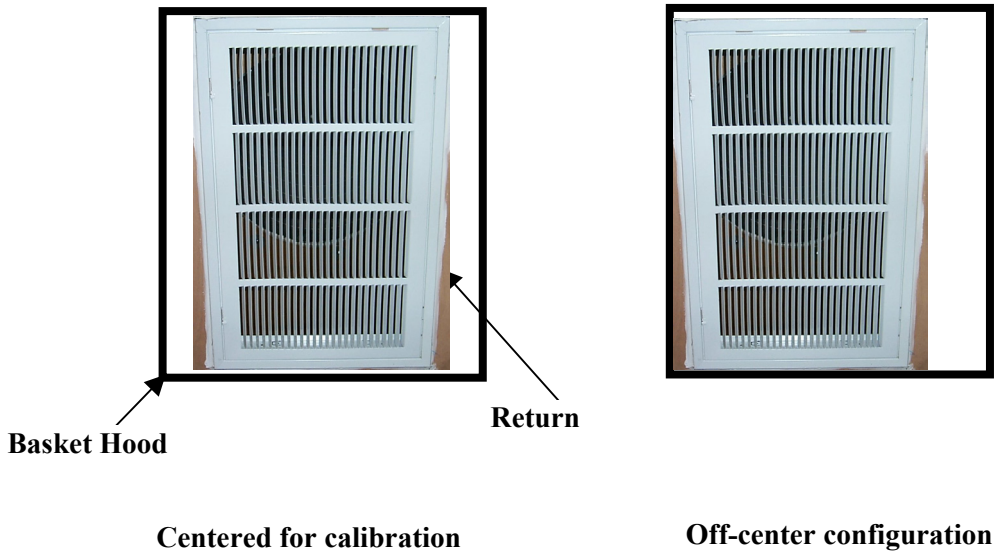

Figure B5. comparison of basket hood edge location for centered and off-centered tests

Field evaluation

The return basket hood was field tested on five residential and three commercial buildings in California. A powered flow hood was used as the reference for these tests. In some systems, a single fan-flowmeter powered flow hood cannot produce enough flow to match the large flows through a single return. In these cases a device was constructed (shown in Figure B6) that allowed the flows from several fan-flowmeters to be combined using a mixing box. Table B1 summarizes the test results for these systems and shows that the return basket hood gives excellent results. The average difference over all theses systems was only –0.2 % and the RMS difference was 2.4 %. This RMS difference is close to the accuracy of the powered flow hood itself, which shows that the return basket hood gives the same results as our reference device within the uncertainty specification of the reference.

The field evaluation also looked at ease of use issues. To use the Basket Hood the operator has to put the device on the register and to hold it tight over the register in order to maintain a seal. The field testing demonstrated that this is easier to do with the basket hood than other flow meters because of its light weight. Figure B6 is a particularly good illustration of the difficulties in applying powered flowhoods in the single large return flow application. In practice, powered flow hood measurements are normally performed with a single fan-flowmeter and measured system pressures are used to extrapolate from the measurement condition to the return flow at operating condition. This introduces extrapolation errors to the calculations. Because the powered flow hood is being used as the reference measurement technique in this study, it was important to reduce the potential errors and so the extrapolation method was not used, and the complex and time consuming multiple fan-flowmeter technique illustrated in Figure 6 was used.

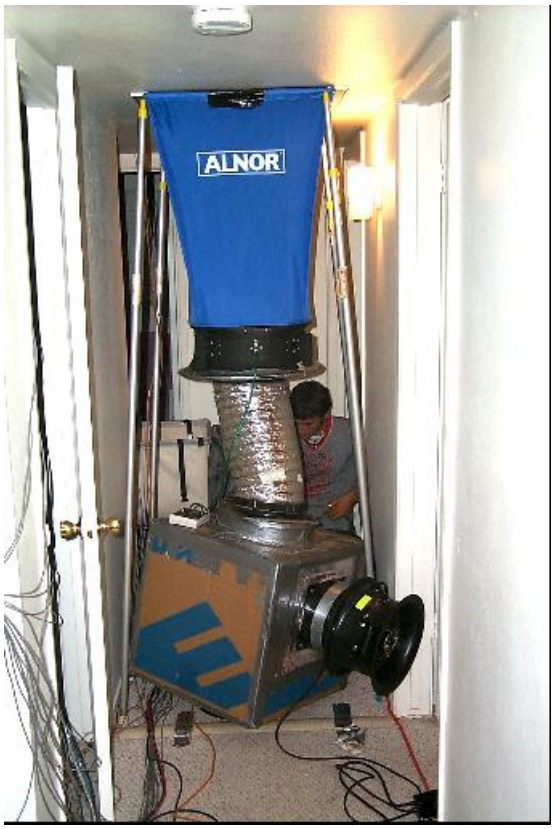

Figure B6. Multiple fan-flowmeter return powered flow hood

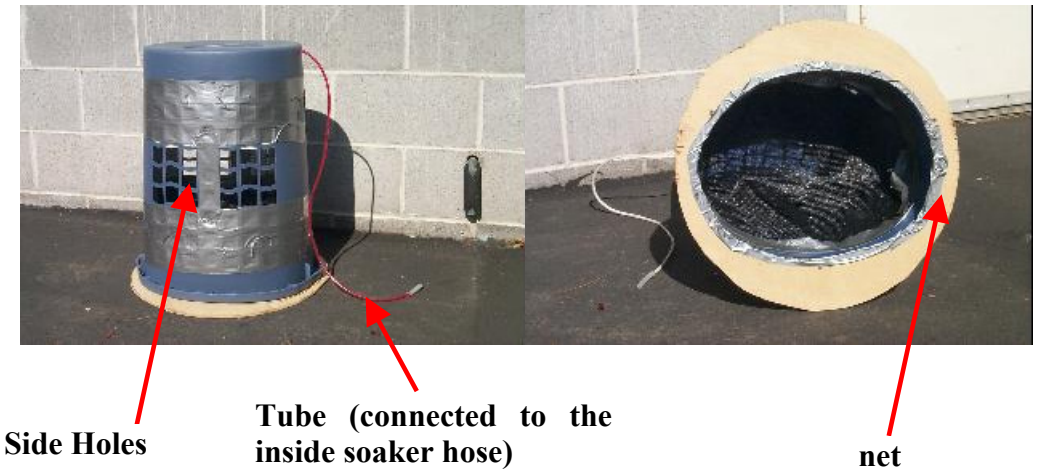

Figure B7. Supply Basket Hood

Table B1. Return Basket Hood field tests results

Building	"Powered flow hood" airflow, cfm (l/s)	"Basket Hood" airflow, cfm (l/s)	Difference (%)
Beauty salon (Sacramento)	981 (463)	990 (467)	+0.9
Bicycles store (Sacramento)	402 (190)	409 (193)	+1.8
Dance studio (Sacramento)	757 (357)	744 (351)	-1.7
One-story house (Fresno)	1039 (490)	1039 (490)	0.0
Dance studio (Sacramento)	620 (293)	637 (301)	+2.7
One-story House (Berkeley)	494 (233)	506 (239)	+2.4
Two-story House (Berkeley)	235 (111)	227 (107)	-3.4
Two-story House (Albany)	683 (322)	700 (330)	+2.5
Two-story House (Alameda)	568 (268)	547 (258)	-3.7

Supply Basket Hood

The supply basket hood (shown in Figure B7) follows the same design technique as the return basket hood. The two supply basket hood prototypes were made from plastic laundry baskets. A typical residential register is 6 × 12 inches (150 mm × 300 mm) and the basket hood openings are large enough to fit over a register measuring 7.5 × 15.5 inches (190 mm x 390 mm). Different taping configurations (illustrated in Appendix 2) were tested in order to find the optimum that gave a reasonable pressure signal of about 5 Pa. The two baskets have different hole taping configurations. The soaker hose is connected to a digital manometer to obtain 5 second time averaged pressures. A net is fixed at the bottom of the Basket Hood in order to make the airflow more homogeneous to reduce measurement errors due to flow non-uniformity. A honeycomb structure is also added at the bottom of the basket as a flow straightener. Figure B8 illustrates how the basket supply flow hood is used on a wall supply register.

Unlike the return measurements, using the basket hood on a supply register can significantly change the airflow. This is because an individual supply branch has a relatively small pressure drop (typically 5 to 10 Pa) and adding the flow hood effectively doubles the pressure drop. The main consequence is a change in the airflow distribution throughout the duct system. Some of the airflow goes through the other branches and the airflow at the register being measured is significantly reduced. One method of accounting for these insertion losses is to use two different flowmeters each with a different flow resistance. The characteristic change in flow as the backpressure is increased for the duct branch being tested can then be estimated. In these prototype tests two physically separate basket flow hoods were used with different flow resistance achieved by systematically blocking off holes in the baskets. The blocking of the holes was carefully designed to result in a flowmeter that was insensitive to entering flow conditions and produced a stable pressure signal.

Figure B8. Residential supply airflow measurement

Supply Basket Flow Meter Calibration

The supply basket flow meters were calibrated using the apparatus illustrated in Figure B9. The setup consisted of a fan, a 6 inch (0.15 m) flow nozzle used as a reference (accuracy +/- 0.5 %) and a supply register mounted in a plywood panel. The register boot used in the calibrations has a 4 inch × 10 inch (100 mm × 250 mm) rectangular exit. The calibrations were repeated with three different register grilles, shown in Figure B10 in addition to the open end of the boot (no grille). The calibrations were done with the supply basket flow meter carefully centered over the register grille. A flow range of 40 cfm (19 l/s) to 200 cfm (94 l/s) was used, which covers most common supply register flows in residential buildings. A total of four basket flow meters were calibrated: a combination of two physically separate baskets (that were colored blue and white), each with two hole taping configurations.

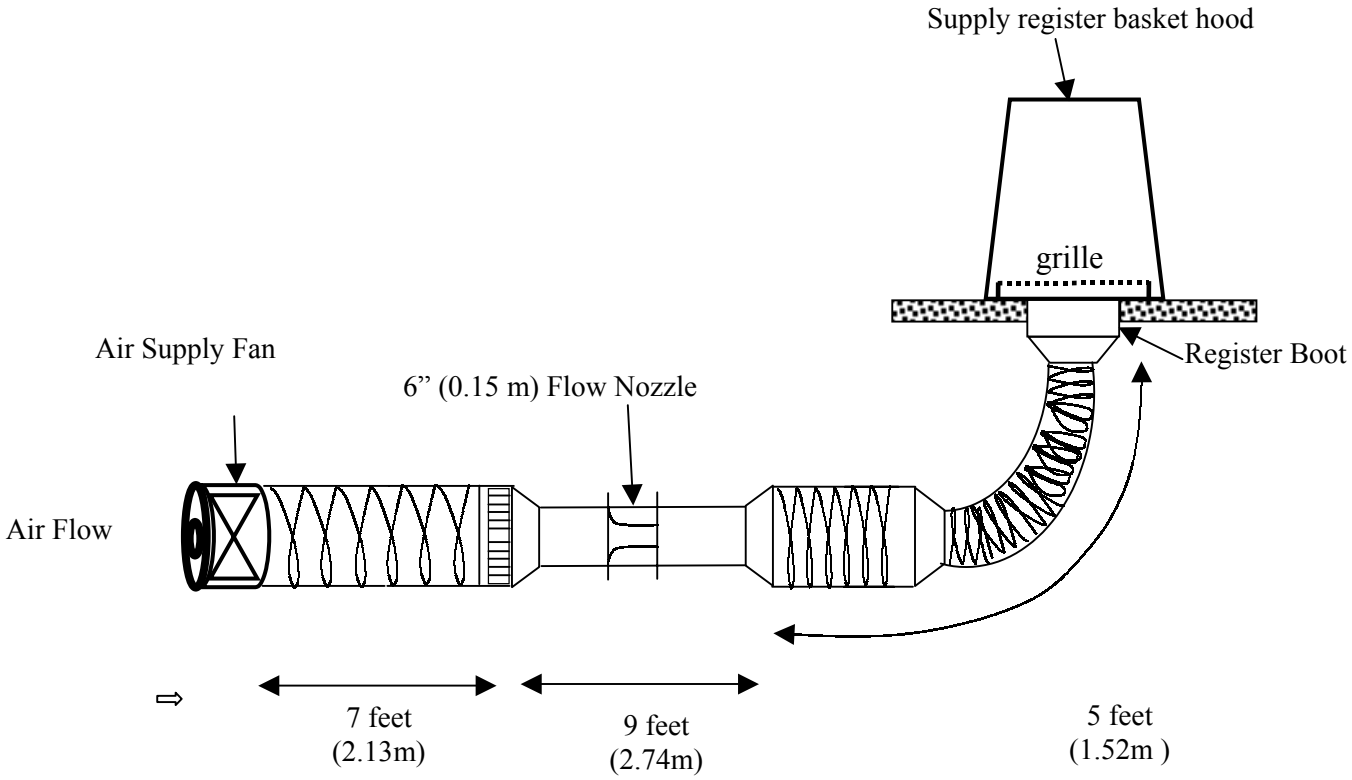

Figure B9. Flow meter test apparatus for supply flows

One-way-throw register Two-way-throw register

Three-way-throw register

Figure B10. Examples of register grilles used for supply basket hood calibration test apparatus

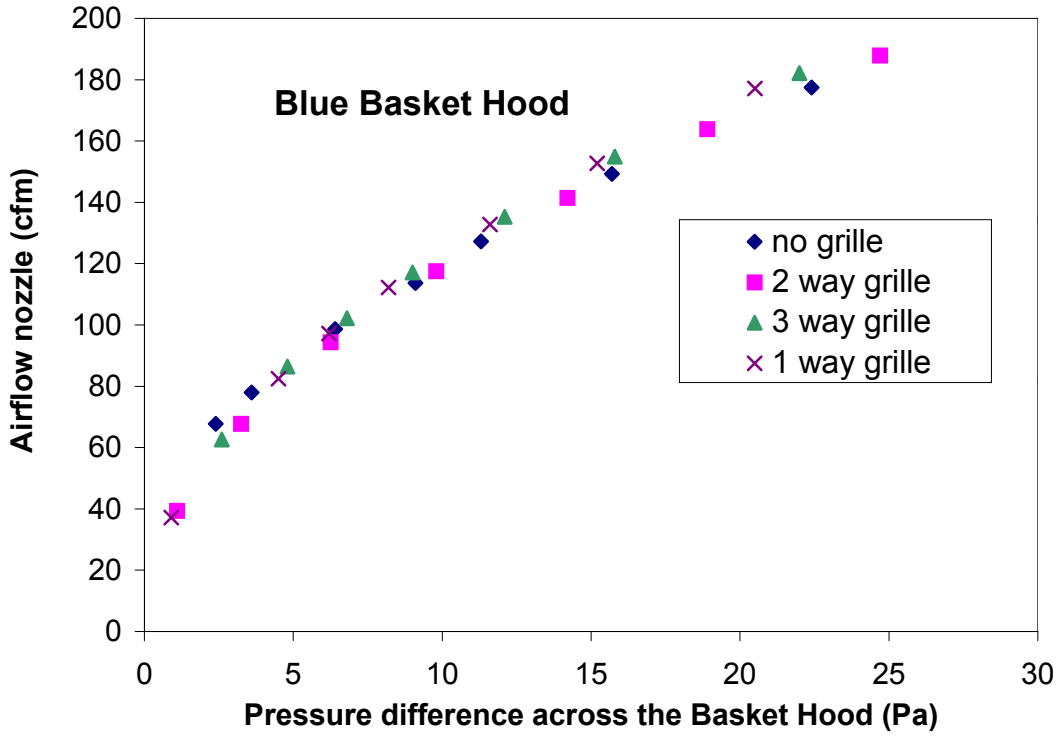

Figure B11. Sensitivity of supply basket hood calibration to grille design

The example calibration results in Figure B11 show that the kind of grille does not make any significant difference to the calibration equation (the coefficients change by only 1%). Therefore, for simplicity the measurements for all four grilles were combined to determine a single calibration equation for each of the basket flow meters. The calibration results for two configurations are shown in Figure B12, and all the calibration results are summarized in Table B2.

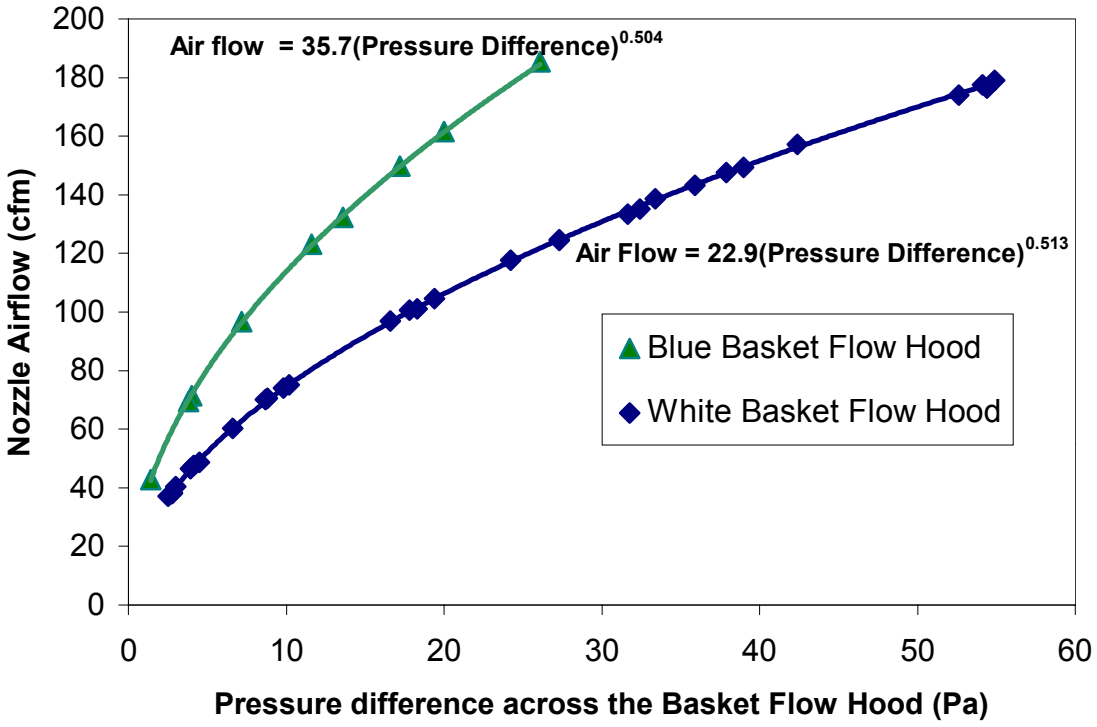

Figure B12. Supply basket flow hood calibration results.

Table B2 Supply basket flow hood calibration results

Configuration name	Number of clear holes on the sides	C (cfm/Pa^n)	95% confidence interval for C	n	95% confidence interval for n
White 1	24	67.6	(66.8, 68.4)	0.496	(0.487, 0.5067)
Blue 1	16	35.7	(35.3, 36.2)	0.504	(0.498, 0.509)
White 2	8	22.9	(22.7, 23.1)	0.513	(0.510, 0.515)
Blue 2	4	10.3	(10.0, 10.7)	0.520	(0.511, 0.528)

Using these two supply basket flowhoods on a register results in two measured flows with two corresponding backpressures. The measured flow hood pressure difference used to calculate the

flow is also used as a surrogate for the additional backpressure. These two points are then used to define an extrapolation relationship that allows the calculation of the flow through the register without the presence of the flow hood. Assuming that the change in flow through the register is proportional to the square root of the flow hood pressure difference, the following extrapolation equation can be used. ΔP_1 and ΔP_2 are the two pressure differences that are read by the basket flow hoods, and Q_1 and Q_2 the two corresponding airflows. The undisturbed flow (Q_o) is given by:

$$Q_0 = \sqrt{\frac{Q_1^2 \Delta P_2 - Q_2^2 \Delta P_1}{\Delta P_2 - \Delta P_1}} \qquad \text{(B5)}$$

Q is the airflow rate through the basket hood, cfm (l/s)

ΔP is the pressure difference across the basket hood, in Pa

Q_0 is the airflow rate through the register when ΔP is 0, cfm (l/s).

Field and laboratory tests

The initial tests only used single taping configurations for the two flow hoods. For both the field and laboratory testing the reference flow meter was the powered flowhood that has an accuracy of about ±2.5%. The laboratory testing was performed on a full scale duct system assembled in an LBNL laboratory. This is the same system as used for the testing of the return basket flow hood and it has 11 supply registers, each with the same style of grille illustrated in Figure B13. Field tests were also performed on six registers in two different houses in Berkeley, CA. Table 3 summarizes the results form these field and laboratory tests. For these tests the mean difference was -6.3 % and the RMS Difference was 7.3 %. In order to reduce these bias errors, the laboratory tests were repeated, with the second set of taping configurations. These results are shown in Table B4. In Table B4, the highlighted boxes correspond to the pressure used in the extrapolation.

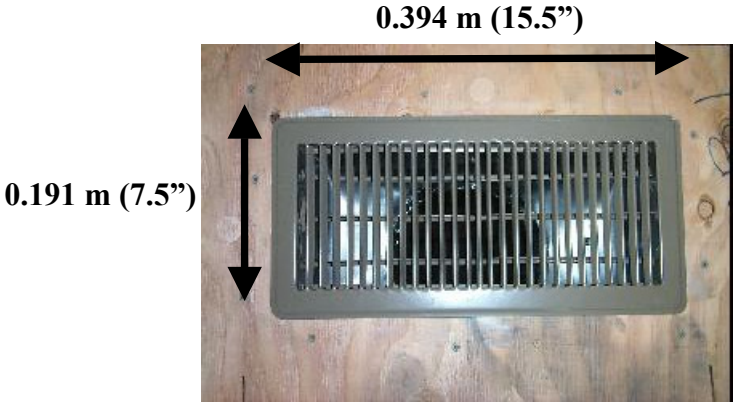

Figure B13. Laboratory test supply grille

Table B3. Initial Two-point Laboratory and field tests

Register location	Pressure difference white (Pa)	Pressure difference blue (Pa)	Airflow (cfm)	Reference Airflow (powered flow hood)	Difference (%)
903-S1	12.75	8	126	139	-9.5
903-S2	4.1	2.15	58	61	-5.2
903-S3	2.45	1.1	38	42	-8.4
903-S4	11.8	7.25	118	132	-10.8
903-S5	7.2	3.85	78	82	-4.7
903-S6	24	16.45	196	212	-7.6
903-S7	8	4.1	79	81	-2.8
903-S8	15.1	9.45	136	157	-13.2
903-S9	8.7	4.8	89	94	-5.5
903-S10	11.85	7.4	120	132	-8.7
903-S11	6.4	3.4	73	77	-5.0
House 1-S1	17.40	8.75	114	124	-8.4
House 1-S2	12.70	5.90	90	93	-3.3
House 1-S2	1.00	0.70	42	43	-2.8
House 2-S3	3.65	1.20	36	42	-13.6
House 2-S4	4.70	2.40	60	62	-2.9
House 2-S5	4.50	2.20	56	59	-4.4
House 2-S6	2.90	1.60	51	54	-3.8

The results in Table B4 show that using 4 taping configurations and selecting the two most appropriate pressures to do the extrapolation improved the results. . The selection procedure was based on having a large enough measured pressure across the flow hood that resolution errors were not dominant (greater than 2 Pa) and on small enough measured pressures that the extrapolation was not too great (less than about 10 Pa). The resolution issue arises from the use of pressure sensors with a resolution of 0.1 Pa. The problem with high pressure extrapolation was verified from the experimental data that showed large errors if large backpressures were developed. The RMS difference decreased from 7.3 to 4.1 %, and the mean difference from –6.3% to –4%. This method of taking the best 2 out of 4 configurations was applied to 33 supply registers in five different houses in California, and the results are shown in Figure B14. These results show that the residential basket flow hood is more accurate than most of the commercially available flow measurement devices (whose RMS errors can be in the 20 to 30 % range (Walker

et al. 2001)). However, the consistent bias found for these tests indicated that the calculation and measurement procedure had the potential for further refinement.

Table B4. Four Point laboratory test

Register	Delta P Blue 2 (Pa)	Delta P White 2 (Pa)	Delta P Blue 1 (Pa)	Delta P White 1 (Pa)	Airflow (cfm)	Reference Airflow (powered Flow hood)	% Difference
S1	20.8	12.75	8	3.3	135	139	-3.0
S2	9.1	4.1	2.15	0.7	58	61	-5.2
S3	6.4	2.45	1.1	0.4	41	42	-2.7
S4	19.5	11.8	7.25	2.95	127	132	-3.9
S5	14.2	7.2	3.85	1.4	78	82	-4.7
S6	35.3	24	16.45	7.3	205	212	-3.3
S7	17.8	8	4.1	1.4	79	81	-2.8
S8	23	15.1	9.45	4	150	157	-4.7
S9	16	8.7	4.8	1.8	89	94	-5.5
S10	19.2	11.85	7.4	3	128	132	-3.2
S11	13	6.4	3.4	1.25	73	77	-5.0

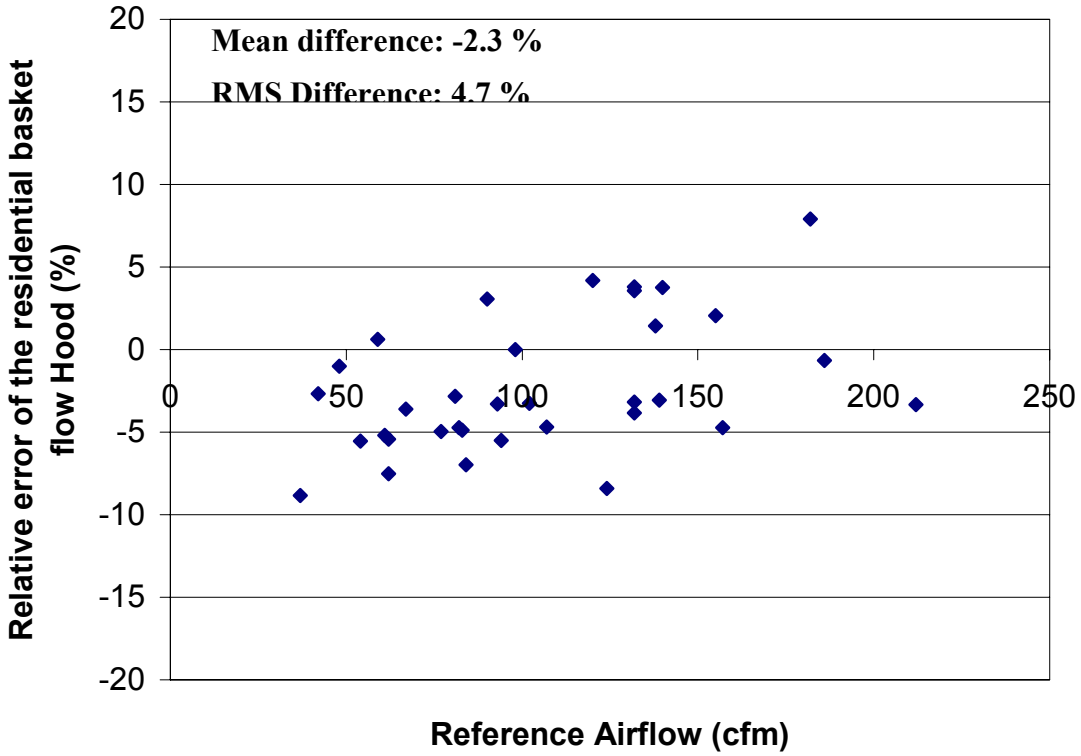

Figure B14. Residential basket flow hood field tests results using the best two out of four measurement points

In an attempt to reduce these biases, the following analysis looks at the system effects of adding flow resistance (the flow meter) to one branch of a duct system. The previous analysis assumed that the flowmeter resistance was added in series with the whole duct system. The simplified system analyzed here has two branches – one of which will have the flowmeter inserted. The pressure drop through both branches is the same and the total flow is assumed to be constant. Additional laboratory tests performed for this study have shown that the adding of a flowmeter to a register only changes the total air handler flow by about 0.1%, which is substantially less than the ±0.5% accuracy of the nozzle used to measure total air handler flow. The pressures and flows are defined as follows:

Q_1=flow through branch 1 (cfm, l/s)
Q_2 = flow through branch 2 (cfm, l/s)
Q_{total} = total flow through the system (cfm, l/s)
C_1=flow coefficient for branch 1 (cfm/$Pa^{0.5}$, l/s/$Pa^{0.5}$)
C_2 = flow coefficient for branch 2 (cfm/$Pa^{0.5}$, l/s/$Pa^{0.5}$)
C_{fm}= flow coefficient for flow meter (cfm/$Pa^{0.5}$, l/s/$Pa^{0.5}$)
C_{comb}= combined flow coefficient for branch and flow meter (cfm/$Pa^{0.5}$, l/s/$Pa^{0.5}$)
R_1 = flow resistance of branch 1 ($Pa^{0.5}$/cfm, $sPa^{0.5}$/l)
R_{fm} = flow resistance of flow meter ($Pa^{0.5}$/cfm, $sPa^{0.5}$/l)
R_{comb} = combined flow resistance of branch and flow meter ($Pa^{0.5}$/cfm, $sPa^{0.5}$/l)
ΔP = pressure difference across both branches (Pa)

Addition subscripts ",a" and ",b" refer to pressures and flows during normal operation and with the flowmeter inserted respectively, such that $Q_{1,a}$ is the true register flow to be measured.

Under normal operating conditions:

$$Q_{total} = (C_1 + C_2)(\Delta P_a)^{0.5} \quad \textbf{(B6)}$$

With the flowmeter added the flow resistance of branch 1 is changed. The flow resistance of the branch and the flowmeter are inversely proportional to their flow coefficients.

$$R_1 = \frac{1}{C_1}; R_{fm} = \frac{1}{C_{fm}} \quad \textbf{(B7)}$$

The total flow resistance of the branch and flowmeter, R_{combo}, is given by the sum of these resistances. The flow coefficient for the branch plus the flowmeter is then:

$$C_{comb} = \frac{1}{R_{comb}} = \frac{1}{\frac{1}{C_1} + \frac{1}{C_{fm}}} = \frac{C_1 C_{fm}}{C_1 + C_{fm}} \quad \textbf{(B8)}$$

Then, the total flow with the flow meter added is:

$$Q_{total} = (C_{combo} + C_2)(\Delta P_b)^{0.5} = \left(\frac{C_1 C_{fm}}{C_1 + C_{fm}} + C_2\right)(\Delta P_b)^{0.5} \quad \textbf{(B9)}$$

With the total flow the same in each case, the change in driving pressures is:

$$Q_{total} = (C_1 + C_2)(\Delta P_a)^{0.5} = \left(\frac{C_1 C_{fm}}{C_1 + C_{fm}} + C_2\right)(\Delta P_b)^{0.5} \quad \textbf{(B10)}$$

which can be rearranged:

$$(\Delta P_b)^{0.5} = \frac{(C_1 + C_2)}{\left(\frac{C_1 C_{fm}}{C_1 + C_{fm}} + C_2\right)}(\Delta P_a)^{0.5} \quad \textbf{(B11)}$$

Next the pressure difference under normal operating conditions is replaced with flow and flow coefficient terms. From

$$Q_{1,a} = C_1(\Delta P_a)^{0.5} \quad \textbf{(B12)}$$

ΔP can be expressed as:

$$(\Delta P_a)^{0.5} = \frac{Q_{1,a}}{C_1} \quad \textbf{(B13)}$$

Substituting Equation B13 in Equation B11:

$$(\Delta P_b)^{0.5} = \frac{Q_{1,a}(C_1 + C_2)}{C_1\left(\frac{C_1 C_{fm}}{C_1 + C_{fm}} + C_2\right)} \quad \textbf{(B14)}$$

The flow through branch one and the flowmeter is given by:

$$Q_{1,b} = \left(\frac{C_1 C_{fm}}{C_1 + C_{fm}} \right) (\Delta P_b)^{0.5} \quad \textbf{(B15)}$$

Substituting Equation B14 in Equation B15 then given the flow through the flowmeter as a function of the flow under operating conditions, $Q_{1,a}$ and the flow coefficients for each branch and the flowmeter:

$$Q_{1,b} = Q_{1,a} \left(\frac{C_1 C_{fm}}{C_1 + C_{fm}} \right) \frac{(C_1 + C_2)}{C_1 \left(\frac{C_1 C_{fm}}{C_1 + C_{fm}} + C_2 \right)} \quad \textbf{(B16)}$$

Now it is possible to examine how the flowmeter branch flow changes with flowmeter resistance and measured pressure difference. In practice, these coefficients are generally not known, instead the system flows and pressures are known (or measured). In the following examples, the branch flow coefficients C_1 and C_2 are determined from the imposed total flow (1000 cfm (472 l/s) in these examples) and the branch pressure differences. I.e. a higher branch pressure difference for the same flow implies a higher branch flow resistance and a lower branch flow coefficient. The flowmeter pressure difference is determined from the flows calculated using Equation B16 and the flowmeter flow coefficient, assuming that the flow is proportional to the square root of pressure difference. A couple of cases are examined: in the first case the total flow is split evenly between two branches and the other case is more typical of residential systems, with 10% of the total flow through the branch being measured.

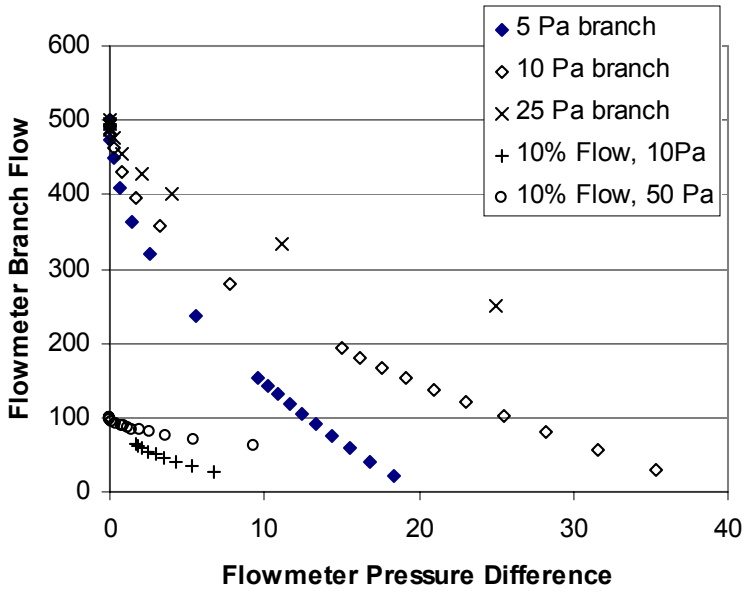

Figure B15a. Example Calculations for Flowmeter Effect on Branch Flow

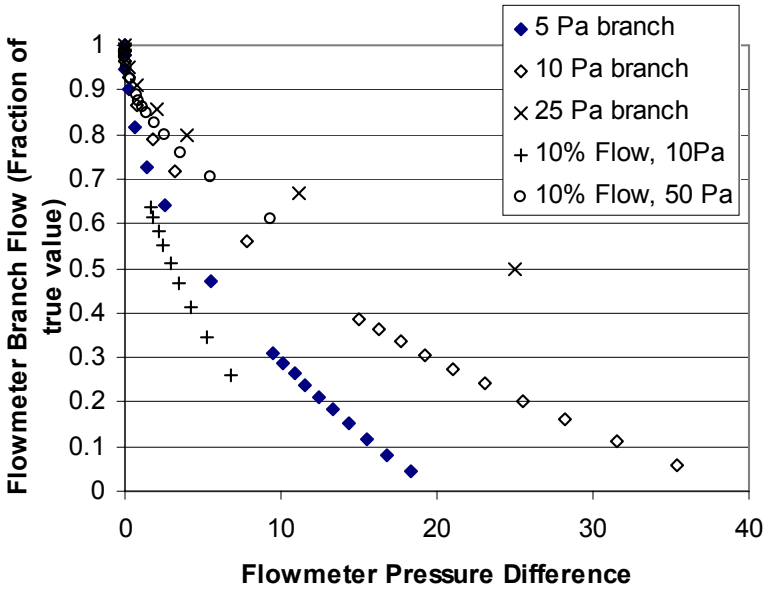

Figure B15b. Example Calculations for Flowmeter Effect on Branch Flow expressed as a fraction of true flow

Figures B15a and B15b show how the branch flow has the opposite trend to that given by Equation B5, i.e., the slope of the pressure/flow relationship increases with decreasing flowmeter pressure difference rather than decreasing. This figure also illustrates how the flowmeter has a greater effect on branches with lower pressure differences under normal operating conditions.

These results suggest that a functional form different from Equation B5 should be used to extrapolate from the measuremed flow meter data. Analysis of the results shows that the "error" term, i.e., the differnece between the measured flowmeter flow and the true flow is proportional the sqare root of the measured flow meter pressure. Using a two-point measurement technique allows for evaluation of the error coefficient and therfore a good prediction of the true flow.

If the two points are labelled "hi" and "lo" for high and low flow resisitance respectively, then the error at low flow resistance is:

$$Q_{error,lo} = C_{error}\Delta P_{lo}^{0.5} \quad \textbf{(B17)}$$

and at high resistance is:

$$Q_{error,hi} = C_{error}\Delta P_{hi}^{0.5} \quad \textbf{(B18)}$$

where, ΔP_{lo} and ΔP_{hi} are the pressure differences across the flowmeter. The equation for the true flow ($Q_{1,a}$) can be written:

$$Q_{1,a} = Q_{lo} + C_{error}\Delta P_{lo}^{0.5} = Q_{hi} + C_{error}\Delta P_{hi}^{0.5} \quad \textbf{(B19)}$$

where Q_{lo} and Q_{hi} are the flowmeter flows. After some algebraic manipulation, Equation B19 yields a relationship for the error coefficient, C_{error}:

$$C_{error} = \frac{Q_{lo} - Q_{hi}}{\Delta P_{hi}^{0.5} - \Delta P_{lo}^{0.5}} \quad \textbf{(B20)}$$

Substituting back into Equation B19 there is the choice of correcting the lo flow or the hi flow. The lo flow will be closest to the correct flow, but have the greater precision errors, whereas the hi flow will have improved precision but a greater extrapolation uncertainty. For the lo flow case:

$$Q_{1,a} = Q_{lo} + \frac{Q_{lo} - Q_{hi}}{\Delta P_{hi}^{0.5} - \Delta P_{lo}^{0.5}} \Delta P_{lo}^{0.5} \quad \textbf{(B21)}$$

For the idealized case considered here, Equation 21 reproduces the true branch flow exactly, with no error. Note that this is a very different functional form from that shown in Equation B5. The issue of which of these functional forms is more appropriate is not clear from measured data. 17 registers in 3 systems (one laboratory and two houses) had three or four different flow/pressure measurements that can be plotted to examine the trend of pressure and flow changes. Figures B16a through B16d illustrate these results and show that it is unclear from measured data which of Equation B2 or Equation B18 would best fit the data.

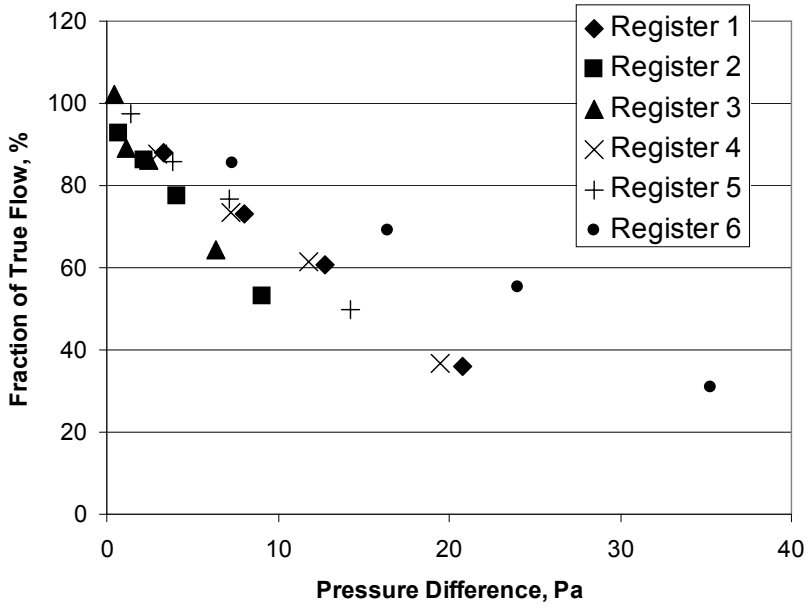

Figure B16a. Multiple Point Measurements on Laboratory System Registers

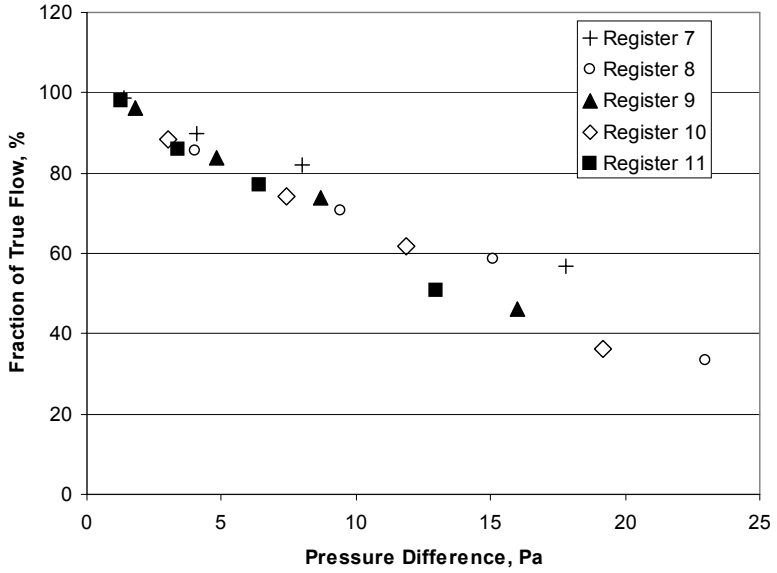

Figure B16b. Multiple Point Measurements on Laboratory System Registers

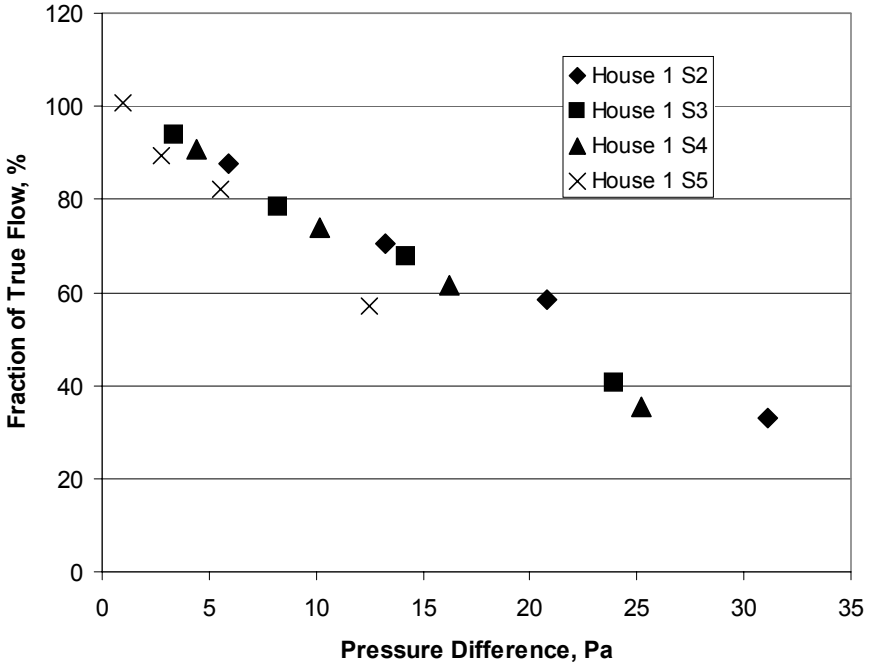

Figure B16c. Multiple Point Measurements on House 1 System Registers

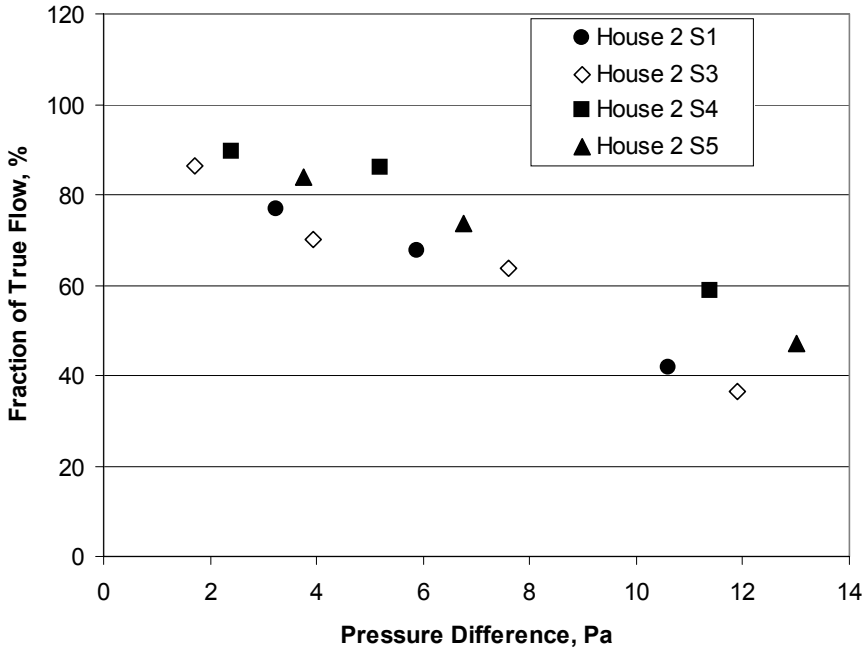

Figure B16d. Multiple Point Measurements on House 2 System Registers

Comparison to Measured data

The next step is to apply these corrections to some measured field and laboratory data on real duct systems. Using the same field and laboratory data discussed earlier the fraction of true flow can be calculated for each individual measurement and flow meter pressure difference. The individual flow and pressure combinations are illustrated in Figure B17. The data trends in Figure B17 are much less clear than the idealized system discussed above. The first issue is that there is significant "scatter" in the field data from a single ideal relationship. This is due to a combination of experimental uncertainties (e.g., how well the flow hood seals against the wall/register and low pressure resolution) and each point being on a different branch of the tested duct systems and having a different set of defining branch flow resistance characteristics.

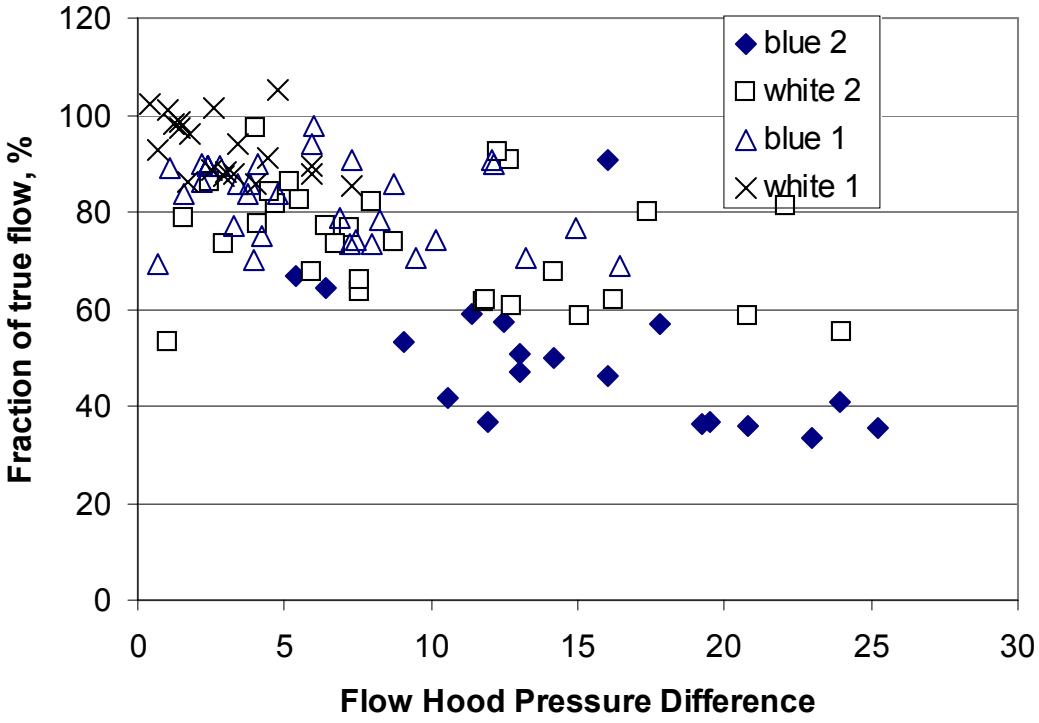

Figure B17. Field Test results for four flow hoods of different resistances.

Applying the corrections from Equation B21 to these data results in predicted flows averaging 15 cfm (13%) too high, with an RMS error of 19 cfm (17%). This bias is a surprising result because it is expected that the "correct" relationship in Equation 18 should be more accurate at extrapolating than the original relationship given in Equation 2. This result indicates that further study is required (including field testing of more duct systems) in order to further evaluate the applicability of these relationships. Another possibility is that the flowmeter pressure drop is not the same as the static pressure differences assumed in the multi-branch analysis above. This is because the soaker hose mounted in the flowmeter may allow some velocity pressure as well as static pressure to be included in the flowmeter pressures. This would result in pressure

differences used in Equation B20 being too high. In turn, this would result in Equation B20 overpredicting the register flow. Conversely, there is some pressure drop across the flow straightener and the diffuser that is not included in the pressure reading from the soaker hose. This would result in the pressure differences being too low and Equation B21 would then underpredict the flow. Both of these effects depend on pressures due the sir flow.

To investigate these effects, the standard assumption that the velocity pressure would be proportional to the square of the velocity was used. Furthermore, it was also assumed that the velocities in side the flowhood were proportional to the volumetric airflow through the flowmeter. The single unknown is the effective pressure coefficient that converts the air velocity into a pressure change in the soaker hose. This coefficient was determined empirically using the measured data shown in Figure B20, and using the following methodology.

In general, the relationship between velocity pressure and velocity is given by:

$$\Delta P_v = C_p \frac{\rho}{2} V^2 \quad \textbf{(B22)}$$

Where:

ΔP_v is the velocity pressure (Pa)

C_p is the pressure coefficient

ρ is the air density (kg/m^3), and

V is the air velocity (m/s).

This can be written in terms of volumetric flow rate, Q, and a coefficient, K, that includes the area of the register, C_p, ρ, and the constant terms:

$$\Delta P_v = KQ^2 \quad \textbf{(B23)}$$

For convenience, in this empirical analysis, K is determined by making the velocity pressure a fixed fraction, F, of the total measured flowmeter pressure difference. In this case, the low flow resistance point is used, such that:

$$\Delta P_{v,lo} = KQ_{lo}^2 = F\Delta P_{lo} \quad \textbf{(B24)}$$

and ΔP_{lo} can be corrected by ΔP_v:

$$\Delta P_{lo,corrected} = \Delta P_{lo} - \Delta P_v \quad \textbf{(B25)}$$

Equation B24 can be rewritten as:

$$K = \frac{F\Delta P_{lo}}{Q_{lo}^2} \quad \textbf{(B26)}$$

then ΔP_{hi} can then be corrected using:

$$\Delta P_{hi,corrected} = \Delta P_{hi} - \Delta P_{v,hi} = \Delta P_{hi} - KQ_{hi}^2 \quad \textbf{(B27)}$$

Substituting the corrected pressures from Equations B25 and B27 in Equation B21 allows the calculation of flowmeter flow using pressures corrected for potential velocity effects. Analysis of

the measured data in Figure B20 has shown that the bias can be reduced to 0.3% (0.9 cfm) and the RMS errors reduced to 7% (7 cfm) by using a velocity pressure fraction (F) of 0.6 (Pa/cfm^2). These results indicate that this empirical velocity pressure correction substantially improves the two-point flowmeter results.

Single Point Residential Supply Testing

Analysis of the data in Figure 17 suggest that a simple empirical relationship could be used to correct the flow hood data to true flows. Both the idealized analysis and the field data indicate that a flowmeter with less back-pressure requires less extrapolation. There is, however, a lower limit implied by the pressure sensor resolution of 0.1 Pa. Looking at the flowmeter with the lowest flow resistance (white 1) a simple linear empirical relationship suggests itself. At a flowmeter pressure difference of 5 Pa, this flowmeter reads 15% too low. Linearizing over the zero to 5 Pa pressure difference leads to a simple linear correction that only requires a single point to be measured:

$$Q_{1,a} = Q_{1,b}\left(1 + \frac{0.15\Delta P_{fm}}{5}\right) \qquad \textbf{(B28)}$$

Where $Q_{1,a}$ is the true register flow, $Q_{1,b}$ is the indicated flowmeter flow and ΔP_{fm} is the pressure across the flowmeter in Pa. Applying this to the laboratory and field data resulted in an average error of only 1% (2 cfm) with a RMS error of 6% (8 cfm). However, using this relationship on flowmeters with greater resistance and pressure drop produced significant errors. For each of the four flowmeters, Equation B28 was optimized to reduce the biases. Table B5 summarizes the optimization results. The higher resistance flow meters that require the greatest correction show the greatest scatter in Figure B20, and have the greatest RMS errors in Table B5. The best single point strategy indicated by these results is to use a flowmeter with the minimum flow resistance or pressure drop when applying these simple linear corrections.

Table B5. Summary of single point optimization results

Flowmeter	Optimization	Bias Error, % (cfm)	RMS Error, % (cfm)
White 1	$Q_{1,a} = Q_{1,b}\left(1 + \frac{0.15\Delta P_{fm}}{5}\right)$	1 (2)	6 (8)
Blue 1	$Q_{1,a} = Q_{1,b}\left(1 + \frac{0.15\Delta P_{fm}}{5}\right)$	-3 (-1)	12 (13)
White 2	$Q_{1,a} = Q_{1,b}\left(1 + \frac{0.2\Delta P_{fm}}{5}\right)$	1 (3)	19 (20)
Blue 2	$Q_{1,a} = Q_{1,b}\left(1 + \frac{0.33\Delta P_{fm}}{5}\right)$	-3 (-5)	24 (17)

* - The fractional (%) errors are the average and RMS of the fractional errors, not the average and RMS flows divided by average flow.

Commercial Supply Basket Hood

The two main differences between a commercial and a residential supply register are the flow range and the size. A typical commercial register is larger – typically 22 inches (560 mm) square and the flow range is from 200 cfm to 500 cfm (95 l/s to 240 l/s) compared to less than 300 cfm (140 l/s) for a residential register. Figure B18 shows how the same plastic laundry basket as for the residential basket flow hood was connected to a fabric hood from a standard flow hood in order to cover the larger square commercial registers. This combination of the basket and the flow capture hood is called the commercial supply basket flow hood. As with the residential measurements, two baskets of different colors (light blue and dark blue) and flow resistances were used to obtain two different flows and their corresponding flow resistances/pressure differences.

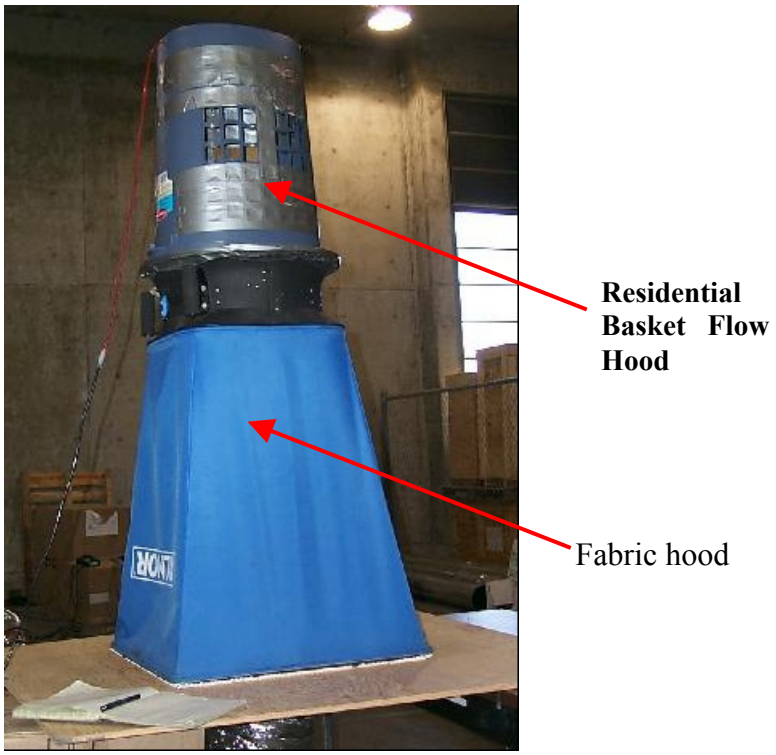

Figure B18. Commercial Supply Basket Flow Hood

Calibration of the Commercial Supply Basket Flow Meter

The commercial flow hoods were calibrated using the same single branch apparatus as for the residential flow meters. The small airflow nozzle introduced too much of a flow restriction at higher flows required for commercial operation, so it was replaced with a less accurate (±3%) combined fan/flow measurement device as shown in Figure B19. The calibrations were performed over a range from 200 cfm to 500 cfm (95 l/s to 240 l/s), which corresponds to typical supply register flows in commercial buildings. The effect of different diffuser grilles (shown in Figure B20) was determined by performing independent calibrations with each of the grilles in place in the apparatus. The test results showed (shown in Figure B21) that the kind of the grille

does not make any significant difference to the calibration equation. Therefore, in the interest of simplicity, the two data sets (square grille and diffuser) were combined to determine a single calibration equation for each basket hood. The calibration results summarized in Table B6 show how the commercial baskets have less flow resistance (higher C) than the residential basket hoods.

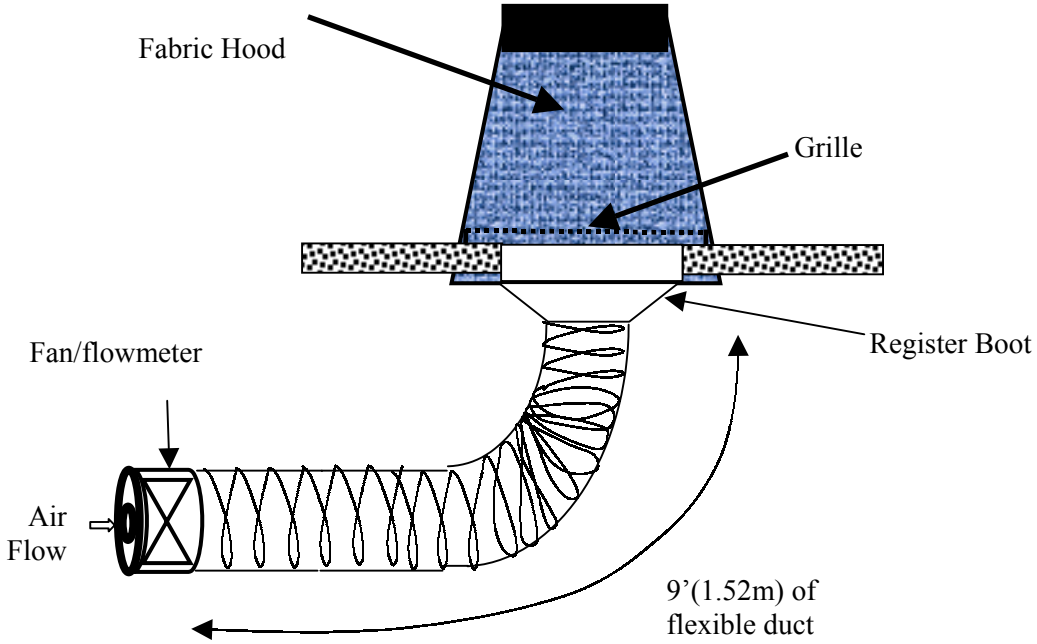

Figure B19. Calibration apparatus for commercial supply basket flow hoods

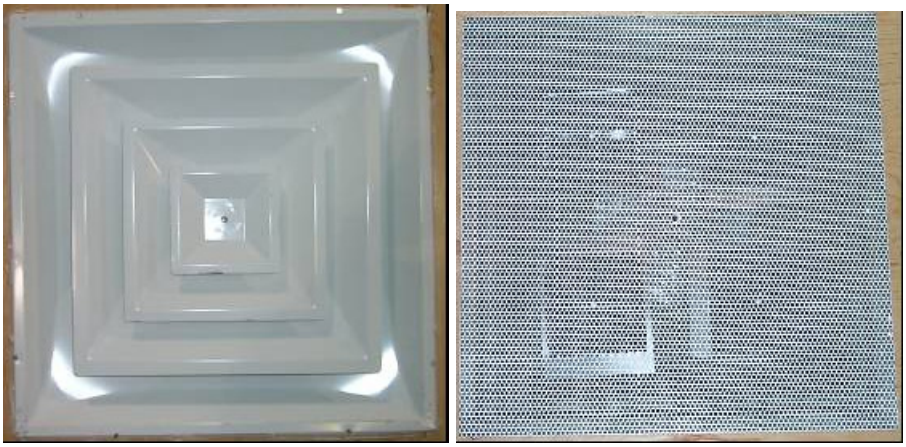

Figure B20: Two different kind of grilles used in the calibration process

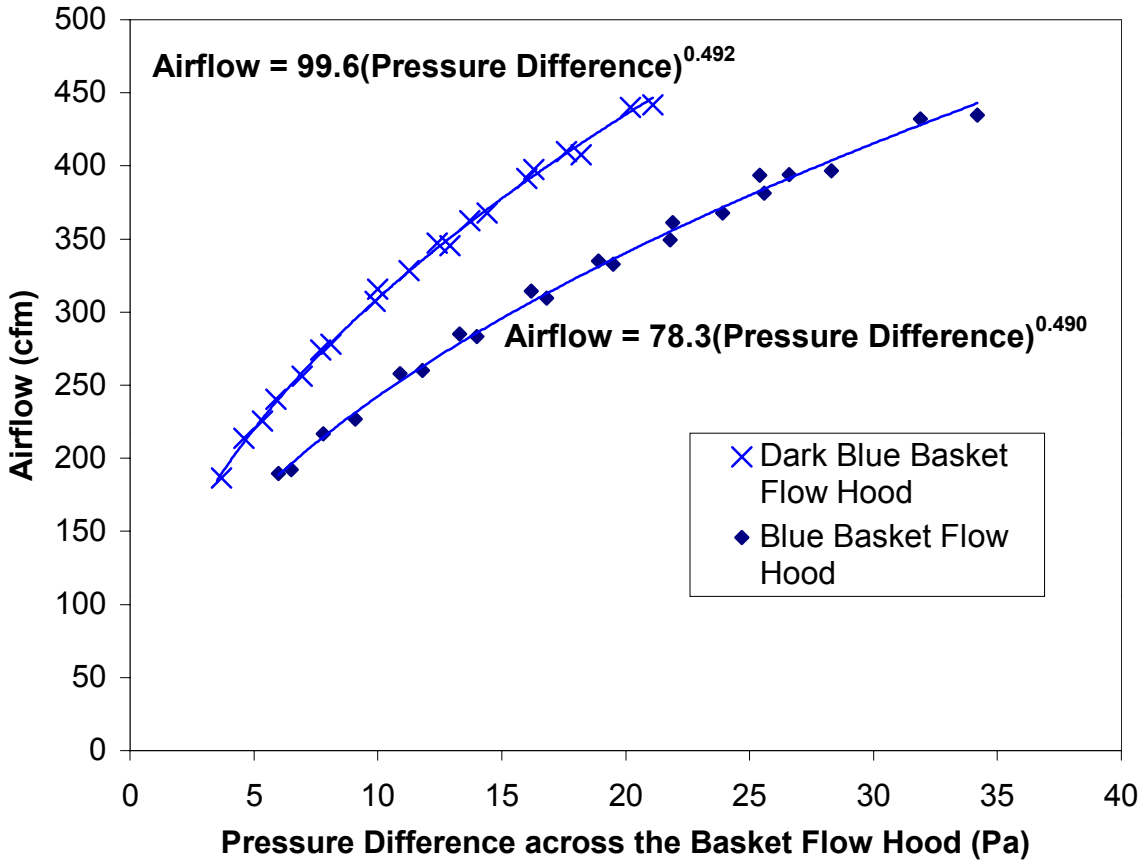

Figure B21. Commercial Supply Basket Flow Hood Calibration Results.

Table B6. Commercial supply basket flow hood calibrations				
Configuration name	C (cfm/Pa^n)	95% confidence interval for C	N	95% confidence interval for n
Blue	78.3	(75.1, 81.7)	0.490	(0.476, 0.505)
Dark Blue	99.6	(97.5, 101.7)	0.492	(0.483, 0.501)

Field testing of commercial supply basket flow hood

The commercial supply basket flow hood was field tested on 11 registers from three commercial building systems located in Sacramento, California. The reference flow hood for these commercial registers was the same powered flow hood used for the residential field testing. Table B7 and Figure B22 show the detailed results of these tests. The test results show that basket flow hood errors are mostly biases. They tend to underpredict the flows, with a mean difference of – 11.6% and an RMS Difference of 14.7%. In addition, the underprediction is greater at higher flow rates, when the backpressure of the flow hood is highest. This indicates that the underprediction is due to the extrapolation of the measured flows to the flow without the flowmeter in place.

Table B7. Commercial basket hood field test results					
Register	Pressure Difference Blue, Pa	Pressure Difference Dark blue, Pa	Basket Flow Hood Airflow, Cfm (l/s)	Reference Airflow, cfm (l/s)	Difference (%)
Beauty Salon 1	10.5	7.45	310 (146)	397 (187)	-21.9
Beauty Salon 2	8.5	6.1	285 (134)	349 (165)	-18.4
Beauty Salon 3	9.0	7.2	367 (173)	413 (195)	-11.2
Dance Studio 1	9.1	6.7	308 (145)	338 (159)	-8.7
Dance Studio 2	8.4	6.0	281 (133)	336 (158)	-16.4
Dance Studio 3	4.4	3.0	189 (89)	205 (97)	-7.9
Bicycle Stores 1	29.8	22.1	563 (266)	721 (340)	-21.9
Bicycle Stores 2	28.4	19.9	497 (235)	664 (313)	-25.1
Bicycle Stores 3	19.8	13.4	393 (186)	486 (229)	-19.1
Bicycle Stores 4	14.3	10.1	358 (169)	360 (170)	-0.5
Bicycle Stores 5	12.5	8.8	333 (157)	344 (162)	-3.0

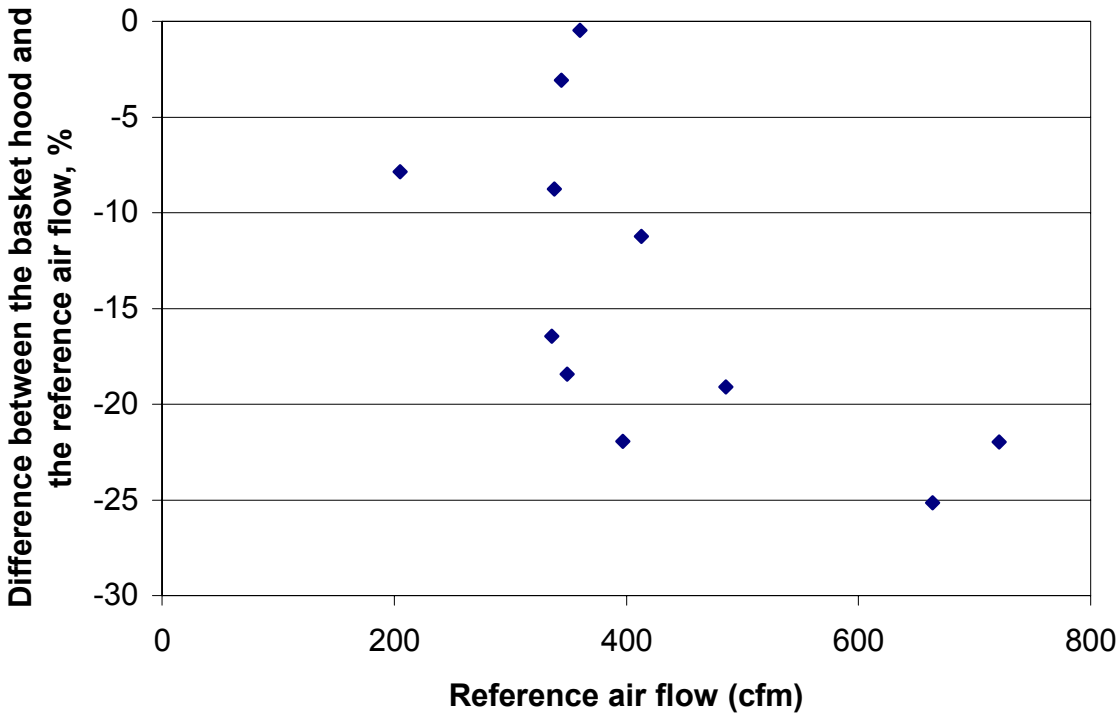

Figure B22: Commercial supply basket hood field test results

Extrapolation error reduction for commercial basket flow hoods

Using the same two point velocity pressure corrections used for residential registers, reduces the errors to a bias of –1 cfm (1.5%) and an RMS uncertainty of 49 cfm (11%). This required the use of a velocity pressure fraction (K) of 0.1 in Equation B24 - substantially less than for the residential flowmeter. This difference is probably because the construction of the commercial flowmeter places the soaker hose pressure sensing element far away form the direct register flow.

The individual measured flows and pressure differences for the commercial register measurements are illustrated in Figure B23. The flow to pressure drop relationship is much less clear than for the residential supplies shown in Figure B17. Because the commercial results did not show definite flow to pressure difference trends, the one point analysis performed for the residential registers was not repeated for commercial registers.

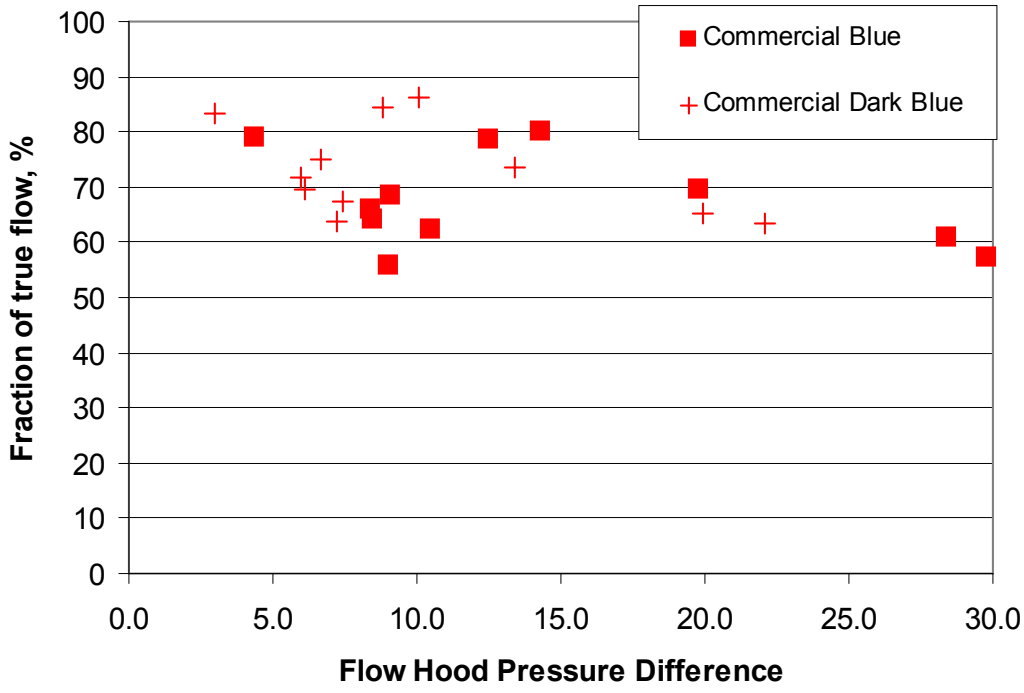

Figure B23: Individual pressure and flow measurements from commercial supply basket hood field test results

Summary

The test results shown here indicate that the basket style flow hood combines sufficient accuracy for most applications while being cheap and easy to use. The development of the basket flow hoods has shown that it is important to balance the need to have flow hoods that introduce small flow resistances with the precision limits of measuring pressures. With modern time-averaging hand held digital manometers, the measured pressure difference requirements can be reduced to a few Pascals. This is significant because this study showed that significant errors can be introduced as a result of poor extrapolation from measurement conditions to operating conditions.

For residential return measurements, using a basket with many evenly distributed holes gave excellent results compared to the reference powered flow hood, with a mean difference (bias) of -0.2% and an RMS difference of 2.4%. This is less than the ±3% accuracy specification for the reference flow meter.

It is more difficult to measure supply flows because the flow hood has to be made insensitive to inlet flow conditions. The basket flow hoods used a combination of honeycomb flow straightener and a mesh diffuser to effectively reduce this problem. This introduced extra flow resistance compared to the return flow hood. Combining this extra flow resistance with the extra sensitivity of multi-branch supply systems to this flow resistance led to the use of up to four basket hood configurations of different flow resistance and a multi-point fitting method to determine the correct flow through the register without the flow meter in place. Additional analysis were performed comparing multi-branch and single branch extrapolation methods and methods of accounting for pressure differences occurring within the flow hood on 33 registers in five houses and a laboratory test facility. The results of this analysis showed how a two-point test and a

velocity pressure correction gave results within 0.3% of the reference on average, with an RMS difference of 7%. Finally, an empirical single point analysis also gave excellent results, with a mean difference of 1% and an RMS difference of 6%. The use of the single point analysis is limited to situations where the extrapolation to the true flow is less than about 20% of the measurement, otherwise these differences can increase significantly. For the user the single point method has significant advantages because only one basket (or a single leakage configuration for a basket) needs to be used.

The residential supply flow hood was adapted to be used on commercial supplies by connecting it to a large flow capture hood while retaining the same flow straightener and diffuser. The commercial flow hood was tested on 11 register in three separate systems. Using the same two point testing combined with the velocity pressure correction factor, the commercial supply basket hood has a bias of 1.5% and an RMS difference of 11% compared to the reference powered flow hood.

In each case the basket flow hood biases were small compared to the reference flow hood. The remaining RMS differences are due to several issues: residual supply flow meter sensitivities to the incoming air flow pattern, pressure measurement resolution and lastly, the ability of the operator to obtain a good seal around the register so that air does not bypass the flow hood.

These basket hoods all proved to be very easy to use due to their light weight compared to other flow meters. The only significant issue for the operator is the need to have a good seal around the base of the flow hood where it surrounds the register. The component cost is minimal – only a few dollars. However, the accurate results obtained in this study require a good time averaging pressure sensor that costs about $600. In addition, as with most measurement instrumentation there is the need to calibrate the basket – which would also add to the cost. However, there remain significant potential cost savings compared to commercially available flow hoods that cost $2000 to $3000 or powered flow hoods that cost about $1500 to $2000.

References

Walker I.S. Wray, C.P., Dickerhoff, D.J. and Sherman, M.H., 2001 ‘Evaluation of flow hood measurements for residential register flows’, Lawrence Berkeley National Laboratory, Berkeley, USA, LBNL 47382

Appendix C. Summary of Diagnostic Tests on Building America Homes in Tracy, CA.

Two houses were tested in Tracy, CA. These houses used the cathedralized attic system, where the insulation is placed under the roof deck rather than at the ceiling, and the attic space should be sealed relative to outside. This makes the attic space look like conditioned space. Because the HVAC system is placed in this attic space, any duct losses should go to conditioned space rather than being lost to outside. The objective of these diagnostic tests is to measure how leaky the attic is relative to outside. If the attic is leaky to outside, then the ducts may leak to outside, with resulting energy losses. In addition, air movement from outside into the attic will make the attic temperatures more like outside than conditioned space. The ducts were also tested for airtightness. More airtight ducts will have less losses to the attic space and will be more likely to deliver the conditioned air to the right part of the house. The individual register flows were also measured to further investigate if these systems were delivering the correct amount of air to each register. The building envelopes were tested for airtightness also, because the building America homes were designed to have limited natural ventilation.

The results showed that:

- the attics need to be better sealed to outside
- the ducts had very low leakage
- damper and control systems needed to be tested for correct operation
- the envelopes met the required airtightness criteria
- the passive single point basket flow hood consistently underpredicted the flows by about 10%, indicating that further work is required on the single point pressure correction algorithm. Also, the difficulty in accessing some registers prevented us from getting a good seal around the passive flowhood. This results in air leakage between the flow hood and the wall/ceiling and a bias in the flow measurement.
- There is a significant difference between the pressurization and depressurization envelope leakage test results. This is due to the valving action of some leaks: specifically those with dampers, for example the dryer and range hood vents. The pressurization test results show a clear change in envelope leakage as the pressure is increased and the dampers open.

House 1: 1120 Lakeview

Single story house, approximately 2459 ft^2.

Envelope leakage: 1683 cfm50

Attic leakage: 892 cfm50

Attic leakage to outside: 568 cfm50

Attic leakage to house: 324 cfm50

Pressurization Total duct leakage: 112 cfm25

Pressurization Total duct leakage with outside air sealed at hallway return register: 107 cfm25

Pressurization Duct leakage to outside: 35 cfm25

Return Flow (large return done with two measurements, with half of return taped off in each case)= 1178 cfm

Supply plenum to house pressure difference (Psupply) = 45 Pa

Return plenum to house pressure difference (Preturn) = -30 Pa

Register Flows at 1120 Lakeview, Tracy, CA	
Register	Powered flowhood
1	29
2	52
3	99
4	116
5	137
6	125
7	45
8	74
9	95
10	64
11	127
12	110
13	26
14	115
Sum supplies	**1177**
R1	490
R2	221
R3	467
Sum returns	**1178**

House 2: 970 Lakeview

2 story house, approximately 2900 ft^2. This house had a single air handler with three zones: second floor, master suite and the result of the first floor minus the master suite.

Envelope leakage:

From ΔQ program fitted to all pressurization points: 1790 cfm50

From ΔQ data at single pressurization point @ 50 Pa: 1805 cfm50

From ΔQ data at single depressurization point @ 50 Pa: 1542 cfm50

From ΔQ data depressurization fitted from 15 to 50 Pa: 1640 cfm50

From TECTITE CGSB (depressurization): 1503 cfm50

From TECTITE CGSB (depressurization) with ducts sealed: 1488 cfm50

From TECTITE CGSB (depressurization) with ducts and fireplace sealed: 1450 cfm50

From TECTITE CGSB (depressurization) with attic hatch open: 1697 cfm50

Pressurization Attic total leakage: 1820 cfm50

Pressurization Attic leakage to outside: 1000 cfm50

Pressurization Attic leakage to house: 820 cfm50

Three zone system, second floor damper closed for all tests (due to damper malfunction)

Pressurization Total duct leakage with outside air sealed at hallway return register: 302 cfm25 (309 cfm25 CEM)

Duct leakage to outside: 167 cfm25

ΔQ: Qs = 8 cfm, Qr = 19 cfm

Supply plenum to house pressure difference (Psupply) = 40 Pa

Return plenum to house pressure difference (Preturn) = -19 Pa

Upstairs calling (All dampers shut): Psupply = 209 Pa

M Bed + upstairs calling: Psupply = 144 Pa

M Bed + up + hall calling: Psupply = 40 Pa

All three dampers open (upstairs damper forced open): Psupply = 21 Pa

Duct Blaster pressure matching single return flow for air handler flow measurement (mounted at return with largest flow and other two returns sealed) = 1277 cfm

Register Flows at 970 Lakeview, Tracy, CA		
Register	Powered flowhood	Passive Basket (1 point)
1	141	109
2	166	139
3	218	168
4	183	141
5	-	98
6	157	122
7	195	177
8	-	25
9	52	49
10	-	10
11	-	18
12	37	22
13	23	9
14	-	-
15	18	9
16	12	7
17	5	5
Sum supplies	**1207**	**1108**
R1	159	164
R2	431	350
R3	558	715
Sum returns	**1148**	**1229**

Appendix D. Summary of Coil Fouling Solid Particle Pressure Drop Tests.

Introduction

The build up of indoor dust on heat exchanger coils can have a deleterious effect on the performance of the exchanger. It affects the performance by reducing air flow (and thus heat transfer) or increasing fan energy use in order to have the same flow rate. The goal of this study is to determine the relationship between the mass of dust deposited and the resulting pressure drop.

The coil and experimental apparatus used in this study are the same as those used in the deposition experiments discussed elsewhere in this report. Experiments were performed to determine the mass of dust deposited in the coil and the static pressure upstream and downstream of the coil. The particles we used were representative of typical fouling agents, and its characteristics are summarized in Table D1.

Table D1. SAE coarse calibrated dust

Lower bound (µm)	Upper bound (µm)	Mass (%)	Uncertainty (%)
0	5	12	2
5	10	12	3
10	20	14	3
20	40	23	3
40	80	30	4
80	200	8	2

Measurement and calculation methods for estimating solid particle deposition

It is difficult to directly measure deposition because of the small difference between the weight of a clean and a fouled coil. Therefore the following indirect alternatives were used and evaluated.

The first alternative is to measure the fraction of dust deposited on the coil by measuring dust concentration upstream and downstream of the coil, with the difference assumed to be deposited on the coil. Fouled air samples are isokinetically drawn through filters placed up and down stream of the coil to determine the dust concentrations. The difference between the mass of the filters up (m_{up}) and down (m_{down}) stream multiplied by the ratio between the duct area and the filter area gives the mass deposited in the coil.

$$M_{coil} = \left(m_{up} - m_{down}\right) \frac{A_{duct}}{A_{filter}} \qquad \text{(D1)}$$

Because the total mass of dust injected into the duct is known, the mass of dust deposited in the coil can be also calculated using Equation D2 using the deposition, D, calculated using the measured filter masses and the upstream and down stream volumetric flow rates.

$$M_{coil} = M_{\substack{dust \\ introduced}} \cdot D \qquad \text{(D2)}$$

A third alternative is to evaluate the mass of dust deposited on the coil using the deposition multiplied by the ducts mass flow and by the experimental time:

$$M_{coil} = D \cdot C_{up} \cdot V_{bulk} \cdot A_{duct} \cdot t \qquad \text{(D3)}$$

The development of these three calculation methods and a simple uncertainty analysis is given in the Appendix.

Each of these three methods for deposition is corrected for the following three factors that affect the dust deposition:

1. Because the nozzle pump flows cannot be adjusted precisely enough to ensure perfect isokinetic sampling through the filters, a correction was performed based on the measured sampling flows and duct velocities.
2. Visual inspection (as shown in Figure D1) showed that a large amount of dust is blocked by the rack and the filter. Also, Figure 1 shows that the deposition occurs less near the sides of the duct. We hypothesized that both are due to non-uniform mixing of dust in the airstream. For this reason, not all of the duct area should be considered in the deposition calculations.
3. Figures D1 and D2 show that a large quantity of dust deposits on duct surfaces due to gravitational settling. Importantly, this phenomenon occurs between the filters and the coil. So this amount was measured at the end of the series of experiments and subtracted from the calculation of mass deposited in coil.

Figure D1. Deposition on filter rack and duct walls upstream of the coil

Figure D2. Dust deposited below the injection site

All the corrections are discussed in more detail in the Appendix. These corrections were found to be extremely large for the experiments performed in this study: they reduced the calculated deposition by factors of about two to three. This shows how important it is to make these corrections for this type of experiment. In order to make good estimates of the correction factors in the calculation procedure all the dust had to be accounted for. This included dust deposited on the filter mounts and duct walls (see Figure 3) as well as any dust remaining in the sifter (Figure D4).

Figure D3. Dust deposited on filter mount and duct wall

Figure D4. Dust remaining inside of the sifter

Experimental Procedure

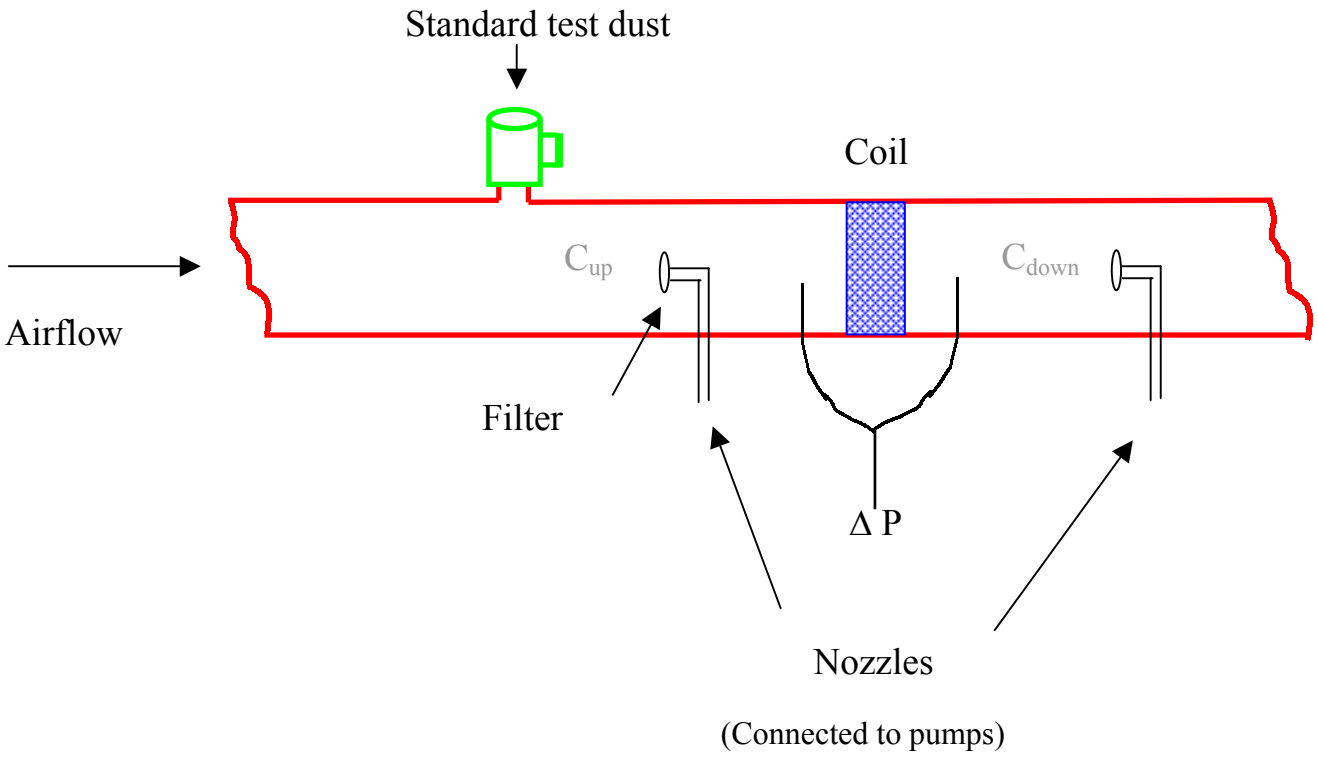

Figure D5. Experimental apparatus

Figure D5 shows the experimental apparatus used to measure solid particles. A fan, with a constant air flow, moved the air in the duct through the coil. The bulk velocity was measured with

a Pitot tube and a micromanometer by averaging sixteen points in the same cross section. This was checked every 5 experiments. The local air velocity near the filters was also measured every experiment.

For each experiment, the same quantity of dust (25 grams) was introduced in the duct with a sifter (shown in Figures D6 and D7) in order to be well mixed. The dust used is relatively massive, so a majority fell by gravitational settling in the duct before the coil. To minimize the amount of dust deposited in the duct before the coil, the dust needs to be added to the duct as close to the coil as possible. However, the dust also needs to be well mixed across the duct that implies the opposite requirement of adding the dust as far upstream, of the coil as possible. A reasonable compromise was to introduce to dust 4.6 m (15 ft) before the coil.

Figure D6. Sifter to introduce the dust in duct

Figure D7. Introduction of dust

The coil pressure drop (the difference between the static pressures before and after the coil) was measured by a micromanometer during all the experiments. Deburred holes were made in each side of the duct to measure the average pressure as shown in Figure D8.

The flow of air through the sampling filter was measured with flow nozzles like the one shown in Figure D9. The goal is to get isokinetic sampling in the filters. Unfortunately, the measured nozzle flows cannot be exactly matched to the local air velocities due the difficulty in controlling the pump flow. However, the highly accurate nozzle flows can be used to perform a correction to the isokinetic case.

Figure 8. Measurement of the coil pressure drop

Figure 9. Nozzle for measuring the air flow through the filter

The series of experiments was considered finished when the pressure drop suddenly fell between two experiments. This indicated that some of the dust deposited on the front of the coil fell off as illustrated in Figure D10.

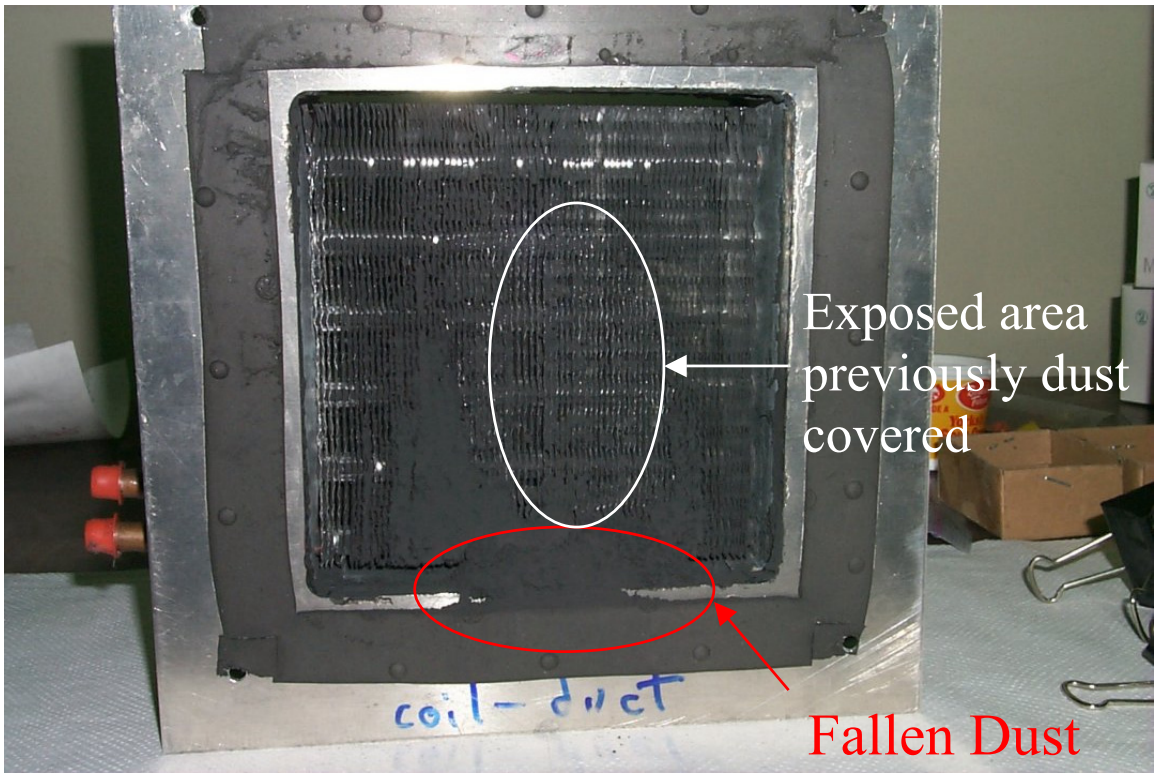

Figure D10. Coil after dust particles have fallen off

Pressure drop results

Figure D11 summarizes up the experimental results for the three mass deposition models at a duct velocity of 1.94 m/s. The first method is based on Equation (D1), the second is based on Equation (D2) and the third method on Equation (D3). The cumulative pressure drop is the additional pressure drop due to coil fouling. The clean coil started with a pressure drop of about 25 Pa, so these results indicate an approximate doubling of the coil pressure drop when it is fouled. In field installations the fouling matter is not a dry loose dust, but includes sticky particles and moisture that tends to allow the particles to adhere to the surface beyond the limits found in these experiments. Therefore these experimental results are more likely to be a lower bound on the effect of coil fouling because material fell off the face of the coil and ended the experiments before the face of the coil was completely fouled.

The results also show that the rate of coil fouling increases as the fouling increases. This is because the fouling dust blocks passages for air flow in the coil which leads to higher air velocities and a larger surface area for fouling to occur.

The error bars in Figure D11 were determined using a simple uncertainty analysis given in the appendix. The uncertainty analysis indicated that the third test method gave the least uncertainty and the first method the greatest. This is because the first method is sensitive to small differences

between two relatively large numbers – the masses of the filters and dust. The other two methods minimize this effect by not using the differences in mass directly.

In the future these experiments should be repeated to examine the repeatability of the results and confirm that the third deposition calculation method produces the most reliable results. Also, the experiments should also be performed at other velocities to test for aerodynamic effects on deposition, pressure drop and face fouling.

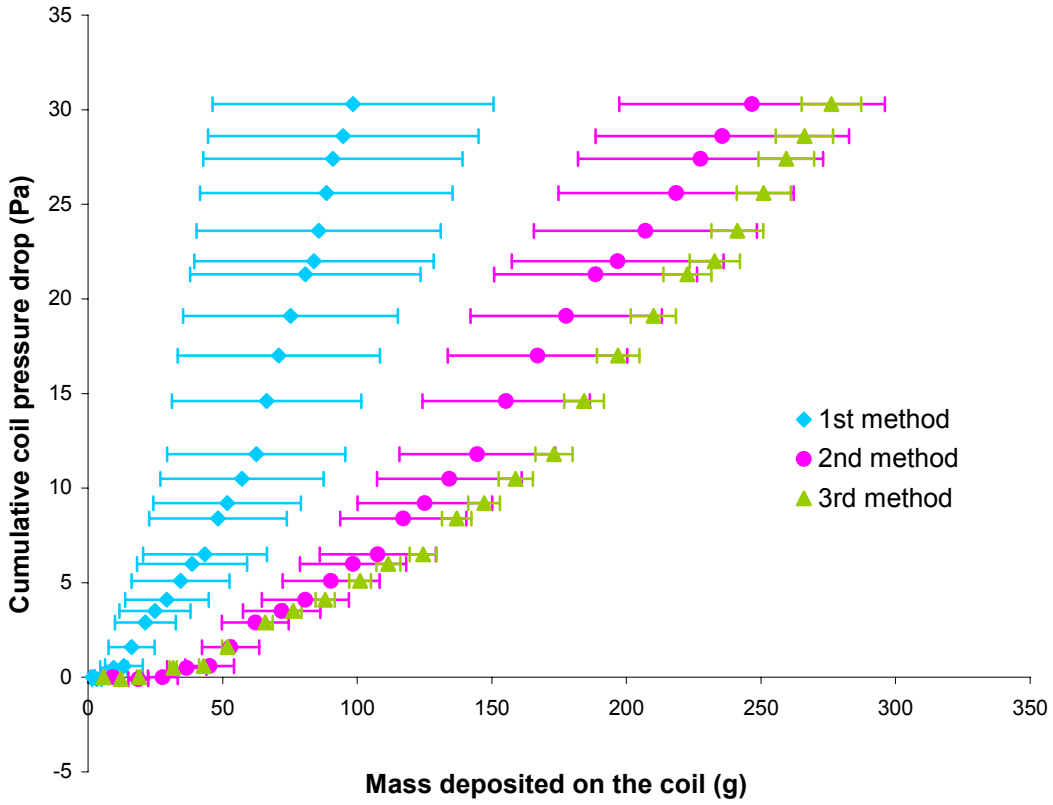

Figure D11. Cumulative coil pressure drop

Nomenclature

A_{duct}	Cross sectional duct area (m^2)
$A_{duct\ corrected}$	Cross sectional duct area corrected (m^2)
A_{filter}	Filter area (m^2)
c_{down}	Average downstream concentration (kg/m^3)

c_{up}	Average upstream concentration (kg/m^3)
D	Deposition fraction (%)
M_{coil}	Mass deposited in the coil (kg)
m_{down}	Mass of the downstream filter (kg)
M_{duct}	Mass deposited in the duct between the two filters (kg)
m_{up}	Mass of the upstream filter (kg)
P	Penetration (%)
Q_{down}	Flow downstream of the coil (m^3/s)
Q_{up}	Flow upstream of the coil (m^3/s)
t	Experimental time (s)
V_{bulk}	Bulk Air velocity (m/s)
$w_1, w_2, \ldots, w_n$	Uncertainties in the independently measured variables

Appendix. Details of mass deposition calculations and uncertainty analysis

The penetration can be expressed by:

$$P = \frac{c_{down}}{c_{up}} = \frac{m_{down}}{Q_{down}} \cdot \frac{Q_{up}}{m_{up}} \tag{D4}$$

Mass deposited in the coil (First method):

$$M_{coil} = \left(m_{up} - m_{down}\right) \frac{A_{duct}}{A_{filter}} \tag{D5}$$

Mass deposited in the coil (Second method):

$$M_{coil} = M_{\substack{dust \\ introduced}} \cdot D \tag{D6}$$

$$M_{coil} = M_{\substack{dust \\ introduced}} \left(1 - P\right) = M_{\substack{dust \\ introduced}} \left(1 - \frac{c_{down}}{c_{up}}\right) \tag{D7}$$

$$M_{coil} = M_{\substack{dust \\ introduced}} \left(1 - \frac{m_{down}}{Q_{down}} \cdot \frac{Q_{up}}{m_{up}}\right) \tag{D8}$$

Mass deposited in the coil (Third method):

$$M_{coil} = D \cdot C_{up} \cdot V_{bulk} \cdot A_{duct} \cdot t \tag{D9}$$

$$M_{coil} = \left(1 - P\right) \cdot \frac{m_{up}}{Q_{up} \cdot t} \cdot V_{bulk} \cdot A_{duct} \cdot t \tag{D10}$$

$$M_{coil} = \left(1 - \frac{m_{down}}{Q_{down}} \cdot \frac{Q_{up}}{m_{up}}\right) \cdot \frac{m_{up}}{Q_{up}} \cdot V_{bulk} \cdot A_{duct} \tag{D11}$$

$$M_{coil} = \left(\frac{m_{up}}{Q_{up}} - \frac{m_{down}}{Q_{down}}\right) \cdot V_{bulk} \cdot A_{duct} \tag{D12}$$

Corrections to deposited mass

Four corrections need to be done:

1. Because of non-isokinetic sampling, the aspiration efficiencies η_{up} and η_{down} are calculated to correct the concentrations on filters.
2. The filters and the racks block some dust that can deposit on the coil, so the duct area A_{duct} should be reduced.

3. The mixing in the duct is not uniform so once again the duct area A_{duct} should be reduced.
4. Some dust is deposited in the coil by gravitational settling. At the end of the experiment, this amount was measured and subtract to the mass deposited in the coil.

In conclusion, the three methods become:

$$M_{coil} = \left(\frac{m_{up}}{\eta_{up}} - \frac{m_{down}}{\eta_{down}} \right) \frac{A_{duct}}{A_{filter}} - M_{duct} \quad \text{(D13)}$$

$$M_{coil} = M_{dust} \left(1 - \frac{m_{down}}{Q_{down} \cdot \eta_{down}} \cdot \frac{Q_{up} \cdot \eta_{up}}{m_{up}} \right) \cdot \frac{A_{duct}}{A_{duct}} - M_{duct} \quad \text{(D14)}$$

$$M_{coil} = \left(\frac{m_{up}}{Q_{up} \cdot \eta_{up}} - \frac{m_{down}}{Q_{down} \cdot \eta_{down}} \right) \cdot V_{bulk} \cdot A_{duct} - M_{duct} \quad \text{(D15)}$$

Uncertainty Analysis

The uncertainty is calculated using Equation D16:

$$w_R = \left[\left(\frac{\partial R}{\partial v_1} \cdot w_1 \right)^2 + \left(\frac{\partial R}{\partial v_2} \cdot w_2 \right)^2 + \ldots + \left(\frac{\partial R}{\partial v_n} \cdot w_n \right)^2 \right]^{1/2} \quad \text{(D16)}$$

where

R is a given function of the independent variables $v_1, v_2, \ldots, v_n$ or $R = R(v_1, v_2, \ldots, v_n)$,

R w_R is the uncertainty in the result,

R $w_1, w_2, \ldots, w_n$ are the uncertainties in the independently measured variables.

Quantity	Uncertainty	Justification
$M_{dust\ introduced}$	12%	Because of the design of the sifter itself, this measure is not really accurate even if we measure the dust remaining in the sifter and in the bag.
M_{duct}	10%	This mass is obtained by taking the ratio of the total dust remained from the duct by the mass introduced each experiments. This uncertainty is also quite large.
m_{up}	14%	This filter had a lot of dust from each experiment, and some deposited on the plastic lip surrounding the filter and was occasionally included inadvertently.
m_{down}	6%	As this filter had very little dust in it and on the plastic lip, the possibility that some extra dust was included in the measurement is relatively small.
Q_{up}	13.6%	This uncertainty corresponds to the ratio between the half range of variations during the experiment over the average flow.
Q_{down}	1%	This flow was quite stable.
V_{bulk}	2%	This measurement was checked frequently, and the repeatability was very good.
$A_{duct\ corrected}$	2%	The area blocked is measurable so the approximation is pretty accurate. The non-uniform mixing between the filters and the coil can't be evaluated.

Uncertainty summary		
M_{coil} from Eq. D10	53%	This method has a very large uncertainty.
M_{coil} from Eq. D11	20%	This method has a large uncertainty.
M_{coil} from Eq. D12	4%	*This method is the most valid because of its reasonable uncertainty.*